



DGK Deutsche Geodätische Kommission
bei der Bayerischen Akademie der Wissenschaften

Reihe C

Dissertationen

Heft Nr. 620

Matthias Butenuth

Network Snakes

München 2008

**Verlag der Bayerischen Akademie der Wissenschaften
in Kommission beim Verlag C. H. Beck**

ISSN 0065-5325

ISBN 978-3-7696-5034-1

**Diese Arbeit ist gleichzeitig veröffentlicht in:
Wissenschaftliche Arbeiten der Fachrichtung Geodäsie und Geoinformatik der Leibniz Universität Hannover
ISSN 0174-1454, Nr. 272, Hannover 2008**



Network Snakes

Von der Fakultät für Bauingenieurwesen und Geodäsie
der Gottfried Wilhelm Leibniz Universität Hannover
zur Erlangung des Grades
Doktor-Ingenieur (Dr.-Ing.)
genehmigte Dissertation

von

Dipl.-Ing. Matthias Butenuth
geboren am 24.02.1976 in Bielefeld

München 2008

Verlag der Bayerischen Akademie der Wissenschaften
in Kommission bei der C. H. Beck'schen Verlagsbuchhandlung München

ISSN 0065-5325

ISBN 978-3-7696-5034-1

Diese Arbeit ist gleichzeitig veröffentlicht in:
Wissenschaftliche Arbeiten der Fachrichtung Geodäsie und Geoinformatik der Leibniz Universität Hannover
ISSN 0174-1454, Nr. 272, Hannover 2008

Adresse der Deutschen Geodätischen Kommission:



Deutsche Geodätische Kommission

Alfons-Goppel-Straße 11 • D – 80 539 München

Telefon +49 – 89 – 23 031 1113 • Telefax +49 – 89 – 23 031 - 1283/- 1100

e-mail hornik@dgfi.badw.de • <http://www.dgk.badw.de>

Prüfungskommission

Referent: Univ.-Prof. Dr.-Ing. Christian Heipke

Korreferenten: Univ.-Prof. Dr.-Ing. Wolfgang Förstner

Univ.-Prof. Dr.-Ing. Monika Sester

Tag der Promotion: 09.06.2008

© 2008 Deutsche Geodätische Kommission, München

Alle Rechte vorbehalten. Ohne Genehmigung der Herausgeber ist es auch nicht gestattet,
die Veröffentlichung oder Teile daraus auf photomechanischem Wege (Photokopie, Mikrokopie) zu vervielfältigen

ISSN 0065-5325

ISBN 978-3-7696-5034-1

Summary

In the thesis a new method of active contour models called *network snakes* is developed. The method enables the optimization of arbitrary graphs representing *networks* and the *boundaries between adjacent objects*. Potential applications are the delineation of road networks or field boundaries from remotely sensed imagery, bio-medical tasks such as the delineation of adjacent biological cells in microscopic images or industrial applications.

Active contour models are a well-known method in computer vision. They bridge the gap between low-level feature extraction or segmentation and high-level geometric representation of objects. But, the original concept is limited to single closed object boundaries. The thesis presents for the first time a general and comprehensive method based on a clear mathematical model enabling a free movement of all nodes and edges of a graph during the optimization without any particular constraints. Three goals of the thesis are defined as follows:

- Development of a new method of active contour models, which optimizes graphs consisting of nodes of an arbitrary degree to enable the delineation of open contours, closed contours and any networks.
- Development of a new method of active contour models, which segments imagery without gaps or overlaps to enable the delineation of adjacent objects or networks.
- Development of a new method of image segmentation and object delineation with a high generality and transferability to enable its applicability for a variety of tasks.

To this end, the concepts of parametric and geometric active contours are compared to each other and the state of the art being relevant to the new developments is presented. The discussion points out, that the explicit representation of topology is only possible in the mathematical model of parametric active contours, which is why the new method is based on this concept. In particular, the possibility to exploit the topology during the minimization of the energy functional prefers the explicit representation of the contour. This allows to deal with applications relying on poor or noisy image data.

The requirements concerning the imagery, initialization and topology are regarded to define the framework for network snakes. The main impact of the thesis is the introduction of new terms into the energy functional to obtain the *novel mathematical model* of network snakes. In particular, the *internal energy* representing the shape model of the contours during the minimization is defined in a new manner to enable the optimization of arbitrary nodes of a graph. The realization of the system is described, the optional topology-preserving energy conserving the initial topology is presented and the general control of the parameters is examined. All developments are illustrated with synthetic examples to highlight the derived achievements compared to traditional parametric active contours.

The developed method of network snakes is analyzed and evaluated with both, synthetic data and real application scenarios. General questions concerning initialization requirements, parameter control, iteration behavior and topology are investigated with exemplary synthetic data to emphasize the benefits and limitations of network snakes with a special focus on the impact of the introduced topology to the concept of parametric active contours. An important goal of the new method of network snakes is the generality and transferability of the solution not only being developed for a specific application, but to delineate arbitrary networks and the boundaries of arbitrary adjacent objects. Two real application scenarios are chosen: the delineation of field boundaries from remotely sensed images and the delineation of adjacent biological cells in microscopic images. The detection of field boundaries is an important task for geosciences and the agricultural sector, for example the derivation of field-based risks of soil loss, precision farming or the monitoring of subsidies. The detection of cells and their properties regarding shape, size and intensity distribution is an increasing task for bio-medical research such as pharmaceutical drug discovery.

Finally, unsolved problems are identified and discussed to show further challenges and to point out possible lines of future research.

Keywords: computer vision, active contour models, network, topology

Zusammenfassung

In dieser Arbeit wird eine neue Methode der Active Contour Models, sogenannte *Network Snakes*, entwickelt. Die Methode ermöglicht die Optimierung beliebiger Graphen zur Repräsentation von *Netzwerken* und *Grenzen zwischen benachbarten Objekten*. Potentielle Anwendungen sind die Optimierung von Straßennetzwerken oder Schlaggrenzen aus Fernerkundungsdaten, bio-medizinische Fragestellungen wie die Abgrenzung von benachbarten biologischen Zellen aus mikroskopischen Bilddaten oder industrielle Anwendungen.

Active Contour Models sind eine bekannte Methode der Computer Vision, die die Lücke zwischen low-level Merkmalsextraktion oder Segmentierung und high-level geometrischer Repräsentation von Objekten überbrückt. Jedoch ist das Konzept auf einzelne geschlossene Objektgrenzen beschränkt. Die Arbeit präsentiert zum ersten Mal eine allgemeingültige und umfassende Methode, die auf einem klaren mathematischen Modell basiert und die eine freie Bewegung aller Knoten und Kanten eines Graphen ermöglicht, ohne dabei durch bestimmte Nebenbedingungen einschränkt zu sein. Drei Ziele der Arbeit sind wie folgt definiert:

- Entwicklung einer neuen Methode der Active Contour Models, die Graphen mit Knoten eines beliebigen Grades optimiert, um offene Konturen, geschlossene Konturen und jegliche Netzwerke zu beschreiben.
- Entwicklung einer neuen Methode der Active Contour Models, die Bilder ohne Lücken oder Überlappungen segmentiert, um benachbarte Objekte abzugrenzen.
- Entwicklung einer neuen Methode der Bildsegmentierung und Objektabgrenzung mit einer hohen Allgemeingültigkeit und Übertragbarkeit, um bei einer Vielfalt von Aufgaben zur Anwendung zu gelangen.

Aus diesem Grund werden die Konzepte der Parametric und Geometric Active Contours gegenübergestellt und der Stand der Forschung in Bezug zu den neuen Entwicklungen präsentiert. Die Diskussion zeigt, dass die explizite Repräsentation der Topologie nur im mathematischen Modell der Parametric Active Contours enthalten ist, weshalb die neue Methode auf diesem Konzept basiert. Insbesondere die Möglichkeit der Topologienutzung während der Minimierung des Energiefunktionalen bevorzugt die explizite Repräsentation, um schlechte oder verrauschte Bilddaten bearbeiten zu können.

Die Voraussetzungen bezüglich Bilddaten, Initialisierung und Topologie werden betrachtet, um einen Rahmen für Network Snakes zu definieren. Der Kern der Arbeit ist die Einführung neuer Terme in das Energiefunktional, um das *neue mathematische Modell* der Network Snakes zu entwickeln. Insbesondere die *interne Energie*, die das geometrische Formmodell der Kontur repräsentiert, ermöglicht durch die neue Definition die Optimierung beliebiger Knoten eines Graphen. Die Realisierung des Systems wird beschrieben, die optionale topologieerhaltene Energie zur Konservierung der Topologie wird präsentiert und die generelle Steuerung der Parameter wird behandelt. Alle Entwicklungen werden mit synthetischen Beispielen bebildert, um die erreichten Ergebnisse herauszustellen und mit traditionellen Parametric Active Contours zu vergleichen.

Die entwickelte Methode der Network Snakes wird mit synthetischen und echten Daten analysiert und bewertet. Allgemeine Fragen bezüglich Initialisierung, Parametersteuerung, Iterationsverhalten und Topologie werden mit synthetischen Daten untersucht, um den Nutzen und die Grenzen von Network Snakes herauszustellen. Ein besonderer Fokus liegt auf der Bedeutung der eingeführten Topologie in die Parametric Active Contours. Ein wichtiges Ziel der neuen Methode ist die Allgemeingültigkeit und Übertragbarkeit der Lösung, um nicht nur spezielle Anwendungen, sondern beliebige Netzwerke und Grenzen benachbarter Objekte beschreiben zu können. Zwei reale Anwendungen werden betrachtet: Die Extraktion von Schlaggrenzen aus Fernerkundungsdaten und die Abgrenzung von benachbarten biologischen Zellen aus mikroskopischen Bilddaten. Die Detektion von Schlaggrenzen spielt eine wichtige Rolle in den Geowissenschaften und der Landwirtschaft, um zum Beispiel schlaggenaue Risiken des Bodenabtrages zu erhalten, für das precision farming oder die Kontrolle von Subventionen. Die Abgrenzung von Zellen und deren Merkmale bezüglich Form, Größe und Helligkeitsverteilung sind eine bedeutende Aufgabe für die bio-medizinische Forschung und die Entwicklung von Heilstoffen. Ungelöste Probleme werden am Ende der Arbeit identifiziert und diskutiert, um zukünftige Herausforderungen zu benennen und mögliche zukünftige Forschungslinien aufzuzeigen.

Schlagnworte: Computer Vision, Active Contour Models, Netzwerk, Topologie

Contents

Summary	3
Zusammenfassung	4
Contents	5
List of figures	7
List of tables	10
1. Introduction	11
1.1. Motivation	11
1.2. Goals of the thesis	12
1.3. Organization of the thesis	13
2. Basics and state of the art	15
2.1. Active contour models	15
2.1.1. Terms and definitions	15
2.1.2. Basics	16
2.1.2.1. Parametric active contours	16
2.1.2.2. Geometric active contours	20
2.1.2.3. Comparison and discussion	22
2.1.3. State of the art	24
2.1.3.1. Introduction	24
2.1.3.2. Parametric active contours	24
2.1.3.3. Geometric active contours	25
2.1.3.4. Multiple active contours	26
2.1.3.5. Coupled active contours	26
2.1.3.6. Related developments regarding network snakes	27
2.1.4. Discussion	27
2.2. Energy minimization of parametric active contours	29
2.3. Related work concerning applications of network snakes	31
2.3.1. Introduction	31
2.3.2. Extraction of field boundaries	32
2.3.3. Delineation of cells	33
3. Network snakes	35
3.1. Introduction	35
3.2. Requirements	36
3.2.1. Outline	36
3.2.2. Imagery	37
3.2.3. Initialization	38
3.2.4. Topology	38
3.3. Energy terms of network snakes	39
3.3.1. Influence of the topology to the energy minimization	39
3.3.2. New internal energy at nodes with a degree $\rho(C) > 2$	40
3.3.3. New internal energy at end points	44
3.3.4. Synthetic example	46
3.4. Implementation	48
3.4.1. Realization	48
3.4.2. Topology-preserving energy	48
3.4.3. Parameters	50
3.5. Discussion	51

4. Results and analysis	53
4.1. Goals of the analysis	53
4.2. Synthetic examples	55
4.2.1. Analysis of the initialization requirements	55
4.2.2. Analysis of the parameter control	59
4.2.3. Analysis of the iteration behavior	65
4.2.4. Analysis of the topology	68
4.2.5. Discussion of the results	72
4.3. Delineation of field boundaries	73
4.3.1. Model, strategy and initialization	73
4.3.2. Results and evaluation of the delineation of field boundaries	75
4.3.3. Discussion of the results	80
4.4. Delineation of cells	81
4.4.1. Model, strategy and initialization	81
4.4.2. Results and evaluation of the delineation of cells	83
4.4.3. Discussion of the results	85
5. Discussion and outlook	87
5.1. Discussion	87
5.2. Outlook	88
References	91
Curriculum Vitae	101
Acknowledgements	102

List of figures

Figure 1: Examples delineating networks depicting the boundaries between adjacent objects	12
Figure 2: Definitions concerning active contour models	16
Figure 3: Parametric active contour: initialization (blue), optimization (gray) and result (red)	19
Figure 4: Geometric active contours: embedded contour as zero level line (red) in the image and height map of the level set function	21
Figure 5: Geometric active contours: change of the topology	22
Figure 6: Two synthetic examples representing networks and adjacent objects	35
Figure 7: Delineating adjacent objects with traditional parametric active contours: initialization (blue), result and zoomed result part (red).....	36
Figure 8: Requirements for network snakes: image energy (left), initialization and topology (right).....	37
Figure 9: Influence of the topology to the internal energy of the energy functional	40
Figure 10: Topology for network snakes	41
Figure 11: Delineating adjacent objects with network snakes: initialization (blue), result and zoomed result part (red); dashed contour part (light red) as comparison to traditional parametric active contours shown in Figure 7	47
Figure 12: Delineating adjacent objects with network snakes: initialization (blue), optimization steps (white) and result (red) of Figure 11	47
Figure 13: Traditional parametric active contours: initialization (blue), optimization steps (white) and result (red)	49
Figure 14: Parametric active contours with topology-preserving energy: initialization (blue), optimization steps (white) and result (red).....	49
Figure 15: Synthetic example with different image energies: original image (left), gradient vectors (center) and distance vector field (right).....	56
Figure 16: Correct initialization of network snakes: initialization (blue), optimization steps (white) and result (red)	57
Figure 17: Critical initialization of network snakes: initialization (blue), optimization steps (white) and result (red)	57
Figure 18: Wrong initialization of network snakes: initialization (blue), optimization steps (white) and result (red)	57
Figure 19: Initialization of network snakes exploiting the topology: initialization (blue), optimization steps (white) and result (red).....	58
Figure 20: Critical initialization of network snakes exploiting the topology: initialization (blue), optimization steps (white) and result (red)	58

Figure 21: Ideal parameter control of network snakes: initialization (blue), optimization steps after 50, 150 and 400 iterations (white) and result (red).....	61
Figure 22: Results of different parameter settings a) – e) to control the internal energy $E_{int}(C(s))$ of network snakes (cf. Table 2): the ideal <i>relative</i> weight of the parameters α and β is displayed in the center	62
Figure 23: Results of different parameter settings a) – e) to control the internal energy $E_{int}(C(s))$ of network snakes (cf. Table 3): the ideal <i>absolute</i> weight of the parameters α and β is displayed in the center	62
Figure 24: Influence of the absolute distance between neighboring nodes C to the parameter control of the internal energy.....	63
Figure 25: Results of different parameter settings a) – e) to control the weight between the internal energy $E_{int}(C(s))$ and the image energy $E_{img}(C(s))$ of network snakes (cf. Table 4): the ideal weight of the parameter κ is displayed in the center	64
Figure 26: Iteration behavior of different parameter settings a) – e) to control the step size γ of network snakes (cf. Table 5): the ideal weight of the parameter γ is displayed in the center.....	65
Figure 27: Iteration behavior of network snakes depicted after 750 iterations of different parameter variations concerning the step size γ	66
Figure 28: Two different strategies to speed up the iteration behavior of network snakes: starting with a step size $\gamma = 15$ (left, white) the final optimization is achieved after 1400 iterations (left, red); starting with $\kappa = 0.5$ (right, white) the final optimization is achieved after 850 iterations (right, red)	67
Figure 29: Optimization of network snakes exploiting a wrong topology with one surplus contour part: initialization (blue), optimization steps (white) and result (red)	69
Figure 30: Optimization of network snakes exploiting a wrong topology with two surplus contour parts: initialization (blue), optimization steps (white) and result (red)	69
Figure 31: Optimization of network snakes exploiting a wrong topology with one missing contour part: initialization (blue), optimization steps (white) and result (red)	70
Figure 32: Optimization of network snakes exploiting a wrong topology with two adjacent missing contour parts: initialization (blue), optimization steps (white) and result (red)	70
Figure 33: Impact of the topology to slightly fragmented object representations in the imagery, white blobs represent holes in the image energy: initialization (blue), optimization steps (light gray) and result (red)	71
Figure 34: Impact of the topology to strongly fragmented object representations in the imagery, white blobs represent holes in the image energy: initialization (blue), optimization steps (light gray) and result (red)	71
Figure 35: IKONOS CIR-image (1000×1000 pixel)	74
Figure 36: Evaluation of the initial segmentation: correctly segmented initial field boundaries (green), missing initial boundaries (red) and falsely segmented boundaries (blue).....	74
Figure 37: Initialization for network snakes using the initial segmentation	76
Figure 38: Final result of the delineation of field boundaries using network snakes	76

Figure 39: Initialization for network snakes using shifted segmentation	77
Figure 40: Final result of the delineation of field boundaries initialized with shifted segmentation	77
Figure 41: Detail of the utilization of network snakes shown in Figure 37 and Figure 38 using the correct initial segmentation: initialization (blue), optimization steps superimposed to the image energy after 10, 50 and 100 iterations (white) and final result (red)	79
Figure 42: Detail of the utilization of network snakes shown in Figure 39 and Figure 40 using the shifted initial segmentation: initialization (blue), optimization steps superimposed to the image energy after 10, 50 and 100 iterations (white) and final result (red)	79
Figure 43: Detail of the utilization of network snakes shown in in Figure 37 and Figure 38: initialization (blue), optimization steps superimposed to the image energy after 10, 50 and 100 iterations (white) and final result (red)	80
Figure 44: Detail of the utilization of network snakes shown in Figure 37 and Figure 38: initialization (blue), optimization steps superimposed to the image energy after 10, 50 and 100 iterations (white) and final result (red)	80
Figure 45: Cell nuclei and microscopic cell imagery (200×200 pixel)	82
Figure 46: Cell nuclei with derived initialization (depicted in blue) and superimposed to the microscopic cell imagery	82
Figure 47: Initialization (blue) and final result of the delineation of cells using network snakes (red)	83
Figure 48: Detail of the utilization of network snakes shown in Figure 47 to demonstrate the general functionality: initialization (blue), optimization steps superimposed to the image energy after 20, 100 and 200 iterations (white) and final result (red)	84
Figure 49: Detail of the utilization of network snakes without the utilization of the topology-preserving energy: initialization (blue), optimization steps superimposed to the image energy after 20, 100 and 200 iterations (white) and final result (red).....	84
Figure 50: Detail of the utilization of network snakes shown in Figure 47 utilizing the topology-preserving energy: initialization (blue), optimization steps superimposed to the image energy after 20, 100 and 200 iterations (white) and final result (red)	84

List of tables

Table 1: Comparison of parametric and geometric active contours	23
Table 2: Parameters of Figure 22 to control the <i>relative</i> weight of the parameters α and β of the internal energy.....	62
Table 3: Parameters of Figure 23 to control the <i>absolute</i> weight of the parameters α and β of the internal energy.....	62
Table 4: Parameters of Figure 25 to control the weight of parameter κ between the internal energy $E_{int}(C(s))$ and the image energy $E_{img}(C(s))$	64
Table 5: Parameters of Figure 26 to control the step size γ of the energy functional of network snakes.....	65
Table 6: Parameters of Figure 27 to control the iteration behavior of the energy functional of network snakes with a varying step size γ and the total number of required iterations.....	66
Table 7: Quality measures before and after the optimization with network snakes	78
Table 8: Quality measures before and after the optimization with network snakes initialized with shifted segmentation	78
Table 9: Quality measures before and after the optimization with network snakes	83

1. Introduction

1.1. Motivation

The goal of *computer vision* is to interpret the world around us obtaining information from imagery and to simulate the human perception with a computer [BALLARD AND BROWN 1982, SHAPIRO AND STOCKMANN 2001, FORSYTH AND PONCE 2002]. Computer vision is one of the most challenging areas of research developed in the last decades with enormous potential for a large variety of applications for reconstruction, detection, recognition and extraction of objects from imagery.

One crucial point to extract information from imagery automatically is *image segmentation*. Traditionally, image segmentation is defined as the partitioning of an image into non-overlapping regions to simplify the representation of an image into more meaningful regions, different aspects of image segmentation are discussed for example in [ROSENFELD AND DAVIS 1979, GURARI AND WECHSLER 1982, HARALICK AND SHAPIRO 1985, ROSIN 1998]. The borderline of image segmentation as a basis for providing a subsequent decision-making process to derive objects is not exactly defined, because an increasing incorporation of modeled knowledge can blur the step of image segmentation to object extraction.

Active contour models are a powerful, physics-based technique which can be employed in various steps during object extraction for segmentation, reconstruction, registration, recognition and manipulation of non-rigid curves or surfaces from images and image sequences. The so-called *snakes* were introduced as a first contribution to this research field with the seminal paper by [KASS ET AL. 1988]. Active contour models are used in computer vision and computer graphics, but are also suitable for image segmentation tasks. The innovation of the method is to bridge the gap between low-level feature extraction or segmentation and high-level geometric representation of objects. The main contribution and success of the method is the mathematical combination of image data with prior modeled object knowledge concerning the shape behavior or movement of the objects during an optimization process. Active contour models can be regarded as a method to delineate subjective contours or surfaces [KANIZSA 1976, SARTI ET AL. 2002], i.e. deriving good results even though the objects of interest are only partly represented in the imagery.

Two directions of active contour models have been developed as complements to each other: the first proposed model of *parametric active contours* [KASS ET AL. 1988] and the later introduced model of *geometric active contours* [CASELLES ET AL. 1993, MALLADI ET AL. 1995]. The idea behind both concepts is quite similar: the coupling of the image data with an internal energy in an energy minimization framework regarding parametric active contours or the combination of the level set method with the curve evolution theory concerning geometric active contours. The common goal of both approaches is to model and control a smooth curve to delineate non-rigid object contours.

Active contour models have received a vast attention in the last two decades, as reflected in numerous contributions comprising further developments and various applications, for an overview see for example [BLAKE AND ISARD 1998, OSHER AND PARAGIOS 2003]. Different applications using active contour models have been investigated, for example concerning the detection of man-made objects such as roads [LAPTEV ET AL. 2000, PETERI ET AL. 2003] and buildings [FUA 1995], the tracking of objects in image sequences [DELAGNES ET AL. 1995, PARAGIOS AND DERICHE 2000a] or medical image applications [MCINERNEY AND TERZOPOULOS 1996, SINGH ET AL. 1998].

Originally, both concepts of active contour models were only defined for single *closed* object boundaries. Newer research deals with the development of multiple and coupled active contours to facilitate solutions dealing with more than one object and tackle the problem of partially touching objects. But, there is still the need to deepen the understanding concerning the delineation of adjacent objects, which are separated by only a single boundary and, in addition, to develop solutions which enable the delineation of networks.

1.2. Goals of the thesis

The main goal of the thesis is the development of a new method of active contour models that enables the delineation of arbitrary graphs representing *networks* and the *boundaries between adjacent objects* with a clearly defined mathematical model. Potential applications are the delineation of road networks or field boundaries from remotely sensed imagery, bio-medical tasks such as the delineation of adjacent biological cells in microscopy cell imagery or industrial applications. Examples illustrating networks depicting the boundaries of adjacent objects are shown in Figure 1.

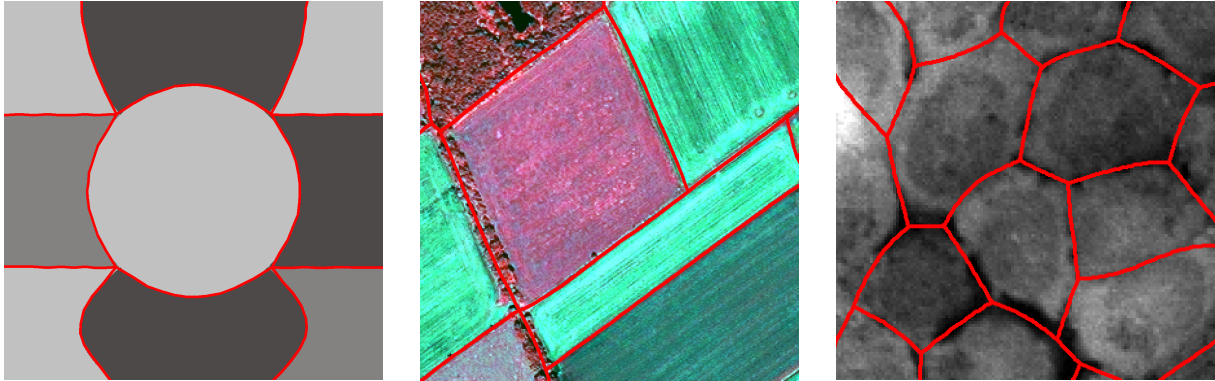


Figure 1: Examples delineating networks depicting the boundaries between adjacent objects

Three sub-goals of the thesis are defined as follows:

- Development of a new method of active contour models which optimizes graphs consisting of nodes of an arbitrary degree to enable the delineation of open contours, closed contours and any networks.
- Development of a new method of active contour models which segments imagery without gaps or overlaps to enable the delineation of adjacent objects or networks.
- Development of a new method of image segmentation and object delineation with a high generality and transferability to enable its applicability for a variety of tasks.

The proposed new method is called *network snakes*. This term was already used in the work of [FUA 1995, FUA ET AL. 1999], but the authors introduce a kind of network with particular constraints only applicable to reconstruct the edges of buildings. In contrast, the goal of this thesis is to develop for the first time a general and comprehensive method with a *clear mathematical model* enabling a free movement of all nodes and edges of a graph during the optimization without any particular constraints.

The aim of the thesis is not just to enable the optimization of nodes with arbitrary degrees to delineate networks and the boundaries between adjacent objects, but also to introduce and exploit the *topology* explicitly during the optimization. The proposed new method of network snakes is implemented with the concept of parametric active contours. This model needs an initialization to start the optimization process of the energy functional. In addition, the exploitation of the topology during the optimization requires a given topology which is assumed to be correct. The strategy behind this concept of active contour models can be divided into two parts: first, a global overview of the scene is derived yielding the coarse structure or topology and, afterwards, this prior information is exploited to detect the details accomplished within the proposed new method with the geometrical refinement of the scene in a comprehensive mathematical model.

An important goal of the new method of network snakes is the *generality* and *transferability* of the solution not only being developed for a specific application, but to delineate arbitrary networks and the boundaries of arbitrary adjacent objects. Two real application scenarios are chosen to demonstrate the transferability of the new method: the delineation of field boundaries from remotely sensed images and the delineation of adjacent biological cells in microscopic cell images. The detection of field boundaries is an important task for the geosciences and the agricultural sector, for example the derivation of field-based risks of soil loss, precision

farming or the monitoring of subsidies. The detection of cells and their derived properties regarding shape, size and intensity distribution is an increasing task for bio-medical research such as pharmaceutical drug discovery. Both examples are chosen to demonstrate the transferability to different applications and, moreover, both examples are well-suited to point out the impact of the proposed new method of network snakes. In particular, the combination of image data with shape behavior and the exploitation of topology can improve the results of these applications compared to the state of the art.

Active contour models have been investigated concerning remote sensing applications, see for example [GÜLCH 1995, FUA 1995, GRÜN AND LI 1997], and concerning bio-medical applications, confer for an overview [SONKA AND FITZPATRICK 2000, SURI ET AL. 2002, MALLADI 2002]. However, the development of a general method satisfying the stated goals of this thesis has so far not been obtained, which not only points out the methodical contribution and relevance, but also emphasizes the impact to different real application scenarios.

1.3. Organization of the thesis

This chapter introduces the topic of the thesis to motivate the defined goals. The organization of the thesis is structured as follows:

In the subsequent Chapter 2, the basics and state of the art concerning active contour models are given to provide the fundamentals required for the new developments presented in this thesis. First, general terms and definitions are shortly introduced and the mathematical definitions of parametric and geometric active contours are given and compared to each other. In addition, the state of the art concerning the concepts relevant to the proposed new method of network snakes is presented. The section is completed with a discussion of the unutilized potential of active contour models and a discussion regarding which concept is suitable to reach the goals of this thesis. Second, the minimization of the energy functional representing parametric active contours is described in detail, which is required for the new developments given in Chapter 3. Third, related work concerning possible applications using network snakes such as the extraction of field boundaries from high resolution satellite imagery and the delineation of adjacent biological cells in microscopy cell imagery is discussed.

In Chapter 3, the new method of network snakes is developed and presented. First, the stated goals of this thesis are taken up to specify the new developments necessary for the current unsolved problems and to identify the challenges related to the work. Second, the requirements concerning the imagery, initialization and topology are discussed to define the framework for the proposed new method of network snakes. Third, the new terms of the energy functional for the chosen concept of parametric active contours are evolved and the new mathematical model is described in detail resulting in network snakes. Afterwards, some general implementation questions regarding the realization of the system, the introduction of the optional topology-preserving energy and the general control of the parameters are examined and illustrated. The chapter is completed with a discussion of the proposed new method of network snakes to highlight the derived achievements.

In Chapter 4, the developed new method of network snakes is analyzed and evaluated. The objective is to point out to which extent the new method can facilitate the established goals and requirements. First, the aims of the analysis are expounded to define the different relevant topics concerning the investigations and their relations to each other. In addition, a framework is specified for the realization of the analysis and evaluation. Second, the general contents of the analysis concerning the initialization requirements, the parameter control, the iteration behavior and the topology are implemented with exemplary synthetic data to emphasize the benefits and limitations of the proposed new method of network snakes. Special attention is given to the introduction of topology to analyze the contribution and effects on the other investigated contents. Third, the generality and usability is demonstrated with results and their analysis of a real application scenario regarding the delineation of field boundaries from high-resolution optical satellite imagery. Fourth, the transferability of the new method of network snakes to different applications is exemplified with the delineation of adjacent cells in medical image data discussing and evaluating the derived results.

In Chapter 5, the developed method of network snakes is discussed considering the stated goals of this thesis to give a concluding evaluation of the proposed new method. Finally, open and unsolved problems and possible further investigations are pointed out in the outlook.

2. Basics and state of the art

In this chapter the basics and state of the art concerning active contour models are given to provide the fundamentals required for the new developments presented in this thesis. First, general terms and definitions are shortly introduced and, afterwards, the mathematical definitions of parametric and geometric active contours are given and compared to each other. In addition, the state of the art concerning active contour models is presented including the basic developments and the latest research relevant to the proposed new method of network snakes. The section is completed with a discussion of the unutilized potential of active contour models and a discussion on why only the concept of parametric active contours is suitable to reach the stated goals of this thesis. Second, the minimization of the energy functional representing parametric active contours is described in detail. The mathematical basics of the energy minimization are required for the new developments introduced in Chapter 3, because the introduction of the topology to the energy functional enabling the optimization of nodes with arbitrary degree is the core of the proposed new method of network snakes. Third, related work concerning possible applications using network snakes such as the extraction of field boundaries from high resolution satellite images and the delineation of adjacent biological cells in microscopic cell images is discussed. The aim is to point out the generality and transferability of the developed new method of network snakes and to demonstrate the contribution to solving these problems.

2.1. Active contour models

2.1.1. Terms and definitions

The general terms and definitions used in this thesis are briefly summarized in this section. Active contour models have received large popularity during the last two decades, for an overview see for example [BLAKE AND ISARD 1998, SINGH ET AL. 1998, OSHER AND PARAGIOS 2003]. Varying definitions have been introduced, the terms and definitions used here are based on the initial considerations introduced by [KASS ET AL. 1988] and [CASELLES ET AL. 1993, MALLADI ET AL. 1995] concerning parametric and geometric active contours, respectively. Furthermore, the required definitions regarding the proposed new method of network snakes are introduced below.

Representation of contours

In Euclidean space \mathbb{R}^2 a *contour* C is defined as a continuous curvilinear object represented in form of a vector model. Vector models contain the geometric information within the *points* C_i with $i = 0, \dots, n \in \mathbb{N}$ and the topological information within the *line segments* L_j with $j = 0, \dots, n-1 \in \mathbb{N}$ connecting the points. Points are defined as coordinate pairs, for example (x, y) in \mathbb{R}^2 . The contour C can be represented as an arbitrary polynomial or spline, but is often approximated by a list of points connected with straight line segments. Besides linear objects $C_{0 \dots n}$, where $C_0 \neq C_n$, representing *open contours*, area objects can be represented by *closed contours* $C_{0 \dots n}$, where $C_0 = C_n$, i.e. with an identical first and end point of the contour.

The aim of active contour models is to let a contour evolve in an *image* I achieving the delineation of an object. In contrast to the definition of the contour in Euclidean space, the image I is represented in discrete space to enable further digital processing. The image is defined by a two-dimensional regular grid in \mathbb{N}^2 , the smallest element is a *pixel* (picture element). The size of the pixels is the limiting factor representing the objects in discrete space. In general, objects should fulfill the Nyquist theorem, i.e. the highest frequency of the imaging system should be sampled more than twice by the pixel spacing.

Graph and topology

A graph consists of a set of *nodes*¹ and *edges* that connect various pairs of nodes, which is a similar definition to the one given above concerning contours. Active contour models can be represented by a graph, in particular to represent topological characteristics of a *contour network*, which is an important requirement of this thesis. The *topology* of the contour can be represented within a graph consisting of nodes, which are characterized by the *degree of nodes* $\rho(C)$. An example is shown in Figure 2: nodes with a degree $\rho(C) = 1$ represent *end points* of a contour, nodes with a degree $\rho(C) = 2$ represent a normal part of a contour and nodes with a degree $\rho(C) > 2$ represent nodes in which more than two edges terminate. In this thesis, the contour network is represented by a *planar graph*, i.e. it can be drawn in a plane without crossing graph edges. Having the possibility to distinguish between different *contour parts*, particularly when forming a network, each part of the whole contour is indexed as C_A, C_B, \dots, C_Z (cf. the red segment C_A in Figure 2 for an example of a contour part). The nodes with a degree $\rho(C) \neq 2$ define the start or end points of the contour parts.

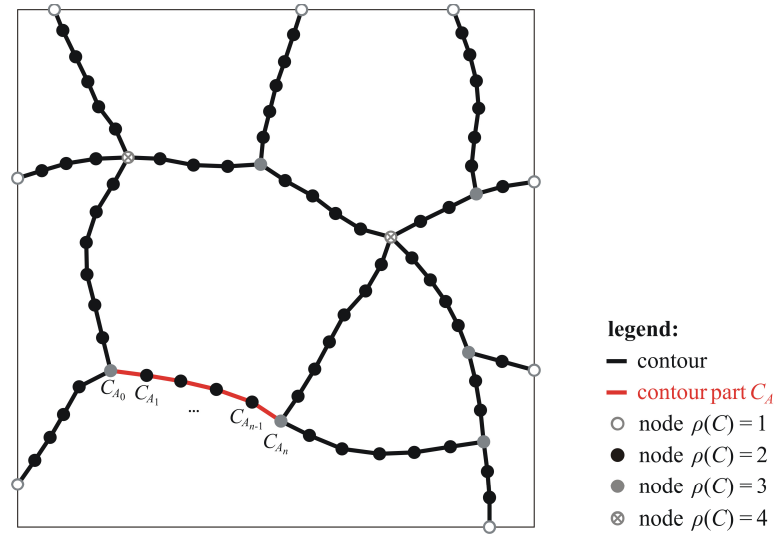


Figure 2: Definitions concerning active contour models

2.1.2. Basics

2.1.2.1. Parametric active contours

As mentioned before, active contour models have received much attention with the seminal paper by [KASS ET AL. 1988], which earlier appeared as [KASS ET AL. 1987]. In addition to this highly referenced paper, further developments by the authors have to be referred to in this context [TERZOPOULOS 1986, TERZOPOULOS ET AL. 1987a, TERZOPOULOS ET AL. 1987b, TERZOPOULOS AND FLEISCHER 1988], a detailed discussion of the literature is given in Section 2.1.3.2. All these contributions have in common a *parametric* representation of active contour models, whose mathematical basics are described in this section.

A traditional parametric active contour, often called a *snake*, is defined as a parametric curve C

$$C(s) = (x(s), y(s)) , \quad (1)$$

where $s \in [0,1]$ is the arc length, and x and y are the coordinates of a closed 2D-curve. The extension to a 3D-curve is straightforward, but is not considered here. The core of active contour models is to let the curve C evolve in an image I delineating the object of interest. This aim is reached by setting and minimizing an

¹ In literature, the term *vertex* is sometimes used as synonym for a *node* of a graph, where two or more edges terminate, cf. for example [HARARY 1994]. Here, the term *node* is generally used and, if required, the degree is added.

appropriate *energy functional* $E(C(s))$, which comprises all necessary energies or costs [KASS ET AL. 1988]:

$$\begin{aligned} E(C(s)) &= \int_0^1 E_{curve}(C(s)) ds \\ &= \int_0^1 [E_{img}(C(s)) + E_{int}(C(s)) + E_{con}(C(s))] ds \end{aligned} \quad (2)$$

$$E(C(s)) \rightarrow \min .$$

The energy functional consists of the *image energy* $E_{img}(C(s))$ representing an optimal description of the object of interest in the image, the *internal energy* $E_{int}(C(s))$ introducing modeled object knowledge concerning the shape and movement behavior of the object and, finally, the *constraint energy* $E_{con}(C(s))$ giving the possibility to insert any external constraints to the energy functional. The minimization of the energy functional $E(C(s))$ is accomplished with an iterative processing starting from an initialization, details are presented in Section 2.2. The three energy terms are explained below in detail.

Image energy

The image energy $E_{img}(C(s))$ describes the object of interest in the image I in an optimal manner, where optimal description means an image function that lets the contour C be attracted by salient features in the image representing the boundaries of the object of interest. In the simplest way, the image energy can be expressed by the image intensities itself with

$$E_{img_{line}}(C(s)) = I(C(s)) \quad (3)$$

to detect light or dark *lines*, depending on the negative or positive sign of the image function, respectively. When the object of interest is characterized by *edges*, the image energy can be defined as

$$E_{img_{edge}}(C(s)) = -|\nabla I(C(s))|^2, \quad (4)$$

where $|\nabla I(C(s))|$ is the norm or magnitude of the gradient image at the coordinates $x(s)$ and $y(s)$. The negative sign results in an attraction of the contour to large image gradients during energy minimization. A further possible image energy is the termination energy in order to find *terminations* of line segments, i.e. end parts of lines, and corners using the curvature of level lines in the image. The termination energy is defined as

$$E_{img_{term}}(C(s)) = \frac{\partial \theta(C(s))}{\partial n_{\perp}(C(s))}, \quad (5)$$

where $\theta(C(s)) = \tan^{-1}(I_y/I_x)$ is the gradient angle and $n_{\perp}(C(s)) = (-\sin \theta, \cos \theta)$ is the unit vector perpendicular to the gradient direction. In addition to the initially defined image energies $E_{img}(C(s))$ by [KASS ET AL. 1988] several other energy terms were introduced to represent the object boundaries within an image: one example is *texture boundaries* [YHANN AND YOUNG 1995, WONG AND WONG 2004], another one is the *standard deviation* of the image intensities within a quadratic mask [BUTENUTH 2007].

A strategy to enhance the utilization of the image energy is the convolution of the image I with a Gaussian kernel G_{σ} , where σ is the standard deviation. One effect of a large σ is a smoothed image and an increase of the capture range of the contour to allow for coarser initializations and/or a faster iteration behavior taking into account blurry object boundaries. A second effect is the elimination of nearly insignificant features which often prevent the motion of the contour towards the positions with lower image energy during the minimization process corresponding to the more salient image features. An approach to be utilized in this context to improve the image energy is the *scale-space theory* introduced by [LINDBERG 1990, LINDBERG 1994].

An alternative image energy that significantly increases the capture range while preserving accurate image boundaries compared to the image energy definition quoted above is the *distance potential force* introduced by

[COHEN AND COHEN 1993]. A *distance map* $d(x,y)$ is derived by calculating the Euclidean distance [DANIELSSON 1980] or Chamfer distance [BORGEFORS 1984] between each pixel and the closest prior extracted edge point (edge map). An appropriate potential energy $P_{dist}(C(s))$ can be defined as

$$P_{dist}(C(s)) = -e^{-d(C(s))^2}, \quad (6)$$

and the corresponding image energy is given by

$$E_{img_{dist}}(C(s)) = -|\nabla P_{dist}(C(s))|. \quad (7)$$

Thus, the contour is always attracted by the nearest boundary in the image and does not remain in uniform image parts.

Another image energy improving the distance map is the *gradient vector flow* (GVF), which aims to overcome the general problem of concave boundary regions, identified in [NEUENSCHWANDER ET AL. 1994a] and [DAVATZIKOS AND PRINCE 1995]. This problem is addressed in [XU AND PRINCE 1997, XU AND PRINCE 1998]: starting from an edge map $f(x,y)$ computed from an image, the image energy $E_{img}(C(s))$ is defined as a non-irrotational vector field $V(x,y) = (u(x,y), v(x,y))$, which minimizes the energy functional

$$E_{img_{GVF}}(C(s)) = \iint \mu(u_x^2 + u_y^2 + v_x^2 + v_y^2) + |\nabla f|^2 |V - \nabla f|^2 dx dy, \quad (8)$$

where μ is a parameter to regularize the trade off between the first and second term. The formulation causes the desired effect of keeping $V(x,y)$ nearly equal to the gradient of the edge map $f(x,y)$ when it is large, but forcing the vector field to vary in homogeneous regions of the image. These regions are filled with interpolated values from the boundaries of the region in a kind of competition among the boundary vectors. Therefore, the GVF image energy allows the delineation of concave object boundaries and has a large capture range causing a relative insensitivity to the initialization.

To conclude, the choice of the image energy or the combination of different terms depends on the application and the characteristics of the object of interest, a short overview of approaches is given in Section 2.1.3.2. The objective is to obtain a distinctive representation of the boundary of the object of interest within the image to attract the contour toward the desired object boundary during energy minimization.

Internal energy

The second term of the energy functional representing the active contour model is the internal energy $E_{int}(C(s))$. The aim is to incorporate modeled prior knowledge about the shape characteristics or movement of the object of interest during the energy minimization. Thus, a geometric representation of the object boundaries can be exploited when optimizing the contour within complex image domains, for example disturbed by noise or occlusions. The internal energy $E_{int}(C(s))$ is defined as

$$E_{int}(C(s)) = \frac{1}{2} \left(\alpha(s) \cdot |C_s(s)|^2 + \beta(s) \cdot |C_{ss}(s)|^2 \right), \quad (9)$$

where C_s and C_{ss} are the first and second derivatives of C with respect to s [KASS ET AL. 1988]. The internal energy can be regarded as a controlled continuity spline being a generalization of a Tikhonov stabilizer [TIKHONOV 1963] while regularizing the ill-posed problem of contour delineation [POGGIO ET AL. 1985]. The first term of the internal energy, weighted by $\alpha(s)$, controls the elasticity or tension of the curve. Large values of $\alpha(s)$ allow the contour to become very straight between two points and hamper stretching, while small values allow a higher bending. The second term of the internal energy, weighted by $\beta(s)$, controls the rigidity of the curve. Large values of $\beta(s)$ let the contour become smooth, and small values allow the generation of corners. The terms $\alpha(s)$ and $\beta(s)$ need to be predefined based on the modeled shape characteristics of the object of interest, often they are fixed during optimization.

Constraint energy

The energy functional of active contour models can optionally incorporate constraint energy terms to consider particular conditions. For example, a typical requirement could be the interaction with the active contour model within a user-aided system to define landmark points P_{lm} , where the contour has to be pushed. This constraint energy $E_{con}(C(s))$ can be defined as

$$E_{con}(C(s)) = -k|P_{lm} - X_c|^2, \quad (10)$$

where X_c is a point on the contour C and k is a positive parameter to weigh the constraint energy compared to the other energy terms of the whole energy functional. This constraint energy can be regarded physically as a spring to minimize the distance between a particular point and the contour. A further possible constraint is to fix a point, for example an end point of an open contour to the image border or an arbitrary context object.

Further possibilities to affect the active contour model are additional energy terms incorporating prior knowledge. One example is the *balloon model* using a pressure force to inflate or deflate the closed contour model to increase the capture range and allow for initializations quite far from the object boundary. This additional energy term $E_{bal}(C(s))$ is defined as

$$E_{bal}(C(s)) = n_{\perp}(s), \quad (11)$$

where n_{\perp} is the inward unit normal of the model [COHEN 1991]. It must be known whether the contour is inside or outside the object of interest to choose the sign of the unit normal vector. Since the additional energy term is independent from the image energy, the pressure force can cause an unwanted jump over object boundaries, which are represented only by weak image features. On the other hand, the balloon model enables the use of an inside or outside initial contour not close to the object boundary.

Example of a parametric active contour

An example of a parametric active contour is given in Figure 3: the underlying binary image is taken from the seminal paper of [KASS ET AL. 1988] to demonstrate the general functionality of parametric active contours to delineate subjective contours [KANIZSA 1976]. Starting from an arbitrary initialization close to the object boundary (depicted in blue), the contour moves automatically to the expected object boundary exploiting the image and internal energy during the minimization process (time steps are depicted in gray). The final result represents a subjective contour (depicted in red), even though there is in parts no image information given. In particular at the parts of the image where no salient image features can support the optimization, the internal energy controls the shape behavior of the contour.

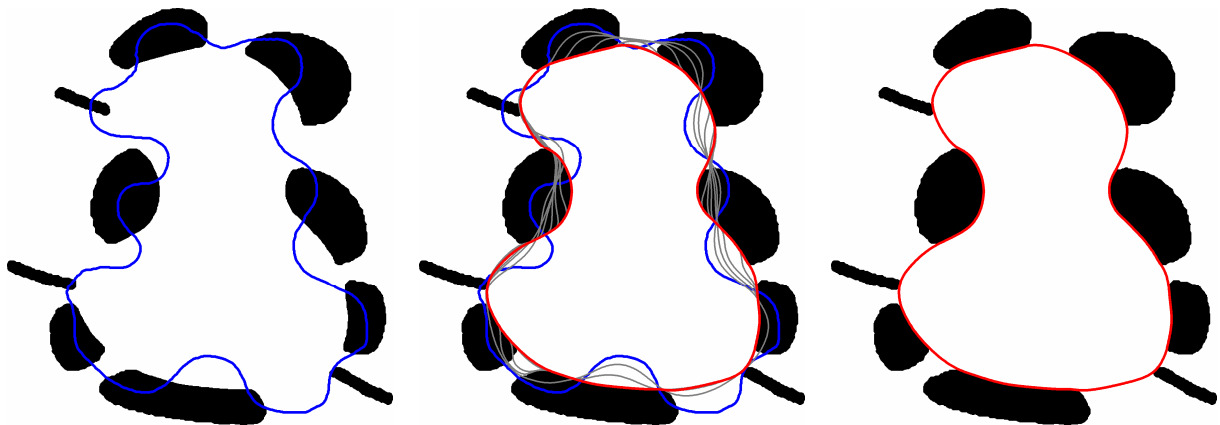


Figure 3: Parametric active contour: initialization (blue), optimization (gray) and result (red)

2.1.2.2. Geometric active contours

Geometric active contours have been developed as a complement to parametric active contours (cf. Section 2.1.2.1), independently proposed by [CASELLES ET AL. 1993] and [MALLADI ET AL. 1993, MALLADI ET AL. 1994, MALLADI ET AL. 1995]. The main difference between geometric active contours and parametric ones is the implicit representation of the curve C as a level line within a higher-dimensional embedding *level set function* Φ . In particular, the curve is only evolved using *geometric* measures, i.e. shape measures, resulting in an evolution that is independent of the parameterization and enables topological changes in a natural manner.

The fundamental concept of geometric active contours is to combine the *curve evolution theory* as discussed in [KIMIA ET AL. 1990, SAPIRO AND TANNENBAUM 1993, KIMMEL ET AL. 1995], i.e. describing the shape behavior or movement of the curve during the evolution, and the *level set method* as introduced in [DERVIEUX AND THOMASSET 1979, DERVIEUX AND THOMASSET 1981] and later reinvented in [OSHER AND SETHIAN 1988], i.e. coupling the curve to the image data. Both concepts are first defined below, before the implementation of geometric active contours is presented.

Curve evolution theory

A closed curve $C(s,t)$, such as defined in Equation 1, is the starting point of geometric active contours. The curve evolution theory is based on the partial differential equation

$$\frac{\partial C}{\partial t} = F(\kappa) n_{\perp} , \quad (12)$$

where $F(\kappa)$ is a *speed function* depending on the curvature κ of the contour, and n_{\perp} is the inward unit normal, for instance see [KIMIA ET AL. 1990, KIMIA ET AL. 1992]. The goal is to let the curve evolve along its normal direction with a specific speed. One possibility of curve evolution depending only on the *curvature* is defined by

$$\frac{\partial C}{\partial t} = \alpha \kappa n_{\perp} , \quad (13)$$

where α is a positive constant. The effect of the above definition is a kind of elasticity resulting in a smooth curve, i.e. highly curved contour parts will move faster than moderately curved parts. This behavior results in a circular blob and finally in a round point [GAGE 1984, GRAYSON 1987]. A second possibility of curve evolution is the use of a *constant* deformation defined by

$$\frac{\partial C}{\partial t} = F_0 n_{\perp} , \quad (14)$$

where F_0 is a constant advection component determining the speed of deformation. This characterization of the speed function is similar to a pressure force used in the balloon model of parametric active contours (cf. Section 2.1.2.1).

The evolution of the curve C depends only on geometric measures, either on a curvature or a constant deformation term, but mostly a combination of both terms is used. The goal of geometric active contours is to couple the speed of deformation to the image data yielding the boundaries of the objects of interest within the image domain.

Level set method

The connection of the evolving curve to the image data is achieved with the level set method, in which the curve is implicitly represented within a time-depending higher dimensional level set function Φ , for example see [OSHER AND SETHIAN 1988, SETHIAN 1989, SETHIAN 1996a]. The contour $C(s,t)$, such as defined in Equation 1, is represented within the level set function $\Phi(x,y,t)$ as zero level line (cf. Figure 4, red line):

$$\Phi(C(s, t), t) = 0 . \quad (15)$$

Differentiating Equation 15 with respect to t and using the chain rule the following equation is derived:

$$\frac{\partial \Phi}{\partial t} + \nabla \Phi \frac{\partial C}{\partial t} = 0 , \quad (16)$$

where $\nabla \Phi$ is the gradient of Φ . The inward unit normal n_{\perp} is defined as $n_{\perp} = -\nabla \Phi / |\nabla \Phi|$, i.e. Φ is assumed to be negative inside and positive outside the zero level set. Using Equation 12 and the definition of the n_{\perp} , Equation 16 can be rewritten yielding the evolution equation

$$\frac{\partial \Phi}{\partial t} = F(\kappa) |\nabla \Phi| , \quad (17)$$

where the curvature κ is derived from $\kappa = \nabla \cdot (\nabla \Phi / |\nabla \Phi|)$. Thus, the contour can be evolved using the level set method.

There are some considerations to be taken into account when implementing the geometric active contours: the initial level set function $\Phi(x, y, t = 0)$ must be defined in a way that the zero level line matches the initial contour (cf. Figure 4, zero level line is depicted in red). A common initial condition is a signed distance function to an initially given curve

$$\Phi(x, y, 0) = \pm d(x, y) , \quad (18)$$

where $d(x, y)$ is the signed distance between the grid point and the zero level line.

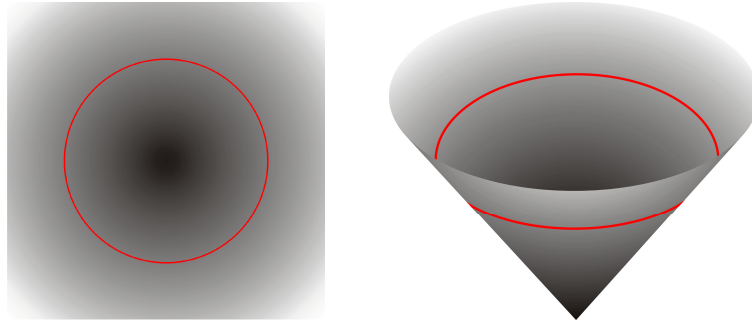


Figure 4: Geometric active contours: embedded contour as zero level line (red) in the image and height map of the level set function

One of the challenges using geometric active contours is the design of the *speed function* F . The difficulty is to reach the object boundary, even if the initial contour is far away and noise or disturbances hamper the evolution, and to avoid a jump over the boundary. One possibility is the introduction of a stopping term c [CASELLES ET AL. 1993, MALLADI ET AL. 1995]:

$$\frac{\partial \Phi}{\partial t} = c F(\kappa) |\nabla \Phi| , \quad (19)$$

with

$$c = \frac{1}{1 + |\nabla (G_{\sigma} * I)|} . \quad (20)$$

The contour reduces the speed at high image gradients, but particularly when the contrast is low or the boundary is blurry or fragmented, the contour can fail to stop and, thus passes the object boundary. A partly different approach is to define an energy concept in order to minimize a weighted length as proposed in [KICHENASSAMY ET AL. 1995, KICHENASSAMY ET AL. 1996] and is known as *geodesic active contours* [CASELLES ET AL. 1997]:

$$\frac{\partial \Phi}{\partial t} = c F(\kappa) |\nabla \Phi| + \nabla c \cdot \nabla \Phi . \quad (21)$$

The design of the function includes an extra term compared to Equation 19 to increase the attraction of the contour towards the desired object boundary, but the contour can also be pulled back if it passes the boundary. In addition to the presented speed functions above, further developments on the design of speed functions have been carried out, an overview is presented in [SETHIAN 1996a]. Furthermore, a short overview of approaches is given in Section 2.1.3.3.

Finally, a solution of geometric active contours can be derived by setting the evolution equation given in Equation 17 equal to zero and using the signed distance function given in Equation 18. A numerical scheme is devised to approximate the solution with a discrete grid together with finite differences. The approximation to the gradient in the evolution equation is required, in a simple scheme defined as

$$\Phi_{ij}^{n+1} = \Phi_{ij}^n - \Delta t \left(\max(D_{ij}^{-x} \Phi, 0)^2 + \min(D_{ij}^{+x} \Phi, 0)^2 \max(D_{ij}^{-y} \Phi, 0)^2 + \min(D_{ij}^{+y} \Phi, 0)^2 \right)^{1/2} , \quad (22)$$

where the difference operator notation is employed, for example $D_{ij}^{+x} \Phi = (\Phi_{i+1,j} - \Phi_{i,j})/(\Delta x)$, and the speed is $F = 1$ [SETHIAN 1996a]. The high computational costs based on the evolution of all level sets lead to further developments such as the narrow-band method introduced in [CHOPP 1993], and later enhanced as fast marching level set method in [SETHIAN 1996b].

Example of a geometric active contour

An example of the general functionality of geometric active contours is presented in Figure 4 and Figure 5. The implicit representation of the contour as zero level line in a higher dimensional level set function is exemplarily demonstrated with a circular object boundary (Figure 4). One of the mostly quoted advantages of geometric active contours is the natural change of the topology: the contour can transform for example from one curve into two curves, while the level set function remains a valid function (Figure 5). Consequently, no prior information about the object topology is necessary, but on the other hand a topological control is difficult and requires additional effort.

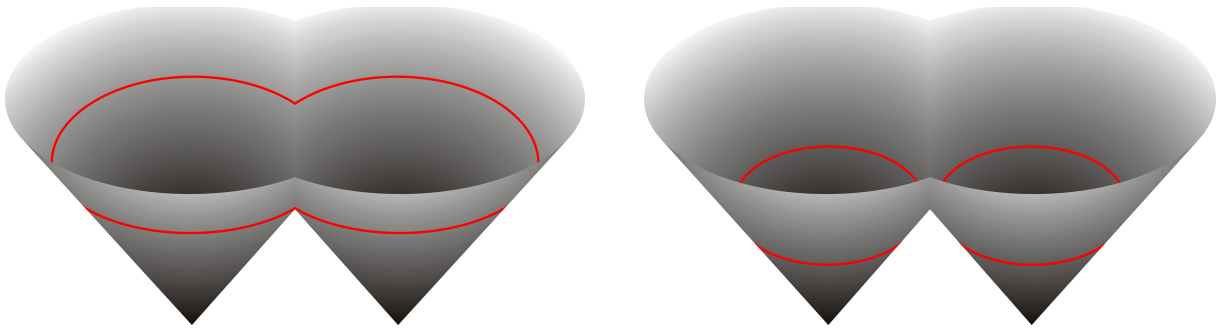


Figure 5: Geometric active contours: change of the topology

2.1.2.3. Comparison and discussion

Summarizing the *basics* concerning active contour models, a comparison and discussion of parametric and geometric active contours is given to highlight the similarities and differences of both concepts. Numerous contributions address active contour models in the literature, but mostly focus on only one concept.

Comprehensive comparisons of both models are presented in [CASELLES ET AL. 1997, AUBERT AND BLANC-FERAUD 1999, XU ET AL. 2000, DELINGETTE AND MONTAGNAT 2001, KERSCHNER 2003].

In addition to the mentioned relationships between parametric and geometric active contours in Section 2.1.2.1. and Section 2.1.2.2., respectively, the aim at this point is to give a brief comparison of the fundamental characteristics of both concepts. The most prominent properties are contrasted in Table 1.

Parametric active contours	Geometric active contours
<ul style="list-style-type: none"> ▪ Explicit representation of contours in their parametric form during deformation ▪ Direct interaction with model during optimization possible, e.g. for a human operator ▪ Rigid object topology ▪ Sensitive to the initialization of the contour, local optimization ▪ High efficiency, suitable also for real-time applications 	<ul style="list-style-type: none"> ▪ Implicit representation of contours as a zero level line of a higher-dimensional level set function ▪ Parameterizations are computed after complete evolution of the contour ▪ Topology changes naturally ▪ Relatively independent to the initialization of the contour ▪ Less efficiency due to the update of at least a narrow band around the contour

Table 1: Comparison of parametric and geometric active contours

The elementary difference is the explicit representation of parametric active contours compared to the implicit representation of geometric active contours, which involves several properties of the respective model. Parametric active contours allow for a direct interaction, for example by a user, while geometric active contours are parameterized after the evolution of the contour and a direct interaction is more difficult. On the other hand, the implicit representation enables topological changes during the evolution naturally, whereas the topology of parametric active contours is rigid and splitting or merging is complicated. When the object topology is known and should be exploited during the optimization, the explicit concept is better suited. Otherwise, the delineation of objects with an unknown topology can be performed ideally with the implicit concept. Parametric active contours are sensitive to the initialization and require a starting point near the object of interest, because the contour is locally optimized. In contrast, geometric active contours are relatively independent to the initialization, for instance a circle within the object or the image border can be chosen. The global deformation causes smaller efficiency compared to the parametric model, even though fast marching methods increase the computational speed.

In spite of the mentioned differences of parametric and geometric active contour models, the idea behind both concepts is quite similar. The coupling of the image data to the internal energy or curve evolution theory, respectively, is a common goal of the explicit and implicit representation. The control of both models enables a smooth curve to delineate non-rigid object contours. In addition, a constant evolution step starting from the initialization to bridge large distances is possible due to the balloon force or the constant speed term, respectively. The decision on which concept is the better one cannot be answered in general, because it depends highly on the application and, thus, on the requirements and characteristics of the object of interest.

In the subsequent sections, the state of the art concerning active contour models and related developments regarding the goals of the thesis are addressed. A concluding discussion bearing in mind the basics *and* state of the art of active contour models together with the defined goals of this thesis regarding the development of network snakes is given in Section 2.1.4.

2.1.3. State of the art

2.1.3.1. Introduction

In the following sections 2.1.3.2. - 2.1.3.5. the state of the art regarding active contour models is presented. The goal is not to give a comprehensive review of the large amount of published work since their introduction in the late eighties, but to give an idea of research lines and applications being relevant in the context of this thesis. First, the model of *parametric active contours* is examined, followed by the complementary model of *geometric active contours*. Originally, both models were only defined for single closed object boundaries, while newer research deals with the development of *multiple active contours* to delineate multiple objects as addressed in Section 2.1.3.4. Further problems occur when several objects of interest are in close proximity and partially touch each other: latest research of *coupled active contour models* incorporating topology is outlined in Section 2.1.3.5.

In addition to the state of the art regarding active contour models, *developments related* to the goals of this thesis concerning network snakes are pointed out in Section 2.1.3.6. Research incorporating topological characteristics of adjacent objects and dealing with the optimization of networks is examined to give a basis to distinguish the latest research against the proposed new method of network snakes presented in Chapter 3. A concluding discussion considering the state of the art and the already presented fundamentals regarding active contour models is given in Section 2.1.4.

2.1.3.2. Parametric active contours

Since their first presentation [KASS ET AL. 1987, KASS ET AL. 1988], the methodology of parametric active contours has received vast attention, as reflected in numerous contributions comprising further developments and various applications, for an overview see for example [MENET ET AL. 1990a, JAIN ET AL. 1998, BLAKE AND ISARD 1998]. Parametric active contours are an example of a more general concept of matching a template or deformable model to an image. Related ideas were already discussed by [WIDROW 1973] with the rubber mask technique and simultaneously by [FISCHLER AND ELSCHLAGER 1973] with the spring-loaded templates. The group of Kass, Witkin and Terzopoulos started their work concerning snakes with the mathematically ill-posed reconstruction problem proposing a general class of controlled-continuity stabilizers as solution [TERZOPOULOS 1986]. Elastic models of deformable curves using physical properties such as tension and rigidity are discussed in [TERZOPOULOS ET AL. 1987a], the 3D case of object reconstruction in [TERZOPOULOS ET AL. 1987b] and the general physically-based models of deformable curves, surfaces and solids for the use in computer graphics are described with the help of dynamic differential equations in [TERZOPOULOS AND FLEISCHER 1988].

Developments regarding parametric active contours can be classified using different criteria, for instance varying kinds of representation, minimization schemes, image energies, particular problems or applications. Here the focus is on the most relevant ones in the context of this thesis. The *representation* of the contour can be defined discretely by a list of points [KASS ET AL. 1988] or continuously with B-splines, called B-snakes [MENET ET AL. 1990b, BRIGGER ET AL. 2000]. Latest research improved B-snakes in order to vary the smoothness during evolution based on rational Gaussian curves termed R-snakes [ZAGORCHEV ET AL. 2007].

Different *minimization schemes* have been discussed in literature to solve the optimization of parametric active contours. The implementation can be realized using the variational calculus approach with finite differences such as accomplished in [KASS ET AL. 1988] (for further details cf. Section 2.2). The dynamic programming approach enables the incorporation of hard constraints avoiding possible numerical instabilities [AMINI ET AL. 1990], later enhanced with the greedy algorithm to speed up the minimization scheme [WILLIAMS AND SHAH 1992].

Several kinds of *image energies* have been developed covering diverse object characteristics within the imagery. Edge-based image energies are useful to delineate objects represented with edges or gradients [GÜLCH 1990, GRÜN AND LI 1997], while region-based energies are chosen to detect objects represented with homogeneous image features, for example with a local region analysis [RONFARD 1994]. An active region model using statistical characteristics of the image is used in [IVINS AND PORRILL 1995] to segment textures and colors, similarly a statistic deformable model is presented in [PUJOL AND RADEVA 2003] to delineate naturally textured objects. It can be helpful to utilize more than one resolution when minimizing the energy functional of active contour models, examples for the combination of different resolutions are given in [LEROY ET AL. 1996, PETERI AND RANCHIN 2003, WOLF AND HEIPKE 2007].

Research dealing with the general solution of *particular problems* incorporated within parametric active contours has been discussed in different contributions. The question of how to *initialize* the contour is regarded in the work of [NEUENSCHWANDER ET AL. 1994b, NEUENSCHWANDER ET AL. 1997], where only the end points of a contour have to be defined resulting in a completely optimized contour. A robust possibility of a dual contour is presented in [GUNN AND NIXON 1997], where an inside and outside initialization overcomes the drawback of sensitivity against the initialization. In the work of [RADEVA ET AL. 1995] a model-based image segmentation is achieved defining an enhanced image energy using only edge points with a suitable gradient direction and an internal energy incorporating a compensating force to avoid deviations from the initial contour. Further developments increasing the capture range of the image energy and, thus, allowing for initializations farther away are addressed in [COHEN AND COHEN 1993] with the distance map and in [XU AND PRINCE 1998] with the gradient vector flow (GVF) approach (cf. Section 2.1.2.1.). A second particular problem of parametric active contours concerns the rigid *topology*: the possibility to change topology is tackled in [SAMADANI 1989], for example to change the connectivity of tracked objects. An affine cell image decomposition is proposed in [MCINERNEY AND TERZOPOULOS 2000] to enable a contour reparameterization aiming at a seamless split or merge. An alternative approach is given in [LI ET AL. 2005] to handle a flexible initialization and topology using an external force with prior segmented enclosures. Current state of the art concerning multiple parametric active contours including the problem of topological changes are discussed in detail in Section 2.1.3.4.

A large variety of *applications* has been examined using parametric active contours. At this point the goal is only to give a short overview of examples where the proposed goal of this thesis concerning network snakes could be a possible enhancement. The tracking of features or objects in image sequences or videos is addressed in [DELAGNES ET AL. 1995, HOCH AND LITWINOWICZ 1996] and concerning 3D-objects in [STARK AND FUCHS 1996]. The delineation of man-made objects such as roads and road networks is discussed in [LAPTEV ET AL. 2000, PETERI ET AL. 2003, SONG ET AL. 2006], the detection of buildings in [FUA 1995]. Further developments using parametric active contours deal with the delineation of natural objects, for example trees [WOLF AND HEIPKE 2007], or cartographic tasks such as cartographic displacement [BURGHARDT AND MEIER 1997], line smoothing [BURGHARDT 2005] or polygon generalization [GALANDA AND WEIBEL 2003]. An important research field are medical applications, where parametric active contours are a very suitable tool, for an overview confer [MCINERNEY AND TERZOPOULOS 1996, SINGH ET AL. 1998]. Particular questions deal with the tracking of leukocytes or cells [RAY ET AL. 2002, LEYMARIE AND LEVINE 1993], the segmentation of vessels [KOZERKE ET AL. 1999] or incorporate shape priors [BOSCOLO ET AL. 2002].

2.1.3.3. Geometric active contours

The introduction of geometric active contours [CASELLES ET AL. 1993, MALLADI ET AL. 1995] as a complement to parametric ones increased the success of active contour models. In particular, the topological flexibility and independent initialization of the model are reasons for this success, for an overview see for example [SETHIAN 1996a, MALLADI 2002, OSHER AND PARAGIOS 2003].

Again, developments regarding geometric active contours can be classified according to different criteria, for instance varying kinds of image energies, shape priors, particular problems or applications. Different kinds of *image energies* have been introduced to cope with varying object representations in the imagery. The classical image energy is based on edges or gradients [MALLADI ET AL. 1995, CASELLES ET AL. 1997], while newer research deals with region-based image energies to segment objects which are not defined by gradients [CHAN AND VESE 2001, CHENG ET AL. 2005]. Alternative image energies integrate boundary and region-based texture segmentation modules [PARAGIOS AND DERICHE 1999, PARAGIOS AND DERICHE 2002a], a survey of a statistical framework in region-based models is given in [CREMERS ET AL. 2007].

The consideration of *shape priors* to the model of geometric active contours to increase the robustness against noisy or occluded data is addressed in [LEVENTON ET AL. 2000]: the authors include a probabilistic approach while computing a prior shape variation using a set of training instances. In a similar fashion, a global shape consistency is combined with the ability to make local deformations, presented in [ROUSSON AND PARAGIOS 2002]. Shape priors are exploited in different tasks, for example in digital building map refinement [BAILLOEUL ET AL. 2005] or the extraction of road networks [ROCHERY ET AL. 2006].

Investigations concerning the general solution of *particular problems* are content of some contributions: The integration of a *multiscale* approach to geometric active contours having the possibility to extract image structures at different scales simultaneously is given in [BRESSON ET AL. 2006]. The introduction of *topological*

constraints to geometric active contours is discussed in the work of [HAN ET AL. 2003]: the preservation of the initial topology is achieved using the simple point criterion from digital topology. An enhanced framework is described in [SEGONNE ET AL. 2005], where prior knowledge is integrated to control the topology. Developments regarding *computational efficiency* of geodesic active contours are proposed by [GOLDENBERG ET AL. 2001], where numerical consistency is combined with a narrow band around the contour and an efficient re-initialization technique.

Geometric active contours have been investigated for a large number of different applications. Again, the aim is here only to give a short overview of examples, where the proposed goal of this thesis could be a possible enhancement. The detection and tracking of moving objects in image sequences or videos is discussed for instance in [CASELLES AND COLL 1996, PARAGIOS AND DERICHE 2000a, FREEDMAN AND ZHANG 2004]. Similar to parametric active contours medical applications are a major research field of geometric active contours, for an overview see [MCINERNEY AND TERZOPOULOS 1996, SINGH ET AL. 1998, MALLADI 2002]. Particular questions define for example feature-based metrics on given imagery which lead to a quick and efficient attraction of the desired features [YEZZI ET AL. 1997], combine prior shapes and intensity information for medical segmentation tasks [CHEN ET AL. 2007] or deal with 3D surface representations to detect and measure objects in 3D medical data [MALLADI ET AL. 1996].

2.1.3.4. Multiple active contours

Both models, parametric and geometric active contours, are originally defined for single closed object contours. For this reason, advanced research extends these models to facilitate solutions dealing with more than one object, called *multiple active contours*.

First, research concerning *multiple parametric active contours* is addressed in [MCINERNEY AND TERZOPOULOS 1995]: the authors introduce an approach to handle multiple snakes with the additional opportunity to deal with topological changes. A domain decomposition framework is proposed with an iterative reparameterization using a superimposed grid. The case of multiple 3D deformable models with automated topology changes is examined in [LACHAUD AND MONTANVERT 1999], based on the work of [LEITNER AND CINQUIN 1992], where a generic model is presented to recover multiple shapes or extract multiple surfaces from 3D data. In [ABE AND MATSUZAWA 2000], a kind of active contour model is presented which enables the control of multiple contours with the help of statistical image characteristics competing with each other to extract sub-regions of uniform image or object properties. The approach of [DELINGETTE AND MONTAGNAT 2000, DELINGETTE AND MONTAGNAT 2001] detects intersections of edges controlling connected components automatically to eliminate overlaps of object contours. A different framework to segment similar objects represented in the image with varying image energies is given in [SRINARK AND KAMBHAMETTU 2001, SRINARK AND KAMBHAMETTU 2006] with the introduction of a so-called group energy, which incorporates sharing information about similar object shapes. In the work of [RAY ET AL. 2003], several contours are initialized and evolve separately with the aim to merge those within homogeneous image regions.

Research regarding *multiple geometric active contours* is also discussed in several contributions. In the work of [ZHAO ET AL. 1996] the authors use as many level set functions as there are expected kinds of regions. Depending on the proximity, each level set moves to the nearest interface, overlaps or vacuums are removed in a reassignment step. Similarly, the exploitation of prior knowledge concerning the number of regions characterized by a predetermined set of statistical features is the starting point presented in [YEZZI ET AL. 1999]. Geodesic active regions are utilized in [PARAGIOS AND DERICHE 2000b, PARAGIOS AND DERICHE 2002b] to deal with frame partition problems. The authors integrate boundary and region-based information within a curve-based minimization framework incorporating expected properties of defined classes. A multiphase level set formulation is given in [CHAN AND VESE 2001, VESE AND CHAN 2002] to avoid the construction problems of vacuum and overlaps during image segmentation.

2.1.3.5. Coupled active contours

The discussed work above concerning multiple active contours does not cover the general problem of adjacent or partly touching objects, where a change of topology is not desired. *Coupled active contours* incorporate topological constraints to cope with similar image energies characterizing neighboring objects.

There are only few contributions regarding *coupled parametric active contours*, one example is the work of [ZIMMER AND OLIVO-MARIN 2005]. The authors include a penalty force during the simultaneous optimization of all contours taking into account that objects cannot merge during the optimization. Thus, tasks such as tracking of objects represented with similar intensities or textures is possible without losing the given topology under the assumption of a homogeneous background.

Work related to *coupled geometric active contours* is a bit more common, firstly discussed in [MERRIMAN ET AL. 1994]. The authors enhance the traditional level set formulation, implying only one interface separating two regions, to a coupled level set method dealing with multiple level sets having multiple junctions. The difficulty is establishing a constraint at triple junctions that couples the three functions at a single point. In the cited approach, this is achieved at each time step with a kind of interface operation. This point is solved in the contribution of [SMITH ET AL. 2002] by replacing each level set function after the movement with a correction term defined by the overlap of neighbored level sets. The handling of multiple objects with multiple level sets is addressed in [ZHANG ET AL. 2004], where a coupling constraint minimizes the overlap of touching objects. However, it is not guaranteed that the boundary between touching objects is correctly located.

2.1.3.6. Related developments regarding network snakes

In this section, related developments concerning the goals of this thesis (cf. Section 1.2.) are examined, incorporating topological characteristics of adjacent objects and dealing with the optimization of networks. The aim is to give a basis to distinguish the relevant research from the proposed new method of network snakes presented in Chapter 3.

The term *network snake* was first introduced in the work of [FUA 1995, FUA ET AL. 1999]. The authors insert a network to reconstruct 3D-buildings: trihedral corners impose constraints of 90 degree angles between the three edges terminating at the corners. Thus, a free movement of all nodes and edges during the optimization is not possible and, additionally, the approach is only suitable for particularly constrained applications.

An adaptive adjacency graph is introduced in [JASIOBEDZKI 1993] and enhanced in [DICKINSON ET AL. 1994] to extract *networks of active contours*. The authors connect active contours at nodes during the deformation. The connectivity of the graph is achieved by imposing external energies in the form of constraints or springs to keep the adjacent contours together. However, a clear mathematical basis of the nodes with a degree unequal to two is not given and holes can appear leading to an incorrect topology.

A *region competition* approach for image segmentation is given in [ZHU ET AL. 1995, ZHU AND YUILLE 1996] combining active contours and region growing techniques to minimize a global cost function. The used generalized minimum description length (MDL) criterion assumes regions with smooth boundaries and homogeneous intensity properties within the image, which are defined by a list of probability distributions. A point of further investigation is the accuracy of the boundaries between adjacent segments and the effects of the initial seed point configuration. A topological control of adjacent objects is not incorporated into the proposed approach.

2.1.4. Discussion

In the previous sections, the mathematical definitions of parametric and geometric active contours were given and compared to each other. Additionally, the state of the art concerning active contour models was presented and related developments regarding the goals of this thesis were examined. The mentioned approaches of multiple active contour models require particular conditions to handle multiple objects such as homogeneous object representations in terms of intensities, colors or statistical properties, which are only suitable for specific applications. Alternatively, additional steps of reparameterizations of the contour are needed during the optimization. The general question of how to represent multiple and adjacent objects, despite having no homogeneous object characteristics available, is unanswered. The approaches concerning multiple and coupled active contours represented with coupled level sets are ad hoc solutions, because triple points are not defined with a clear mathematical basis.

A concluding discussion involving all quoted aspects is given in this section to point out which potential of active contour models not utilized up to now is available and why only parametric active contours are suitable

for reaching the defined goals of the proposed new method of network snakes. Taking up the goals defined at the beginning of this thesis (cf. Section 1.2.), the following research issues are still to be solved:

- A method of active contours, which optimizes graphs consisting of nodes of arbitrary degree:

No contribution can be found in the literature which solves this question. The work of [JASIOBEDZKI 1993, DICKINSON ET AL. 1994] addresses this task partly, but the graph is built with constraints in the form of springs. No clear mathematical definition of nodes with a degree $\rho(C) > 2$ is given and, consequently, no single point can be defined at these positions in the graph. Alternative approaches fix nodes to overcome this problem, but the aim in this thesis is to allow a free movement of any node independently of their degree incorporating a complete shape control. The question of how open contours can be represented at the end points ($\rho(C) = 1$) using active contour models is difficult to answer: in traditional approaches using parametric active contours, constraints are introduced to enable a shape control at the end points. This solution is undesirable here due to the aim of developing a constraint-free procedure at the end points. In addition, the problem of contour shrinking because of the definition of the internal energy is generally unsolved (cf. Section 2.1.2.1. and for details Section 2.2.). The alternative representation of nodes with a degree $\rho(C) = 1$ with geometric active contours is not possible because the implicit representation with a level set in a higher dimension is exclusively defined for closed contours and, thus, cannot represent open contour parts. In sum, a method of active contours optimizing any kind of graphs does not exist so far, and only parametric active contours are suitable to represent open contour parts due to their explicit representation.

- A method of active contours, which segments imagery without gaps or overlaps:

Contributions regarding active contour models dealing with the segmentation of imagery without gaps or overlaps by construction are addressed in the work of [ZHU AND YUILLE 1996] and [VESE AND CHAN 2002]. Further articles claim to deal with segmentation tasks, too, but no clear mathematical definition is given to cover the segmentation in its original definition, where gaps and overlaps are impossible (cf. for example the work regarding multiple active contours discussed in Section 2.1.3.4.). The region competition approach [ZHU AND YUILLE 1996] requires homogeneous segments in terms of prespecified probability distributions of the intensity values. The multiphase level set framework [VESE AND CHAN 2002] defines classes with a disjoint decomposition and coverage of the image. Both approaches use region information to define the boundaries of the segments, which is only reasonable for the delineation of particular object classes. When the objects of interest vary in terms of intensities, colors or textures, the quoted methods will probably fail. This problem increases when the image information between the graph meshes is perturbed causing wrong segmentation results. In sum, a method of active contours segmenting imagery without gaps or overlaps is only covered by geometric active contours using region-based image information representing only a particular object class. A complete segmentation using parametric active contours is not treated in the literature, only transitionally touching objects are content of the work of [ZIMMER AND OLIVO-MARIN 2005] using coupled parametric active contours.

- An image segmentation and object delineation method with a high generality and transferability:

Active contour models have been continuously enhanced, mostly for specific object types represented in specific kinds of images, Sections 2.1.3.2. - 2.1.3.6. give an overview of research lines and applications. In contrast, the goal of this thesis is to develop a method of active contour models with a high generality and transferability concerning the delineation of adjacent objects and any kinds of networks. The aim is to enable a free optimization of the whole network incorporating a complete shape control of any contour parts. The incorporation of constraints and, thus, the limitation of the method to only particular applications is not desired.

The proposed new method of network snakes aims to delineate any graphs representing networks and boundaries of adjacent objects. One important criterion is the possibility to control and utilize the topology, particularly when dealing with applications being represented with weak or noisy image data. This fact prefers parametric active contours for further investigations due to their explicit representation of the contours. A method to deal with nodes with a degree $\rho(C) \neq 2$ as discussed concerning the stated goals is not known in the literature (cf. Section 2.1.3.6.) and, thus, aim of the developments of this thesis presented in Chapter 3.

A second important point is the underlying image energy. Geometric active contours incorporate methodically the whole image domain, even though approaches use often only a narrow band around the contour to speed up the processing. Parametric active contours use local image information during the optimization, which is a

disadvantage when the object topology is unknown, but an advantage when the topology is known or no (region-based) image information is available to specify topological changes.

The discussed reasons result in a solution based on the concept of parametric active contours to develop the new method of network snakes. The next section presents the details of the energy minimization concept of parametric active contours to provide a mathematical basis for the proposed new method given in Chapter 3.

2.2. Energy minimization of parametric active contours

In this section the *minimization* of the energy functional $E(C(s))$ of parametric active contours is given in detail. The aim is to provide the mathematical basics to initiate a discussion considering the goals of this thesis defined in Section 1.2. resulting in the new developments of network snakes presented in Chapter 3.

The energy functional $E(C(s))$ of a parametric active contour was defined in Section 2.1.2.1. as

$$E(C(s)) = \int_0^1 [E_{img}(C(s)) + E_{int}(C(s))] ds \rightarrow Min, \quad (23)$$

whereas the optional constraint energy term $E_{con}(C(s))$ is disregarded in order to derive a minimization without any restrictions. However, the constraint energy can be introduced to the energy functional at any time if required. The solution of Equation 23 can be derived with the *calculus of variations* as proposed in [KASS ET AL. 1988].

In general, the calculus of variations deals with seeking a curve (or surface), for which a given functional $F(C)$ in the form of

$$F(C) = \int_0^1 E(s, C, C_s, C_{ss}) ds \quad (24)$$

has a minimum or maximum considering the boundary conditions

$$C(0) = C_b, C(1) = C_e, \quad (25)$$

where the values $C_e > C_b$ are given, and with

$$C_s = \frac{\partial C}{\partial s}, \quad C_{ss} = \frac{\partial^2 C}{\partial s^2}, \quad (26)$$

see for example [BRONSTEIN ET AL. 2005]. The solution of functional $F(C)$ defined in Equation 24 is obtained with setting up the condition

$$C(s) = C_0(s) + \varepsilon \eta(s), \quad (27)$$

where $\eta(s)$ is a function with $\eta(0) = \eta(1) = \eta_s(0) = \eta_s(1) = 0$ and ε is a parameter. Using Equation 24 and Equation 27 the functional $F(C)$ is replaced with the function $F(\varepsilon)$, i.e. the variation problem becomes an extremum problem

$$F(\varepsilon) = \int_0^1 E(s, C_0 + \varepsilon \eta, C_{0s} + \varepsilon \eta_s, C_{0ss} + \varepsilon \eta_{ss}) ds, \quad (28)$$

fulfilling the condition

$$\frac{\partial F}{\partial \varepsilon} = 0 \quad \text{for } \varepsilon = 0 . \quad (29)$$

Using the Taylor expansion [BRONSTEIN ET AL. 2005] one gets

$$F(\varepsilon) = \int_0^1 \left(E(s, C_0, C_{0s}, C_{0ss}) + \frac{\partial E}{\partial C}(s, C_0, C_{0s}, C_{0ss}) \varepsilon \eta + \frac{\partial E}{\partial C_s}(s, C_0, C_{0s}, C_{0ss}) \varepsilon \eta_s + \frac{\partial E}{\partial C_{ss}}(s, C_0, C_{0s}, C_{0ss}) \varepsilon \eta_{ss} \right) ds . \quad (30)$$

The required condition defined in Equation 29 leads to

$$\int_0^1 \eta \left(\frac{\partial E}{\partial C} \right) ds + \int_0^1 \eta_s \left(\frac{\partial E}{\partial C_s} \right) ds + \int_0^1 \eta_{ss} \left(\frac{\partial E}{\partial C_{ss}} \right) ds = 0 , \quad (31)$$

and with integration by parts considering the boundary condition for $\eta(s)$ it follows

$$\int_0^1 \eta \left(\frac{\partial E}{\partial C} - \frac{d}{ds} \left(\frac{\partial E}{\partial C_s} \right) + \frac{d^2}{ds^2} \left(\frac{\partial E}{\partial C_{ss}} \right) \right) ds = 0 . \quad (32)$$

The integral of Equation 32 vanishes for every function $\eta(s)$ resulting in

$$\frac{\partial E}{\partial C} - \frac{d}{ds} \left(\frac{\partial E}{\partial C_s} \right) + \frac{d^2}{ds^2} \left(\frac{\partial E}{\partial C_{ss}} \right) = 0 , \quad (33)$$

which represents the general *Euler differential equation*.

This general solution is now applied to the minimization of the energy functional $E(C(s))$ of parametric active contours. With constant weight parameters $\alpha(s) = \alpha$ and $\beta(s) = \beta$ in order to simplify the representation, the energy functional $E(C(s))$ of parametric active contours given in Equation 23 can be minimized by solving the corresponding Euler equations:

$$\frac{\partial E_{img}}{\partial C} - \alpha \frac{\partial^2 C}{\partial s^2} + \beta \frac{\partial^4 C}{\partial s^4} = 0 . \quad (34)$$

As the contour C is represented with the coordinates x and y (cf. Equation 1) Equation 34 results in two independent equations. The required Euler equations are independent of each other concerning the coordinates x and y . The derivatives are approximated with finite differences since they cannot be computed analytically:

$$\begin{aligned} & \frac{\partial E_{img}}{\partial C} \\ & + \alpha ((C_i - C_{i-1}) - (C_{i+1} - C_i)) \\ & + \beta (C_{i-2} - 2C_{i-1} + C_i) - 2\beta (C_{i-1} - 2C_i + C_{i+1}) + \beta (C_i - 2C_{i+1} + C_{i+2}) = 0 . \end{aligned} \quad (35)$$

With $\frac{\partial E_{img}}{\partial C} = f_C(C)$ Equation 35 can be rewritten in matrix form as

$$AC + f_C(C) = 0 . \quad (36)$$

A is a pentadiagonal band matrix of dimension n , which depends only on the parameters α and β . With substitution of $a = \beta$, $b = -\alpha - 4\beta$ and $c = 1 + 2\alpha + 6\beta$ the matrix A has the following structure for a closed contour:

$$A = \begin{bmatrix} c & b & a & 0 & \dots & 0 & a & b \\ b & c & b & a & 0 & \dots & 0 & a \\ a & b & c & b & a & 0 & \dots & 0 \\ 0 & a & b & c & b & a & \ddots & \vdots \\ \vdots & \ddots & \ddots & \ddots & \ddots & \ddots & \ddots & 0 \\ 0 & \dots & 0 & a & b & c & b & a \\ a & 0 & \dots & 0 & a & b & c & b \\ b & a & 0 & \dots & 0 & a & b & c \end{bmatrix} . \quad (37)$$

In general, the calculus of variations defines boundary conditions [BRONSTEIN ET AL. 2005], which are in terms of parametric active contours incorporated by fixed boundary values. For closed contours, this condition is introduced leading to entries beside the banded structure in the corner of the matrix A (cf. Equation 37).

A solution to Equation 36 can be derived by setting the right hand side equal to the product of a step size γ and the negative time derivatives of the left hand side. It is assumed that the derivatives of the image energy $f_C(C)$ are constant during a time step, i. e. $f_C(C_t) \approx f_C(C_{t-1})$, resulting in an explicit Euler step regarding the image energy. In contrast, the internal energy is an implicit Euler step due to its specification by the band matrix A . The resulting equation reads

$$AC_t + f_C(C_{t-1}) = -\gamma(C_t - C_{t-1}) . \quad (38)$$

The time derivatives vanish at the equilibrium ending up in Equation 36. Finally, a solution can be derived by matrix inversion:

$$C_t = (A + \gamma I)^{-1}(\gamma C_{t-1} - \kappa f_C(C_{t-1})) , \quad (39)$$

where I is the identity matrix and κ is an additional parameter in order to control the weight between internal and image energy (not to be confused with the symbol for curvature, cf. Section 2.1.2.2).

In the presented energy minimization process, two assumptions have been made. First, the approximation of the derivatives with finite differences (cf. Equation 35) requires unit distances between neighboring points representing the contour. This prerequisite is important because parameterization changes can involve unwanted shape modifications [DELINGETTE AND MONTAGNAT 2001]. In addition, the approximated curvature of the contour using finite differences will result in somewhat incorrect terms. Second, the parameter s is assumed to be the arc length to represent the curvature with the derivatives correctly [WILLIAMS AND SHAH 1992]. Avoiding reparameterizations during the minimization process, a preservation of unit distances between neighboring points can be incorporated in the energy functional.

A further problem which may occur during the minimization process is self-looping, which is caused by the setting of the weighting parameters of the internal energy. Parameters enabling high curvatures for delineating corners or deep concave or convex shapes facilitate self-loopings. A possible solution is given in [JI AND YAN 2002a, JI AND YAN 2002b], where an anterior loop control and a posterior elimination process can cope with self-looping cases and handle their topological transformations automatically. Alternatively, a dense discretization coupled with stronger internal energy weights can minimize self-loopings.

2.3. Related work concerning applications of network snakes

2.3.1. Introduction

One goal of this thesis is to explore and demonstrate the generality and *transferability* of the proposed new method of network snakes. The achievement of this aim will be examined in terms of more general and basic

investigations using synthetic examples to avoid any disturbing conditions only focusing on the points of interest. The transferability of network snakes will be regarded with two different, real application scenarios. The goal is to identify how the proposed method can contribute to varying applications. The first application from geosciences and agricultural sector deals with the extraction of *field boundaries* from high resolution optical satellite images. The second application from the bio-medical sector investigates the delineation of adjacent biological *cells* in microscopic cell images. The following two sections address the state of the art concerning these different applications to point out possible limitations of the current research and to identify potential improvements using the proposed new method of network snakes.

2.3.2. Extraction of field boundaries

The extraction of field boundaries has become a task of increasing interest during the last years. One application area are the geosciences, for example for the derivation of potential wind erosion risk fields, which can be generated with field boundaries and additional input information about the prevailing wind direction, wind shelters and soil parameters [THIERMANN ET AL. 2002]. Another area is the agricultural sector, where information about field geometry is important for tasks such as the monitoring and control of subsidies [OESTERLE AND WILDMANN 2003] or precision farming [AUERNHAMMER 2001].

An approach to reconstruct agricultural land-use units by fusing multitemporal and multisensoral raster images with digital vector map data is presented in [LÖCHERBACH 1994, LÖCHERBACH 1998]. The author proposes a global estimation of the location of the vector polygons of the land-use units to update and refine the geometry. The polygons consist of straight line segments representing the real world only in a generalized manner. However, the acquisition of new field boundaries is not incorporated in the approach.

The work of [TORRE AND RADEVA 2000, TORRE AND RADEVA 2004] deals with the problem of segmenting agricultural fields by a semiautomatic region competition technique. The system combines region growing and deformable models to segment areas in aerial images which are assumed to be homogeneous enough to be represented by a Gaussian distribution. The proposed contribution needs manually defined seed regions typifying the characteristics of the fields to initialize the processing. Each field is treated on its own, whereby no topological properties of neighboring fields are incorporated in the model.

In the contribution by [MÜLLER 2001, MÜLLER ET AL. 2004] an object-orientated segmentation framework is discussed to extract agricultural fields from panchromatic satellite imagery. The authors combine region- and edge-based techniques through the inclusion of extracted shape knowledge in a subsequent region growing algorithm. However, no topological control is exploited within the model leading to results containing frayed borders at field boundaries and, furthermore, a partial oversegmentation occurs within fields.

A technique for predicting missing field boundaries to increase the accuracy of a subsequent per-field classification is presented in [APLIN AND ATKINSON 2004]. The authors introduce an approach based on a comparison of the within-field proportion of modal land cover and the average local variance per field to provide an indication of the likelihood of missing boundaries. The framework requires a manual post processing, because only fields with a high likelihood of missing boundaries are identified, not field boundaries directly.

Prior knowledge from a GIS-database is incorporated in the field segmentation process addressed in the work of [BUTENUTH AND HEIPKE 2005, BUTENUTH ET AL. 2007]. Global context knowledge is used to focus only on open landscapes and, additionally, the GIS-objects roads, tree rows, hedges and rivers describe already fixed field boundaries. Exploiting the GIS-knowledge enables one to partition the imagery deriving regions of interest and to concentrate the following segmentation algorithm only on the fields within these regions.

The work of [TRIAS-SANZ 2006, TRIAS-SANZ ET AL. 2007] starts with prior information, too, by using a cadastre graph as a rough approximation to partition the land into fields. The authors propose two approaches to solve the matching problem of the cadastre graph and the image: the first one finds the best match between the graph and segmented edges using simulated annealing, the second one finds a near-optimal match between the faces in the graph and homogeneous regions in the image. The question of which cadastre edges actually exist in the image in terms of splitting or merging adjacent cadastre regions is not answered in the contribution.

The existing contributions describing different approaches on the extraction of field boundaries do not provide fully automatic solutions nor exploit topological knowledge. To avoid semiautomatic approaches, as much

knowledge as possible has to be incorporated in the model representing field boundaries within the complex environment of vegetation. Prior knowledge, for example from a GIS, can be used to restrict the search space and, thus, to ease the segmentation task, e.g. [BUTENUTH ET AL. 2003]. In addition, not only knowledge about each single object on its own has to be regarded, but topological properties of neighboring objects can be exploited to compensate the heterogeneities, which often occur at the borders of fields. The question concerning the extraction of field boundaries is how the proposed new method of network snakes can include image information, shape control and topological constraints to improve the results of this application.

2.3.3. Delineation of cells

The second application scenario investigating the transferability of network snakes is related to the bio-medical sector dealing with the delineation of adjacent biological cells in microscopy cell imagery. In general, bio-medical image segmentation has received much attention in recent years due to improved possibilities for data capture and, obviously, due to the enormous application potential [SONKA AND FITZPATRICK 2000, SURI ET AL. 2002]. The automatic segmentation and tracking of cells is one important task in the field of biological research because the understanding of the cell migration and shape analysis is a basic requirement for tasks such as drug discovery, confer for example [CHICUREL 2002, ZIMMER ET AL. 2006, BUTENUTH AND JETZEK 2007]. In the following, some relevant approaches for cell delineation are discussed to give an idea of the state of the art and to point out possible limitations and improvement opportunities.

In the work of [YOUNG ET AL. 1998], a template matching algorithm is presented identifying and measuring living cells in differential interference contrast (DIC) microscope images. The template is defined in a particular way to represent the pseudo bas-relief image generated due to the capturing process, i.e. dark and light cell boundaries. The model requires a homogeneous background without any features, which cannot be guaranteed in general. Furthermore, the measurement of overlapping cells or the incorporation of topological properties is not considered.

The approach of [ZIMMER ET AL. 2002] deals with the segmentation and tracking of cell dynamics from in vitro videomicroscopy data. The proposed technique is based on parametric active contours and overcomes the shortcomings of the inability to correctly segment pseudo-pods and cells in contact. The model needs a homogeneous background to localize weak object boundaries, which do not allow any features or noise in the image data. To tackle the problem of cell interactions producing partly invisible boundaries, the authors introduce in a later approach a region-based model based on geometric active contours [ZHANG ET AL. 2004]. To handle multiple cells, a coupling constraint is incorporated to minimize overlaps of touching cells, but the technique does not guarantee that the boundary between cells is located correctly.

A procedure for finding boundaries between adjacent cells sharing a common border in microscopy images is addressed in [JONES ET AL. 2005]. The authors start with manually segmented seed regions and define a metric in the image by calculating distances from the seed regions according to this metric. Prior information concerning the cell shape is only included in a simple way together with local image properties. Therefore, the boundary localization of the common cell borders is not very precise and sometimes fails.

In the work of [JETZEK AND KAISER 2007], a geometric model is incorporated into the segmentation process of biological cells in confocal microscope images. The authors include biological knowledge in their model to characterize the cytoskeleton and to describe the architecture of the cells. A tree-based model is used to predict locations of inner adhesion within the cells. While describing the geometric model of each cell in much detail, the proposed framework does not consider neighboring cells and their influence on each other.

An approach for segmenting and tracking of cellular shape and motion from dynamic 3-D microscopy data is given in [DUFOUR ET AL. 2005]. The authors describe a method using multiple active surfaces coupled by a penalty for overlap handling touching cells and a constraint conserving the volume of cells. The proposed framework requires the existence of a background in the image data, while only partly touching cells can be covered and further improvements are essential to deal with tight cell clusters.

Many discussed approaches initiate the cell delineation process with cell nuclei defined beforehand. This strategy is reasonable because the cell nuclei are well defined against the background and are thus much easier to detect than the boundaries of the cytoplasm. To exploit this prior information, automatic procedures are needed in particular for high-throughout biological research to detect the cell nuclei. One possibility is given in

[BAMFORD AND LOVELL 1998], where the cell nucleus segmentation is accomplished by a global search-based dual active contour. The approach fails when there are high image gradients near the true nuclei border. Another framework to detect cell nuclei is presented in [ORTIZ DE SOLORZANO ET AL. 2001], where the authors propose an approach based on object size estimation and, thus, require homogeneous object sizes and shapes.

Several approaches deal with the delineation of biological cells, but often manual work is required to initialize the processing or only particular microscopy images representing few cells can be treated. Knowledge about single cells is sometimes incorporated to define comprehensive models. The influence of neighboring cells on each other is often not regarded, even though the objects share a common border. These topological properties of adjacent objects can be exploited to compensate image properties such as noise or disturbances together with the modeled shape properties of cells. Similar to the first application scenario concerning the extraction of field boundaries (cf. Section 2.3.2.), it must be examined how the proposed new method of network snakes can include image information, shape control and topological constraints to improve the results regarding the delineation of cells.

3. Network snakes

In the previous chapter it was concluded, that the optimization of graphs with nodes of an arbitrary degree delineating networks or adjacent objects cannot be solved with existent active contour models. To overcome this limitation, the new method of network snakes is presented in this chapter. First, the goals of this thesis are taken up and are illustrated with a synthetic example to specify the new developments necessary and to identify the challenge of this thesis. Second, the requirements concerning the imagery, initialization and topology are discussed to define the framework for the proposed new method of network snakes. Third, the new terms of the energy functional for the chosen concept of parametric active contours are presented and the new mathematical model is described in detail resulting in network snakes. In addition, the general functionality is demonstrated using the synthetic example. Fourth, some general implementation issues regarding the realization of the system, the introduction of the optional topology-preserving energy and the general parameter control are examined and illustrated. This chapter is completed with a discussion of the proposed new method of network snakes to highlight the obtained results.

3.1. Introduction

The presentation of the mathematical basics of parametric and geometric active contours and the discussion of the state of the art demonstrate that the stated goals of this thesis cannot be reached with existing active contour models or related methodologies as discussed in Chapter 2. Neither the optimization of arbitrary graphs nor the delineation of adjacent objects based on a clear mathematical model is available. In Figure 6 two synthetic examples are given to depict exemplarily the general problem treated: potential applications of arbitrary networks and adjacent objects are illustrated and will be used in this chapter to emphasize the new developments.

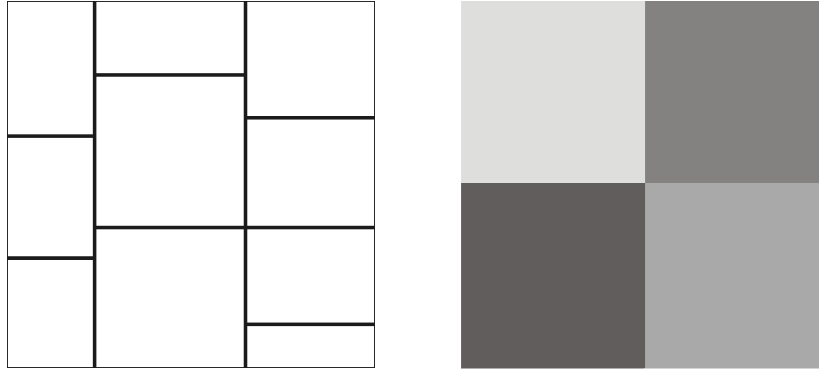


Figure 6: Two synthetic examples representing networks and adjacent objects

The new method of network snakes will be developed based on the concept of *parametric active contours* as discussed in Section 2.1.4. However, regarding the goals of this thesis, parametric active contours cannot meet the challenges using the traditional concept because the original concept is only defined for single and *closed* object contours, i.e. only for nodes with a degree $\rho(C) = 2$. The reason for this fact is the definition of the *internal energy* $E_{int}(C(s))$ of the energy functional $E(C(s))$ representing the shape model of the object of interest. The solution of the energy functional is obtained using the corresponding Euler equations, whose derivatives are approximated with finite differences as shown in detail in Section 2.2. Thus, each node requires neighboring nodes on both sides to set up the approximated derivatives comprising the shape model of the contour (cf. Equation 35). Obviously, this condition is only fulfilled for closed object contours and, consequently, a new definition of the energy functional at the nodes with a degree $\rho(C) \neq 2$ has to be developed.

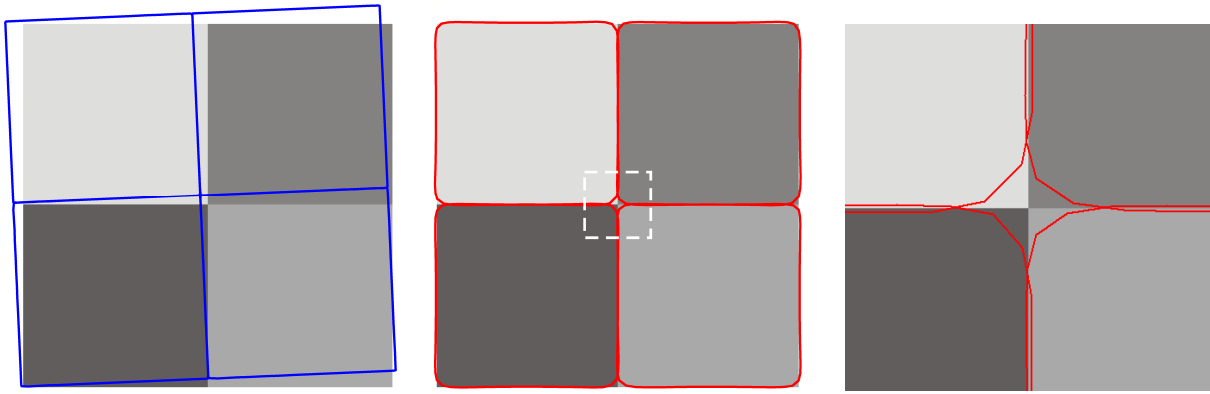


Figure 7: Delineating adjacent objects with traditional parametric active contours: initialization (blue), result and zoomed result part (red)

In Figure 7 the synthetic example is taken to demonstrate the general functionality and limitation of the traditional concept of parametric active contours: the exemplary four regions cannot be delineated with one contour jointly, instead for each segment a single and closed contour is required. Starting from a topologically correct initialization (Figure 7, left, initialization depicted in blue), the optimization leads to a loss of the topology and thus to incorrect results (Figure 7, middle, result depicted in red). Focusing on the center of the synthetic example (dashed white line), the gaps and overlaps of the result are more apparent (Figure 7, right, result center depicted in red). At that time the extent of the gaps and overlaps is not important, but only the effect on its own. This consequence is mathematically obvious, because the individual contours do not consider adjacent ones due to the fact that no topological knowledge about the objects of interest is incorporated in the model of parametric active contours. Similarly, the effect of gaps and overlaps is observable at the borders of the example, where the individual contours result in rounded corners.

In contrast, the new method of network snakes to be developed will include a complete topology to solve arbitrary problems regarding the optimization of networks and boundaries of adjacent objects to overcome the drawbacks of traditional single parametric active contours. The incorporation of any constraint in the mathematical model is omitted to enable a free optimization of the whole graph including a complete shape control at any contour parts. Consequently, a new mathematical model has to be developed. The goal is to define the energy functional in a new manner to enable a connection of arbitrary contour parts in *one* point representing the topology of a graph. At the same time, the control of the shape of the different contour parts is a further important advantage of the concept of parametric active contours, which has to be maintained during the optimization of the energy functional.

3.2. Requirements

3.2.1. Outline

Parametric active contours are defined as an energy functional $E(C(s))$ consisting of the image energy $E_{img}(C(s))$ given an optimal description of the object of interest in the image, the internal energy $E_{int}(C(s))$ introducing modeled object knowledge concerning the shape behavior or movement of the object and the optional constraint energy $E_{con}(C(s))$ offering the possibility to insert an external constraint to the energy functional (cf. Equation 2). The constraint energy is not considered here because the new method of network snakes will be developed without any restrictive conditions. However, the introduction of optional constraints to represent particular applications, for example the fixing of special points or contour parts due to additionally available prior knowledge, is possible at any time.

In this section, the conditions concerning the required *imagery* and the *initialization* of the contour are addressed to define a framework for the new method of network snakes. In addition, *topology* is introduced to the concept of parametric active contours to point out the prerequisites of this powerful information being exploited during the optimization of the energy functional. The requirements concerning the synthetic example of Figure 6 (right) are displayed exemplarily in Figure 8 and are explained in detail in the subsequent sections: the required image energy is obtained by computing the inverse gradient amplitude image of the input image as depicted on the left, the requirements concerning the initialization of the contour and the given topology are illustrated on the right of Figure 8.

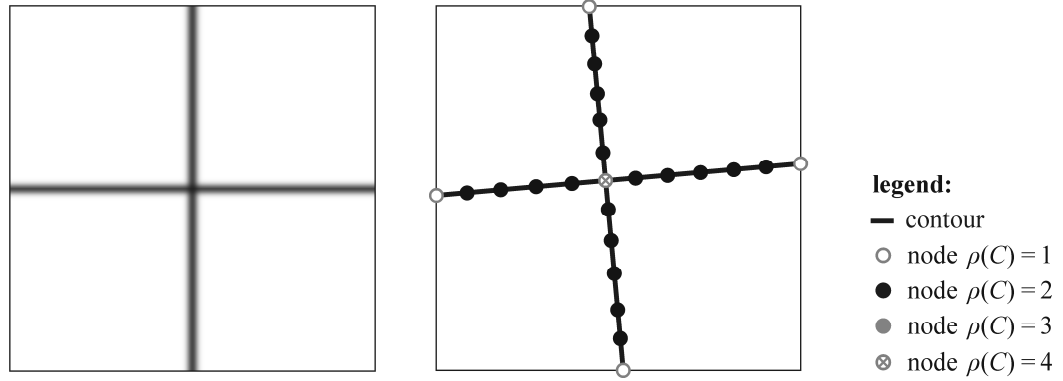


Figure 8: Requirements for network snakes: image energy (left), initialization and topology (right)

3.2.2. Imagery

The imagery is a basic input information required for any kinds of active contour models. The image energy $E_{img}(C(s))$ describes the object of interest in the image I in an optimal manner, where optimal means an image function letting the contour C attract salient features in the image, which represents the boundaries of the object of interest (cf. Section 2.1.2.1.). The choice of the best image energy or the combination of different terms depends on the application and the characteristics of the object of interest. The objective is a distinctive representation of the object boundary within the image to attract the contour towards the desired object boundary during energy minimization. A short overview of approaches using different kinds of image energy is given in Section 2.1.3.2.

One important issue concerning parametric active contours is the fact that the imagery is regarded as the “truth of the real world” and, thus, represents the reference of the object of interest during the optimization of the energy functional. However, as a result of occlusions of the object of interest caused by local context objects in the real world and noisy or blurry image data due to the sensor properties or weakly represented object boundaries due to the local environment of the object, the image energy can represent the object of interest only in a partially correct way in terms of the assumed true real world or, even worse, it pictures a wrong real world. These limitations of the image energy apply to any concept of active contour models and, moreover, to any other methods segmenting or detecting objects automatically in imagery. The prominent characteristic of parametric active contours is the combination of the image energy with the internal energy $E_{int}(C(s))$. The goal is to compensate complex or disturbed image properties with prior modeled object knowledge about the shape characteristics or movement of the object of interest. This feature and advantage of parametric active contours will be furthermore extended with the incorporation of the topology to the model, because poorly represented object boundaries in the imagery can potentially be delineated exploiting the topology.

Examples of possible image energies depending on the respective object characteristics are given in Section 2.1.2.1 and concerning particular applications are cited in Section 2.1.3.2. The image energy of the synthetic example of Figure 6 is depicted symbolically as a gradient amplitude image in Figure 8 on the left side, which is used within this chapter to demonstrate the general functionality of the traditional concept of parametric active contours compared to the proposed new method of network snakes.

3.2.3. Initialization

The initialization of the contour representing the starting point to minimize the energy functional is the second requirement for active contour models. The concept of parametric active contours needs an initial contour close to the true object boundary, because the optimization of the energy functional $E(C(s))$ considers only the local environment of the current position of the contour. The minimization of this energy functional is an iterative procedure as shown in Section 2.2., because the procedure requires the introduction of a step size γ for finding a solution (cf. Equation 36 and Equation 38). Thus, a preceding step deriving the initial contour is essential before starting the optimization of the energy functional.

The question on what exactly an initial contour *close* to the true object boundary means in this context cannot be answered in general. There are dependencies between the initialization, the image characteristics compared to the object characteristics, the parameter control of the energy functional and the topology of the objects of interest, which have to be discussed in a comprehensive analysis. Investigations concerning these tasks will be presented in Chapter 4 to develop possible rules and boundary conditions. Obviously, an initialization very close to the true object boundary will speed up the optimization process compared to an initialization farther away.

An important issue is the requirement of unit distances between neighboring nodes representing the initial contour, which is assumed when starting the energy minimization process (cf. Section 2.2.). The reason is the approximation of the derivatives with finite differences (cf. Equation 35) representing the shape model of the contour within the internal energy. This condition is significant for the whole energy minimization process, because parameterization changes can cause unwanted shape variations. In addition, the approximated curvature of the contour using finite differences without unit distances will result in incorrect values (cf. Section 2.2.). Avoiding reparameterizations during the minimization process, a preservation of unit distances between neighboring nodes can be incorporated in the energy functional, a detailed examination of this requirement is given in Section 3.4.1.

Besides the unit distances between the nodes, an appropriate number of nodes representing the object boundaries has to be chosen. The approximation of the object contour depends on the level of detail to be represented. Many nodes facilitate a precise delineation of the object of interest, less nodes speed up the processing. It should be noted that only a sufficient number of nodes can represent the shape characteristics of the contour due to the approximation of the derivatives of the internal energy with finite differences. A general statement of how many nodes are required for an adequate representation depends highly on the object characteristics: object parts with large curvature need more nodes than relatively straight parts.

Examples of different initialization strategies are stated and discussed in Section 2.1.3.2. However, the cited approaches follow the solution of particular applications rather than more general statements concerning the necessary requirements of the initial contours. The reason could be the very complex challenge of finding general initialization rules. A detailed examination and discussion proposing possible answers is given in Section 3.4.1. Regarding the synthetic example of this chapter, the initial contour requiring unit distances between the nodes representing the contour is symbolically shown in Figure 8 on the right side.

3.2.4. Topology

The first two requirements quoted above, the imagery and the initialization, are prerequisites for any kind of parametric active contours. Concerning the goals of this thesis, developing a solution optimizing arbitrary networks and delineating the boundaries of adjacent objects, the additional introduction of the *topology* to the concept of parametric active contours is the prominent challenge. Consequently, the topology representing the graph structure has to be given or derived from the initialization before starting the optimization process. Details on the incorporation of topology to the active contour model are explained in the next Section 3.3.

Besides enabling the optimization of nodes with a degree $\rho(C) \neq 2$ enhancing the concept of parametric active contours it is also an aim to *exploit* the topology during the minimization of the energy functional (cf. Section 1.2.). Obviously, the requirement is a given topology which is assumed to be correct. The exploitation of a given correct topology during the energy minimization process presumes the preservation of this initial topology during optimization. This fact cannot be guaranteed in general, because close contour parts can merge or nodes with higher degrees can move around each other. These undesired effects mean that the criterion of a

planar graph is no longer satisfied. Thus, the preservation of the correct initial topology must be ensured within the complete processing to avoid touching or overlapping contour parts changing the original topology. Details of a potential solution addressing the problem of topology control are presented in Section 3.4.2.

The utilization of the topology of adjacent or multiple objects concerning active contour models is regarded in the Sections 2.1.3.2. - 2.1.3.6., but a complete topological control with a clearly defined mathematical basis in terms of the defined goals of this thesis is not given in the literature (cf. Section 2.1.4. for a detailed discussion). The synthetic example provided in this chapter is used to identify symbolically the required topology for the proposed new method of network snakes as depicted in Figure 8 on the right side. The graph contains the different connected contour parts representing the topology and enables the derivation of each node with its degree, which has to be integrated in the proposed new method of network snakes. The aim is to point out which mathematical definition is required when optimizing the energy functional of a parametric active contour incorporating the topology.

3.3. Energy terms of network snakes

3.3.1. Influence of the topology to the energy minimization

In the following sections the energy terms of the new method of network snakes are defined to incorporate the topology into the concept of parametric active contours. In this section, the influence of the topology to the energy minimization is examined concerning the different terms of the energy functional. Afterwards, the required new internal energy terms for arbitrary nodes with a degree $\rho(C) > 2$ and for nodes with a degree $\rho(C) = 1$ representing end points of open contours are defined (cf. Section 3.3.2. and Section 3.3.3.). This separation was chosen to ease the presentation of the new mathematical definitions, even though the developments are highly related to each other. The general functionality of network snakes compared to traditional parametric active contours is demonstrated using the introduced synthetic example (Section 3.3.4.).

The traditional concept of parametric active contours including the solution of the energy functional does not provide the introduction of topology to the model. Thus, the influence of the topology to the mathematical model has to be examined to point out further investigations concerning the goals of this thesis (cf. Section 3.1.). A detailed analysis is necessary to identify which energy terms of the parametric active contour model (cf. Equation 2) have to be modified to incorporate the topology control, leading to an optimization of arbitrary networks and the boundaries of adjacent objects.

The influence of the topology to the *image energy* $E_{img}(C(s))$ is nonexistent in terms of the mathematical solvability of the new energy functional of parametric active contours resulting in network snakes. This fact is apparent because the image energy represents the object of interest within the imagery independently of any topological or geometrical constraints. It is unimportant which object appearances such as open contours, closed contours or any kinds of networks are formed by the object. Consequently, the image energy $E_{img}(C(s))$ is not influenced by the topology and can be kept unchanged when developing the new energy functional of network snakes.

Similarly, the influence of the topology to the *constraint energy* $E_{con}(C(s))$ is not relevant. Although the incorporation of any constraints is not considered methodically to avoid the dependency on any conditions and to enable a free optimization of any contour parts, the later introduction of constraints is left open. Obviously, the topology has no influence on the optional constraint energy $E_{con}(C(s))$, because further conditions can be introduced anytime at any contour parts to fulfill special requirements of particular applications. Thus, the introduction of the topology to the concept of parametric active contours does not need to consider special mathematical criteria concerning the influence of the constraint energy $E_{con}(C(s))$.

The influence of the topology to the *internal energy* $E_{int}(C(s))$ is highly significant in terms of the mathematical solvability of the new energy functional for network snakes and, thus, is the central issue concerning this thesis. Regarding the minimization of the energy functional as defined in the Equations 23 - 39 in Section 2.2., a solution of the required Euler equations optimizing the internal energy $E_{int}(C(s))$ is only given for the traditional concept of parametric active contours. The incorporation of topology into the model having the possibility to

represent and optimize arbitrary networks is not defined. The reason is the approximation of the required derivatives with finite differences since they cannot be computed analytically (cf. Equation 35). The consequence of this prerequisite is that each node of the graph requires two neighboring nodes on both sides to build the approximated derivatives. Obviously, this condition is only fulfilled for closed object contours solely composed of nodes with a degree $\rho(C) = 2$ with an identical first and end point of the contour, i.e. $C_0 = C_n$.

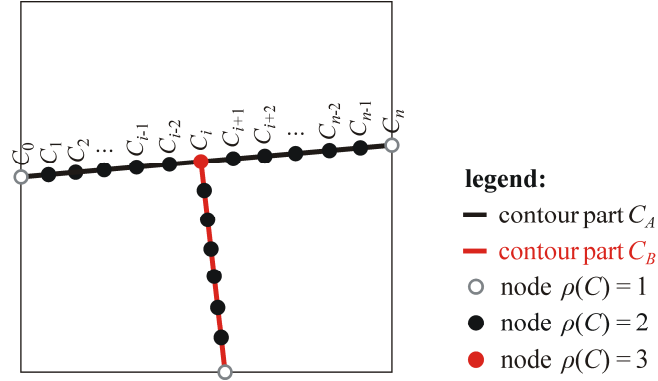


Figure 9: Influence of the topology to the internal energy of the energy functional

In Figure 9 an exemplary parametric active contour is depicted to illustrate the general problem. Initially, the focus is only on the *black contour part* C_A : the second derivative of Equation 34 requires for all nodes C_i one neighboring node on either side, respectively, which are located on the black contour part C_A as C_{i-1} and C_{i+1} (cf. Figure 9, center). Concerning the fourth derivative of Equation 34, the nodes C_{i-2} and C_{i+2} are required additionally resulting in Equation 35. The interesting issue arises if a node with a degree $\rho(C) \neq 2$ is considered, depicted in Figure 9 at the borders of the image for nodes with a degree $\rho(C) = 1$ representing end points and in the center of Figure 9 for an exemplary node with a degree $\rho(C) = 3$ at the position of the node C_i where the *red contour part* C_B is connected resulting in a *contour network*. In this case, the utilized derivatives approximated by finite differences are not defined because the required neighboring nodes are either not available ($\rho(C) = 1$) or exist multiple times ($\rho(C) > 2$). Thus, a new definition of the internal energy $E_{int}(C(s))$ has to be developed to offer the possibility of representing nodes with arbitrary degree enabling a complete shape control of any contour part.

In conclusion, the influence of the topology to the energy minimization of parametric active contours requires a new definition of the *internal energy* $E_{int}(C(s))$ to enable a shape control at any contour part. The new definition of the internal energy is presented in the subsequent Sections 3.3.2. and 3.3.3. First, the new mathematical model for nodes with a degree $\rho(C) > 2$ is introduced allowing the representation of arbitrary graphs. Second, nodes with a degree $\rho(C) = 1$ are addressed to consider the special properties at end points of open contour parts.

3.3.2. New internal energy at nodes with a degree $\rho(C) > 2$

In this section, the new *internal energy* $E_{int}(C(s))$ for the concept of parametric active contours is developed for arbitrary nodes with a degree $\rho(C) > 2$ to enable the optimization of contour networks resulting in the new method of *network snakes*. Regarding the discussed requirements in Section 3.2., the topology is utilized additionally compared to the common used imagery and initialization of traditional active contour models. The aim is to define a mathematically clear solution representing the contour network with its given topology while simultaneously controlling the complete shape of every contour part. The boundaries of adjacent objects will be defined by *single contour parts* each ending in *single nodes*, where several contour parts are connected to each other. Obviously, the same definition is valid for the minimization of networks itself, which cannot be represented by the traditional concept of parametric active contours. Thus, the goal representing a correct topology is ensured during the optimization.

In more detail, the given initial graph representing the topology is divided into separate contour parts C_A, \dots, C_Z connected at nodes C_n with a degree $\rho(C) > 2$. In Figure 10 the synthetic example is taken to exemplarily show the contour parts of the required network: the four contour parts C_A, C_B, C_C and C_D represent the boundaries

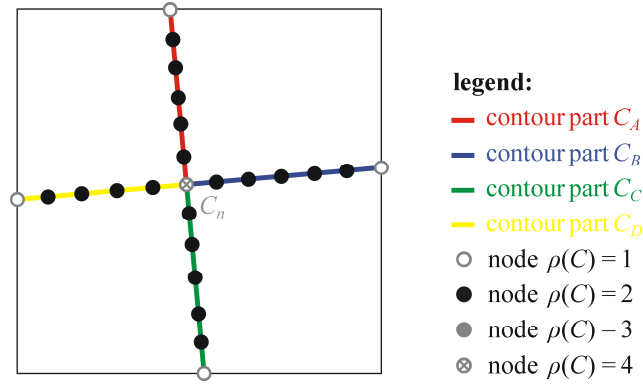


Figure 10: Topology for network snakes

between the adjacent objects, each of them is depicted with a separate color. The contours are connected in the node C_n with a degree $\rho(C) = 4$ (cf. Figure 10, center). In general, the contour parts $C_{A_0, \dots, n}, \dots, C_{Z_0, \dots, n}$ meet with their respective end points C_{A_n}, \dots, C_{Z_n} in the common node C_n in such a way that the end points of the respective contour parts define an identical point, i.e. depending on the number of terminating contour parts $C_n = C_{A_n} = C_{B_n} = \dots = C_{Z_n}$. Thus, the node C_n is contained in each connected contour part representing the topology and, simultaneously, depends on the specific shape model of each contour part. Regarding the given synthetic example in Figure 10, only one common node C_n is required to represent the topology symbolically. In general, an arbitrary number of nodes C_n is possible within the network, each of them defining one point of connected contour parts.

The influence of the topology to the internal energy $E_{int}(C(s))$ was identified as the crucial point (cf. Section 3.3.1.). The approximated derivatives with finite differences are required to control the shape of the contour, but they are not usable in the common way at nodes with a degree $\rho(C) > 2$. Referring to the definition of the internal energy $E_{int}(C(s))$ in Equation 9, two terms are responsible for the shape control of the contour: the first term of the internal energy, weighted by the parameter α , controls the elasticity or tension of the curve, and the second term of the internal energy, weighted by the parameter β , controls the rigidity of the curve. The second and fourth derivatives are required to find a solution of the internal energy contained in the total energy functional $E(C(s))$ within the minimization process (cf. Equation 35).

The first term of the internal energy (cf. Equation 35), weighted by the parameter α is shown as part of the whole energy functional in Equation 40 as

$$\dots + \alpha((C_n - C_{n-1}) - (C_{n+1} - C_n)) + \dots = 0 \quad . \quad (40)$$

This term cannot support the control of the internal energy in the vicinity of C_n during the energy minimization. Regarding one contour part C_A, \dots, C_Z , the finite differences of the first term approximating the required derivatives are only available for the two nodes C_{n-1} and C_n but *not* for C_{n+1} , because this node exists multiple times as an element of the respective connected other contour parts. Thus, no shape control is possible and the first term of the internal energy cannot be considered during the energy minimization in the vicinity of nodes with a degree $\rho(C) > 2$.

The second term of the internal energy, weighted by the parameter β and shown as part of the whole energy functional in Equation 41 as

$$\dots + \beta(C_{n-2} - 2C_{n-1} + C_n) - 2\beta(C_{n-1} - 2C_n + C_{n+1}) + \beta(C_n - 2C_{n+1} + C_{n+2}) + \dots = 0 \quad , \quad (41)$$

can only partly support the control of the shape behavior in the vicinity of C_n . Similar to the first term of the internal energy, the finite differences approximating the required derivatives of this second term are only available for the nodes C_{n-2} , C_{n-1} and C_n , but *not* for the nodes C_{n+1} , and C_{n+2} . Again, the node C_{n+1} and

additionally the node C_{n+2} cannot support the calculation of the internal energy in the vicinity of the C_n , because these nodes belong to multiple available connected further contour parts.

Thus, the shape behavior of the contours represented within the internal energy $E_{int}(C(s))$ and utilized during the minimization of the total energy functional cannot be derived at the node C_n and in the direct vicinity of C_n in a traditional way using the approximations of the derivatives with finite differences. The consequence is to rewrite the internal energy in the vicinity of the nodes C_n using the available finite differences for the nodes C_{n-2} , C_{n-1} and C_n . The new definition of the internal energy aims at controlling the shape of each contour part separately concerning its specific curvature up to each node C_n with degrees $\rho(C) > 2$ contained in the contour network. Simultaneously, the connectivity of the terminating contours at the nodes C_n has to be ensured during the processing.

Equation 42 gives the new definition of the energy functional of network snakes fulfilling the goals of this thesis and considers the mathematical conditions described above. The proposed definition includes a newly developed internal energy valid for every node C_n with a degree $\rho(C) > 2$ and the direct vicinity. Each possible contour part C_A, \dots, C_Z terminating in one common node C_n is represented by one line in the following Equation 42. The new total energy functional for network snakes at the common nodes with a degree $\rho(C) > 2$ with $C_n = C_{A_n} = C_{B_n} = \dots = C_{Z_n}$ is defined as

$$\begin{aligned}
 & \beta(C_{A_n} - C_{A_{n-1}}) - \beta(C_{A_{n-1}} - C_{A_{n-2}}) + f_{C_A}(C_A) = 0 \\
 & \beta(C_{B_n} - C_{B_{n-1}}) - \beta(C_{B_{n-1}} - C_{B_{n-2}}) + f_{C_B}(C_B) = 0 \\
 & \beta(C_{C_n} - C_{C_{n-1}}) - \beta(C_{C_{n-1}} - C_{C_{n-2}}) + f_{C_C}(C_C) = 0 \\
 & \dots \\
 & \beta(C_{Z_n} - C_{Z_{n-1}}) - \beta(C_{Z_{n-1}} - C_{Z_{n-2}}) + f_{C_Z}(C_Z) = 0 .
 \end{aligned} \tag{42}$$

The terms on the left side weighted by the parameter β represent the new internal energy, the other terms $f_{C_A}(C_A), \dots, f_{C_Z}(C_Z)$ represent the image energy at the respective contour parts. Now, all contour parts C_A, \dots, C_Z intersect in the joint and single node C_n and can be optimized *simultaneously* when minimizing the energy functional of network snakes. The energy definition of Equation 42 allows for an energy minimization controlling the shape of each contour part *separately* up to the common node C_n without interacting concerning their particular shape. At the same time, the exploitation of the topology is ensured during the energy minimization process due to the connectivity.

The new definition of the internal energy in the vicinity of nodes with a degree $\rho(C) > 2$ introduced in Equation 42 is similar to the part of the traditionally defined internal energy weighted by the parameter α (e.g. shown in Equation 40). But, the parameter weighting the new internal energy is chosen to be β , because it controls the shape behavior of the contours more naturally compared to α in terms of curvature and rigidity (cf. Section 2.1.2.1).

The new energy functional for network snakes developed above and defined in Equation 42 is given exemplarily for a node with a degree $\rho(C) = 3$, additionally presented in Equation 45 between the dashed lines:

$$\begin{aligned}
 & \frac{\partial E_{img}}{\partial C} \\
 & + \beta(C_{A_{n-2}} + C_{B_{n-2}} + C_{C_{n-2}}) - 2\beta(C_{A_{n-1}} + C_{B_{n-1}} + C_{C_{n-1}}) + 3\beta(C_n) = 0 .
 \end{aligned} \tag{43}$$

The general form can be written in matrix form as

$$A_n C + f_C(C) = 0 . \tag{44}$$

The known substitution used for the energy minimization of traditional parametric active contours to display the matrix A in detail is used here again with $a = \beta$, $b = -\alpha - 4\beta$ and $c = 1 + 2\alpha + 6\beta$ (cf. Equation 37). Furthermore, the new definition of network snakes incorporating nodes with degrees of $\rho(C) > 2$ requires an enhanced procedure for the new matrix A_n . If a node with a degree $\rho(C) = 3$ is to be represented, the further substitutions of $d = 1 + 3\beta$, $e = 1 + \alpha + 5\beta$ and $f = -2\beta$ are necessary; an exemplary matrix A_{n_3} is shown in Equation 45 to present the details:

Matrix A_{n3} shows only one node with a degree $\rho(C) = 3$ and the neighboring elements of the terminating three contour parts C_A , C_B and C_C . Possible further parts of the contour network are ignored to focus only on the definition of the new energy functional. The matrix element enclosed by the two dashed lines represents the node C_n with a degree $\rho(C) = 3$ connecting the three contour parts, contour part C_A on the left/top and contour part C_B in the middle position. The dotted line on the right/bottom marks the beginning of the third contour part C_C . The additionally filled matrix elements besides the banded structure express the connecting parts representing the topology within the matrix. The structure of the matrix A_n points out that the shape of each contour part is controlled independently of any other contour parts contained within the network, because there is no connection of the respective contour ends concerning their specific shape. The only link is given in the single node C_n representing the topology of the three contours within the network.

The described structure of a node with a degree $\rho(C) = 3$ contained in the matrix in Equation 45 can be extended in a straightforward manner to nodes with higher degree. In order to clarify the design of the matrices A_n , an

example of a matrix A_{n4} representing nodes with a degree $\rho(C)=4$ is given in Equation 46. The known substitution is used again with $a=\beta$, $b=-\alpha-4\beta$, $c=1+2\alpha+6\beta$, $e=1+\alpha+5\beta$ and $f=-2\beta$. The possibility to represent nodes with a degree $\rho(C)=4$ requires the additional substitution of $g=1+4\beta$, which represents the node C_n connecting four different contour parts:

$$A_{n4} = \left[\begin{array}{cccc|cccc|cccc|cccc|cccc|cccc} \ddots & \ddots & \ddots & \ddots & & & & & & & & & & & & & & \\ & c & b & a & 0 & \dots & & & & & & & & & & & & \\ & b & c & b & a & 0 & \dots & & & & & & & & & & & \\ & a & b & e & f & 0 & 0 & \dots & & 0 & 0 & & & & 0 & 0 & & \\ \dots & 0 & a & f & g & f & a & 0 & \dots & 0 & f & a & 0 & & 0 & f & a & 0 \\ \dots & 0 & 0 & f & e & b & a & 0 & \dots & 0 & 0 & & & & 0 & 0 & & \\ & \dots & 0 & a & b & c & b & a & 0 & \dots & & & & & & & & \\ & & \dots & 0 & a & b & c & b & a & 0 & \dots & & & & & & & \\ & & & & \ddots & \ddots & \ddots & \ddots & \ddots & \ddots & \ddots & & & & & & & \\ & & & & & & & & & 0 & \dots & & & & & & & \\ & & & & & & & & & 0 & 0 & \dots & & & & & & \\ & & & & & & & & & 0 & 0 & 0 & \dots & & & & & \\ \dots & & & & 0 & f & 0 & & \dots & 0 & 0 & 0 & e & b & a & 0 & \dots & & \\ & & & & 0 & a & 0 & & \dots & 0 & 0 & 0 & b & c & b & a & 0 & \dots & \\ & & & & & & & & \dots & 0 & & & a & b & c & b & a & 0 & \dots \\ & & & & & & & & & & & & \ddots & \ddots & \ddots & \ddots & \ddots & \ddots \\ & & & & & & & & & & & & & & & & 0 & \dots \\ & & & & & & & & & & & & & & & & 0 & 0 & \dots \\ & & & & & & & & & & & & & & & & 0 & 0 & 0 & \dots \\ \dots & & & & 0 & f & 0 & & & & \dots & 0 & 0 & 0 & e & b & a & \ddots & \\ & & & & 0 & a & 0 & & & & & \dots & 0 & 0 & b & c & b & \ddots & \\ & & & & & & & & & & & & \dots & 0 & a & b & c & \ddots & \\ & & & & & & & & & & & & & & & & \ddots & \ddots & \ddots & \ddots \end{array} \right] \quad (46)$$

The structure of the matrix A_{n4} in Equation 46 is enlarged with the fourth contour part starting at the dotted line on the right/bottom side compared to Equation 45. Again, the focus is only on one node C_n with a degree $\rho(C)=4$ and its neighboring contour parts, other possible parts of the contour network are ignored. Concluding, this identified structure of the matrices A_n representing nodes with arbitrary degrees is straightforward for every nodes with higher degrees as defined in Equation 42.

3.3.3. New internal energy at end points

The new *internal energy* $E_{int}(C(s))$ needs to be extended for the nodes with a degree $\rho(C)=1$ which up to now has not been considered in order to enable the optimization of *end points* representing open contour parts within the framework of *network snakes*. Thus, the optimization of contour networks with arbitrary nodes will be achieved. Again, the aim is to define a mathematically clear solution which represents open contour parts of a network with its given topology and, simultaneously, which comprises a complete shape control of these contour parts (cf. Section 3.3.2.). Solutions such as the fixing of end points during the energy minimization process are not desired, because a free optimization of any contour parts of the network is aimed including a complete shape control up to the end points.

Open contour parts are represented within a network as contours C_A, \dots, C_Z with end nodes C_{A_0}, \dots, C_{Z_0} having a degree $\rho(C)=1$, respectively. Thus, no further contour parts are connected at those points; an example of open contour parts is given in Figure 10 at the image borders. Here, only the case of *one* end point of an open contour

is regarded, but obviously a contour part can have open ends on both sides. Similarly as defined in the above Section 3.3.2. for nodes with a degree $\rho(C) > 2$, the crucial point of nodes C_0 with a degree $\rho(C) = 1$ is the approximation of the derivatives with finite differences, which are required to control the shape of the contour during the energy minimization.

Regarding the first term of the internal energy, weighted by the parameter α and shown as part of the whole energy functional in Equation 40, the term cannot support the control of the internal energy at the node C_0 and in the vicinity of C_0 during the energy minimization. The development of a new definition of the internal energy requires a solution to consider open contours within the framework of network snakes. The finite differences of the first term approximating the utilized derivatives are only available for the two nodes C_0 and C_1 , but obviously *not* for the node C_{-1} , because this node does not exist. Thus, no shape control is possible and the first term is once more not considered during the energy minimization at the node C_0 and in the vicinity of nodes with a degree $\rho(C) = 1$.

The second term of the internal energy, weighted by the parameter β and shown as part of the whole energy functional in Equation 41 can aid the control of the shape behavior in the vicinity of C_0 partly. Similar to the definition concerning nodes with a degree $\rho(C) > 2$, the second term is rewritten using the available finite differences for the nodes C_0 , C_1 and C_2 of the open contour part to control the curvature at nodes with a degree $\rho(C) = 1$. Obviously, the nodes C_{-1} and C_{-2} cannot support the internal energy in the vicinity of C_0 , because these nodes are not available at open contour parts. Consequently, the new total energy for network snakes at a node with a degree $\rho(C) = 1$ is defined as

$$\beta(C_{A_0} - C_{A_1}) - \beta(C_{A_1} - C_{A_2}) + f_{C_A}(C_A) = 0. \quad (47)$$

Now, open contour parts C_A, \dots, C_Z can be optimized at the node C_0 and in the vicinity of end points C_0 within the framework of network snakes. The energy definition of Equation 47 allows for an energy minimization controlling the shape of open contour parts up to the nodes C_0 .

The new energy functional for network snakes defined for open contour parts in Equation 47 can be written in matrix form equivalent to Equation 44. Similarly, the characteristics of the new matrix A_n are the same as described in Section 3.3.2. The required adaptation of Equation 36 representing traditional parametric active contours is highlighted for open contour ends in Equation 48. The known substitution used for the energy minimization of network snakes (cf. Section 3.3.2.) is used again with $a = \beta$, $b = -\alpha - 4\beta$ and $c = 1 + 2\alpha + 6\beta$. Additionally, the new definition of network snakes including nodes with a degree $\rho(C) = 1$ requires the substitution with $e = 1 + \alpha + 5\beta$ and $f = -2\beta$. An exemplary new matrix A_{n1} is shown in Equation 48 to present the details of the incorporation of open contour ends:

$$A_{n1} = \begin{bmatrix} a & f & a & 0 & \dots & & & & \\ f & e & b & a & 0 & \dots & & & \\ a & b & c & b & a & 0 & \dots & & \\ 0 & a & b & c & b & a & 0 & \dots & \\ & \ddots & \ddots & \ddots & \ddots & \ddots & \ddots & \ddots & \\ & \dots & 0 & a & b & c & b & a & 0 \\ & & \dots & 0 & a & b & c & b & a \\ & & & \dots & 0 & a & b & e & f \\ & & & & \dots & 0 & a & f & a \end{bmatrix}. \quad (48)$$

The matrix A_{n1} focuses only on the nodes with a degree $\rho(C) = 1$ and the neighboring elements, possible other parts of the contour network are ignored. The two matrix elements at the very left/top and at the very right/bottom represent a node C_0 of an open contour end. The new definition and structure given in Equation 48 points out that the shape control of every contour part is possible up to the end point.

One additional problem concerning open contours arises due to the definition of the internal energy of parametric active contours, which is generally unsolved: contours have the tendency to *shrink* during the energy minimization. The reason for this fact is the approximation of the internal energy with finite differences (cf.

Section 2.1.2.1. and for details Section 2.2.). Two arbitrary neighboring nodes C_i and C_{i+1} will contribute nothing to the energy of the energy functional if they converge to one single point, which is why a contour generally shrinks. This effect applies to closed contours, too, but other energy terms such as the standard required image energy or the optional balloon energy counteract this process (cf. Section 2.1.2.1. for further details). However, these energy terms cannot prevent shrinking of open contours. One possible solution of the problem is a very prominent blob within the image representing the end point, which chains the end point of a contour to prevent the shrinking process during energy minimization. However, this fact cannot be guaranteed at all, which is why a methodical solution is strived. A reasonable answer can be the introduction of an additional term to the energy functional: the conservation of the distances between neighboring nodes C_i and C_{i+1} can be reached by minimizing the difference of the distance $d = C_i - C_{i+1}$ before and after each iteration step between two neighboring nodes. This solution preserves the length of an open contour, but requires a given correct initial length, which is an additional constraint.

3.3.4. Synthetic example

The general functionality of the developed new method of network snakes is demonstrated in this section using the synthetic example introduced in Figure 6 (right). The starting point is again a topologically correct initialization as depicted in blue in Figure 11 and Figure 12 on the left side. Contrary to traditional parametric active contours, the four regions of the image are represented and delineated simultaneously with one contour using the proposed new method of network snakes. The four contour parts C_A, \dots, C_D are connected at the common node C_n with a degree $\rho(C) = 4$ describing the objects of interest in the image incorporating the given topology (cf. Figure 10). Each contour part is assumed to consist of six nodes C_0, \dots, C_5 , the number is arbitrarily chosen aiming at a concrete example with a completely given matrix $A_{example}$. The new energy functional of network snakes defined in the Sections 3.3.2. and 3.3.3. above is taken to set up Equation 44 with a special focus on the new matrix A_n representing the topology of the contour network. The known substitution for the energy minimization of network snakes is used with $a = \beta$, $b = -\alpha - 4\beta$, $c = 1 + 2\alpha + 6\beta$, $e = 1 + \alpha + 5\beta$, $f = -2\beta$ and $g = 1 + 4\beta$ to define the complete matrix $A_{example}$ of the synthetic example:

$$A_{\text{example}} = \begin{array}{cccccc|cccc|cccc|cccc} a & f & a & 0 & \dots & & & & & & & & & & \\ f & e & b & a & 0 & \dots & & & & & & & & & \\ a & b & c & b & a & 0 & \dots & & & & & & & & \\ 0 & a & b & c & b & a & 0 & \dots & 0 & 0 & & & 0 & 0 & \\ \dots & 0 & a & b & e & f & 0 & 0 & \dots & 0 & f & a & 0 & & 0 & f & a & 0 \\ \hline \dots & 0 & a & f & g & f & a & 0 & \dots & & 0 & 0 & & & 0 & 0 & \\ \hline & \dots & 0 & 0 & f & e & b & a & 0 & \dots & & & & & & & \\ & & \dots & 0 & a & b & c & b & a & 0 & \dots & & & & & & \\ & & & \dots & 0 & a & b & c & b & a & 0 & \dots & & & & & \\ & & & & \dots & 0 & a & b & e & f & 0 & 0 & \dots & & & & \\ & & & & & 0 & \dots & 0 & a & f & a & 0 & 0 & 0 & \dots & & \\ \hline & & 0 & f & 0 & & \dots & 0 & 0 & 0 & e & b & a & 0 & \dots & & \\ & & 0 & a & 0 & & & \dots & 0 & 0 & b & c & b & a & 0 & \dots & \\ & & & 0 & & & & & \dots & 0 & a & b & c & b & a & 0 & \dots \\ & & & & & & & & & \dots & 0 & a & b & e & f & 0 & 0 & \dots \\ & & & & & & & & & & \dots & 0 & a & f & a & 0 & 0 & 0 & \dots \\ \hline & & 0 & f & 0 & & & & & & \dots & 0 & 0 & 0 & e & b & a & 0 & \dots \\ & & 0 & a & 0 & & & & & & & \dots & 0 & 0 & b & c & b & a & 0 \\ & & & 0 & & & & & & & & & \dots & 0 & a & b & c & b & a \\ & & & & & & & & & & & & & \dots & 0 & a & b & e & f \\ & & & & & & & & & & & & & & \dots & 0 & a & f & a \end{array}. \quad (49)$$

The matrix element enclosed by the two dashed lines represents the node C_n with a degree $\rho(C) = 4$ connecting the four contour parts C_A, \dots, C_D , the additionally dotted lines mark the beginning and end of the respective contour parts. The additionally filled matrix elements besides the banded structure express the connecting parts representing the topology within the matrix. Moreover, the omitted elements of the matrix $A_{example}$ point out that there is no connection of the contour ends concerning their specific shape. The only link is given in the single node C_n representing the topology of the four contours within the network. Each contour part C_A, \dots, C_D is connected to the common node C_n on one end, and has an open contour end on the opposite side. The open contour endings of the four contour parts are chained to the image borders and are allowed to move only along the borderline, i.e. the x or y coordinate is fixed, respectively.

The new definition of parametric active contours introducing the topology to the energy minimization process enables an optimization of nodes with arbitrary degree including a complete shape control of each contour part separately. The energy minimization of the synthetic example using network snakes is depicted in Figure 11 and in Figure 12 to demonstrate the general functionality: starting from the initialization (blue), the contour optimizes step by step (white) to the desired result (red). The given initial topology is maintained during the energy minimization process and, moreover, is exploited. For example, the contour part C_A (top) is not close to the desired object boundary at the beginning, but the exploitation of the topology as a result of the connection of the contour part to the network pulls the contour part C_A to the true object boundary (cf. Figure 12). Focusing on the center of the synthetic example (dashed white line), no gaps or overlaps arise: compared to the result of traditional parametric active contours (Figure 7, center) and the zoomed result part (Figure 7, right), the new method of network snakes preserves by definition the topology during the optimization leading to a correct result (Figure 11, center) and zoomed result part (Figure 11, right). The zoomed result of Figure 7 (right) is depicted in Figure 11 (right) as dashed light red contour to provide a simplified comparison.

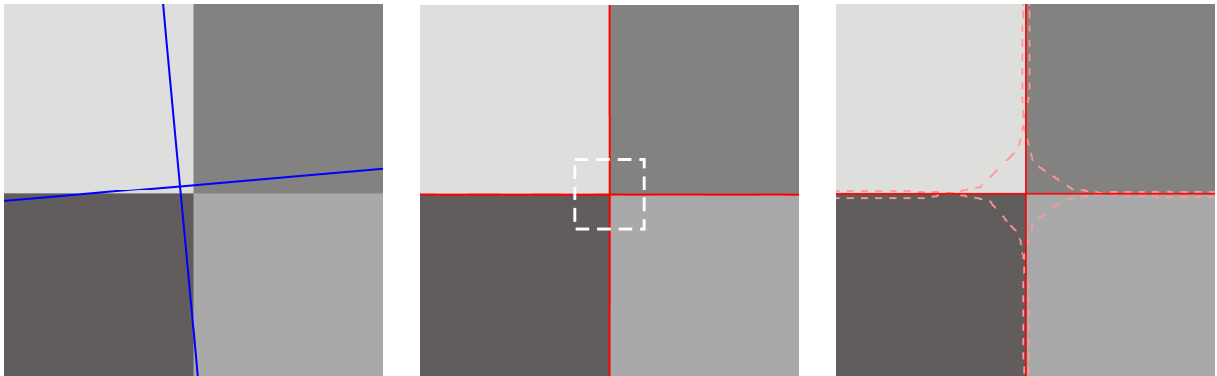


Figure 11: Delineating adjacent objects with network snakes: initialization (blue), result and zoomed result part (red); dashed contour part (light red) as comparison to traditional parametric active contours shown in Figure 7

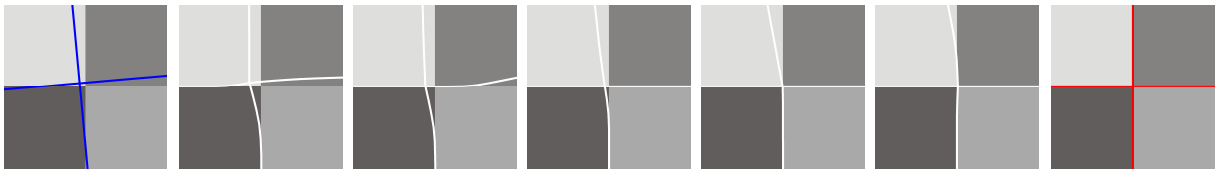


Figure 12: Delineating adjacent objects with network snakes: initialization (blue), optimization steps (white) and result (red) of Figure 11

3.4. Implementation

3.4.1. Realization

In this section, general implementation questions regarding the *realization of the system* of network snakes are examined. The introduction of an optional topology-preserving energy and the required parameters including their control are found in the subsequent Section 3.4.2. and Section 3.4.3., respectively. The new mathematical definitions of the energy functional introduced in the previous Section 3.3. are implemented in an object-based computer language. Two general tasks are regarded here which must be considered realizing the system of network snakes: the unit distances of neighboring nodes during the energy minimization process and the stopping criterion used for the required iterative solution.

Unit distances of neighboring nodes

The solution of the energy functional of network snakes utilizes the approximation of the derivatives with finite differences representing the internal energy (cf. Section 2.2. and Section 3.3.). Thus, the energy minimization process assumes *unit distances* between neighboring nodes representing the shape behavior of the contour during the complete energy minimization process. This prerequisite is important because parameterization changes are unwanted and lead to shape modifications. Avoiding reparameterizations during the minimization process, a preservation of unit distances between neighboring nodes has to be considered in the energy functional. The proposed solution minimizes the difference of neighboring node distances at all nodes of the contour and incorporates this additional term in the energy minimization framework of network snakes:

$$|C_{i-1} - C_i| - |C_i - C_{i+1}| \rightarrow \text{Min} . \quad (50)$$

Thus, the neighboring distances at any node C_i with $i = 1, \dots, n-1$ are aimed to be equal to both sides of the node during the energy minimization process enabling a correct approximation of the derivatives with finite differences. Obviously, this condition is fulfilled for the nodes of each contour part separately and only for nodes with a degree $\rho(C) = 2$, because adjacent contour parts are independent in terms of their shape control represented by the internal energy.

Stopping criterion of energy minimization

The solution of the total energy functional is achieved with an iterative method (cf. Section 2.2. and Section 3.3.). This procedure requires both an initialization and a *stopping criterion* to finish the minimization of the energy functional. Different approaches are feasible to stop the processing: from a methodical point of view, the energy minimization has converged, when the movement of the contour network is zero. The stopping criterion is practically activated when the movement is below a specified threshold. The reason is that for example small movements are caused by a persistent jumping of the contour between pixels. The solution is a modification of the parameter control during the last iteration steps to halve the step size γ (cf. Section 2.2.) or to calculate an average of the last positions of the contour network. Independent of the chosen stopping criterion, the number of iterations is identical for every contour part contained in the network, even though some parts may have already converged, because the minimization of the contour network is done simultaneously exploiting the topology.

3.4.2. Topology-preserving energy

The introduction of topology to the concept of parametric active contours aims to enable the optimization of arbitrary networks and delineation of adjacent objects. Moreover, the goal is to *exploit* the topology during the minimization of the energy functional allowing for coarser initializations of the contour or less concise object characteristics within the image. Obviously, the requirement is a given topology which is assumed to be correct and, in addition, the exploitation of the topology during the energy minimization process presumes the *preservation* of this initial topology during the optimization of the energy functional (cf. Section 3.2.4.). This presumption cannot be guaranteed in general, because close contour parts can merge or nodes with higher degrees can move around each other. These undesired effects mean that the criteria of a planar graph and a fixed

topology can no longer be satisfied. Thus, the preservation of the topology must be ensured within the complete processing to avoid touching or crossing contour parts changing the initial correct topology.

To solve this problem, a *topology-preserving energy* $E_{topo}(C(s))$ is introduced in this section to conserve the topology during the complete processing to avoid touching or crossing contour parts. The goal is to satisfy the criteria of a planar graph during the energy minimization to guarantee an optimal exploitation of the topology. Hence, the positioning of neighboring contour parts within the network is monitored and controlled during the processing.

The proposed *topology-preserving energy* $E_{topo}(C(s))$ conserving the given topology during the complete processing is defined as:

$$E_{topo}(C(s)) = \frac{1}{d_{topo}(C(s))^2} . \quad (51)$$

The parameter $d_{topo}(C(s))$ with $0 < d_{topo} < d_{max}$ describes the distance between two neighboring contour parts. Consequently, a convergence of two contours becomes more and more expensive within the energy minimization process and, thus, practically inhibits merging. The distance is not introduced as a linear force, because the interesting point of control arises when object contours are *close* to each other. In addition, the influence of the topology-preserving energy to the total energy functional can be restricted by an upper limit d_{max} , because neighboring contours will only influence each other within a specific spacing. The weighting of the topology-preserving energy $E_{topo}(C(s))$ compared to the other energy terms of the total functional has to be done in a manner in which it is activated only when two contours converge. The behavior of two contour parts far away is not influenced, because the image and internal energy superimpose the proposed topology-preserving energy at those parts. In the vicinity of nodes with a degree $\rho(C) > 2$ representing the junctions of a contour

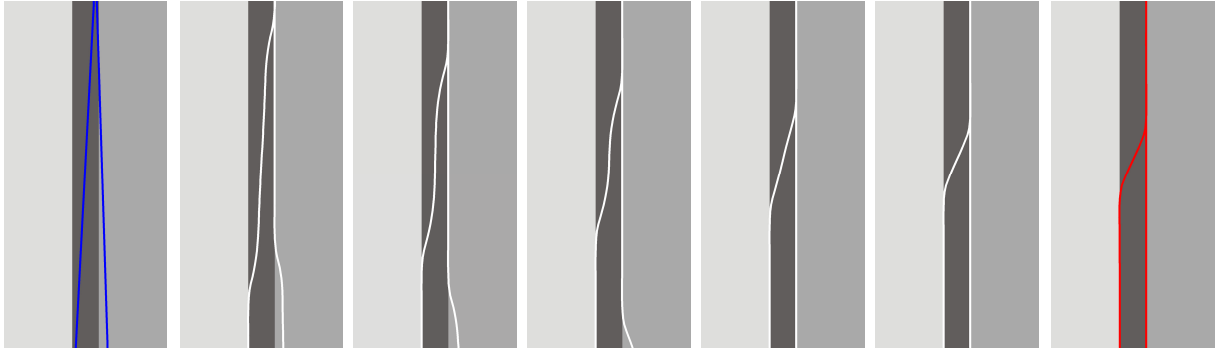


Figure 13: Traditional parametric active contours: initialization (blue), optimization steps (white) and result (red)

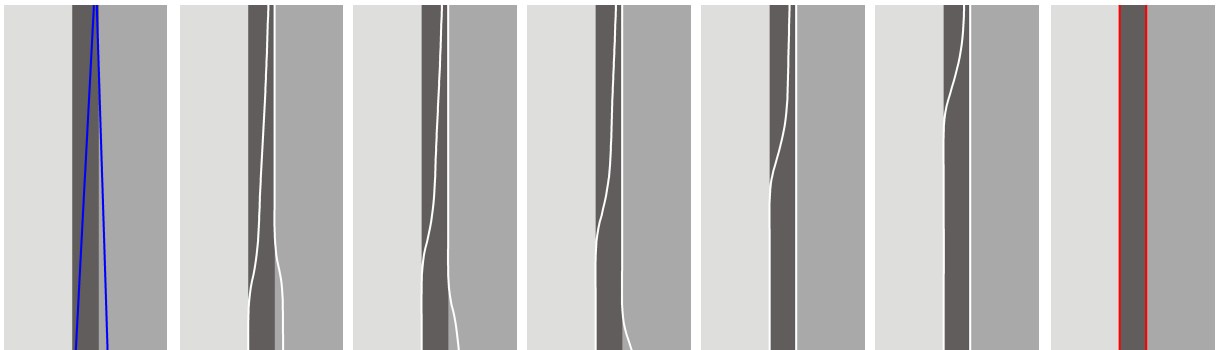


Figure 14: Parametric active contours with topology-preserving energy: initialization (blue), optimization steps (white) and result (red)

network, the topology-preserving energy is not considered due to the intended convergence. The distance of neighboring contour parts must be calculated at each iteration step, but depending on the application, a speed up by less frequent calculations is possible.

In Figure 13 a synthetic example of a traditional parametric active contour as part of a contour network is shown. The starting point are two separate contours (depicted in blue), which merge very fast during the optimization (depicted in white) leading to an obviously wrong result (depicted in red). The reason is very plausible, because due to the image energy the left contour moves to the closest object border, which is at the upper part within the synthetic example the right one. The existence of a second contour is without any consequence here, because this fact is not considered in the traditional framework of parametric active contours. The introduction of the new topology-preserving energy $E_{topo}(C(s))$ to the minimization process yields a correct result as shown in Figure 14 using the same synthetic example. The starting point is again the two separate contours (depicted in blue), but now the topology-preserving energy avoids a merging of the contour parts (depicted in white). Instead, each contour moves step by step to the desired true object boundary yielding the correct result (depicted in red). Thus, the new energy definition enables the exploitation of topology during the energy minimization of network snakes preserving the initial topology over the complete optimization.

3.4.3. Parameters

The energy functional of network snakes is controlled by several parameters. The parameters comprise the image energy $E_{img}(C(s))$, the internal energy $E_{int}(C(s))$, the optional *constraint energy* $E_{con}(C(s))$ and the topology-preserving energy $E_{topo}(C(s))$. All four energy terms can be manipulated to optimize the respective function separately and, in addition, can be weighted against each other to control the influence of each energy term to the total result of the energy functional.

The *image energy* $E_{img}(C(s))$ as part of the total energy functional of network snakes is independent of any parameters and, thus, is incorporated in the energy functional as a constant energy without the control of any parameters during processing. However, the generation of the image energy offers several possibilities, which can include the setting of parameters aiming at the derivation of an optimal description of the object of interest in the image (cf. Section 2.1.2.1. for a detailed discussion). Optionally, the general constant image energy can be adapted during the processing, if it is required for a particular application. For example, the utilization of scale space can be reasonable to initially pull the contour to a coarse solution and, finally, to delineate the precise position of the contour network using the highest resolution of the image.

The *internal energy* $E_{int}(C(s))$ is influenced by two parameters $\alpha(s)$ and $\beta(s)$, see Section 2.1.2.1. for details. The first term of the internal energy, weighted by the parameter $\alpha(s)$, controls the elasticity or tension of the curve. The second term of the internal energy, weighted by the parameter $\beta(s)$, controls the rigidity of the curve. The parameters $\alpha(s)$ and $\beta(s)$ are predefined based on the modeled shape characteristics of the object of interest to incorporate the prior known object characteristics into the total energy functional. The control between the parameters $\alpha(s)$ and $\beta(s)$ is generally chosen with a high weight concerning the second term of the internal energy, because the second term models the shape behavior more naturally in terms of the curvature of the contour compared to the first term, which in addition tends to shrink the contour. The parameters are often taken to be constant during the optimization, but an adaptation during the energy minimization process is possible to change the shape behavior or to control different contour parts individually due to varying shape characteristics. A further opportunity is to define the parameters of the internal energy automatically with given reference contours in terms of a supervised parameter tuning. In this case, the manual definition of $\alpha(s)$ and $\beta(s)$ is not necessary.

In general, the optional *constraint energy* $E_{con}(C(s))$ needs no parameters to weight its internal conditions. This fact is founded by usual constraints such as the fixing of particular points or parts of the contour network, when additional available knowledge facilitates those conditions. Accordingly, the introduction of the constraint energy can be done without any parameter control.

The optional *topology-preserving energy* $E_{topo}(C(s))$ is introduced to the total energy functional to preserve the given topology during the complete energy minimization process (cf. Section 3.4.2.). The influence of the topology-preserving energy to monitor the distance d_{topo} between two neighboring contour parts can be restricted by an upper limit d_{max} , because neighboring contours will only influence each other within a specific spacing. Thus, the control of the spacing where the topology-preserving energy is activated is the only parameter to be

defined. In addition, the spacing includes areas in the immediate vicinity of nodes with a degree $\rho(C) > 2$ representing the connectivity of a contour network, where the topology-preserving energy is not considered due to the intended convergence.

Besides the setting of the individual parameters of the above mentioned energy terms of network snakes, the control of the different energy terms *against each other* incorporated within the total energy functional are of special interest. In particular, the weight between the image energy $E_{img}(C(s))$ and the internal energy $E_{int}(C(s))$ controlled by the parameter κ is an important means to include modeled knowledge in the minimization process (cf. Section 2.1.2.1). The shape characteristics of the contours are important in defining the extent of the image force. For instance, different shape characteristics of the object of interest compared to image disturbances or noise contained in the image energy can allow for strong internal energies exploiting the shape model to ignore non-purposive image properties. On the other hand, concise image features describing the object of interest very comprehensively facilitate the choice of strong image features. To summarize, the parameter κ has to be defined based on the image information compared to the shape characteristics depending on the specific problems to be solved.

The weighting of the topology-preserving energy $E_{topo}(C(s))$ compared to the image energy and the internal energy of the total functional has to be done in a manner that it is only activated when two contours are close to each other and tend to converge. The behavior of two contour parts far away is not influenced, because the image and internal energy overlay the topology-preserving energy at those parts. Thus, the weight of the topology-preserving energy has to be chosen to act only as dominant energy term when two contours are close to each other.

The energy functional includes the parameter γ to define the step size during the iterative processing (cf. Section 2.1.2.1). Large values allow for a fast convergence of the contour network, but tend to jump over the true object boundaries at the last iterations of the energy minimization. The reason is the fact that for example small movements caused by a persistent jumping of the contour between pixels cause a multiplication of the movement as result of a large γ . Thus, a modification of the parameter control during the last iteration steps to halve the step size γ or to calculate an average of the last positions of the contour network is appropriate (cf. Section 3.4.1).

3.5. Discussion

In this section the developed new method of network snakes is discussed to highlight the reached goals and to name the deficits in terms of the general proposed method. Obviously, a comprehensive discussion including the analysis of network snakes can only be given at the end of the thesis.

The first aim was to optimize any kinds of contour networks with nodes with arbitrary degrees. The solution of this aim can only be represented with the concept of parametric active contours as argued in the concluding discussion of the state of the art (cf. Section 2.1.4.). Thus, the developed new method is based on the concept of parametric active contours incorporating the topology in the model to optimize arbitrary networks. The second aim was to segment images without gaps or overlaps. This goal has the identical solution, because the boundaries between adjacent objects represent a network, too. The new method of network snakes enables the optimization of *any kinds of nodes* of an arbitrary graph including a *complete shape control* without the requirement of constraints developing a solution with a *clear mathematical definition* (cf. Section 3.3.). The third aim claims a new method of active contour models with a high generality and transferability concerning the delineation of adjacent objects and any kinds of networks. The goal is not a solution being only applicable for a particular application with for instance particular image data considering particular boundary conditions, but a *general method* with the possibility to transfer the solution to various applications. This aim has been achieved on the basis of the new mathematical definition; a further analysis will be given in Chapter 4.

One important innovation of this thesis is the introduction of topology to active contour models and, moreover, the *exploitation of the topology* during the energy minimization process. The goal is to overcome poor or fragmented object representations within the imagery utilizing the topology of the objects of interest. In addition, some contour parts could be only detectable when exploiting topology. Consequently, a high quality is demanded regarding the initial given topology to be used and, furthermore, is claimed in terms of the preservation of the topology during the minimization of the energy functional. The second requirement is considered using the proposed topology-preserving energy (cf. Section 3.4.2.), but the first item is up to now not

covered. In general, the exploitation of topology can allow for coarser initializations of the contour or less concise object features within the image. The question on to which extent the topology can support the optimization process, in particular the dependencies to the initialization, the iteration behavior, the object properties and the image quality, will be part of investigations in Chapter 4. A problem still unsolved at this point is the influence of a wrong topology to the new method of network snakes, because the initial given topology is assumed to be correct. The question of how a wrong topology affects the final result of the correct parts of the graph will be part of further analysis as well.

One general limitation of active contour models are *open contour ends*: while the new mathematical definition of network snakes enables a complete shape control up to the end point of open contours, the internal energy representing the shape characteristics of the object of interest causes a contour shrinking. Approaches to preserving the contour length or to fix the end points are a possible solution, but a mathematically clear and general solution is not yet given. Thus, the treatment of end points within a contour network has to be done depending on the specific application.

Network snakes need an *initialization* close to the true object boundary, because parametric active contours are based on a local minimization process. Thus, an initialization has to be derived within a preceding step. The question of how a close initialization can be defined precisely is at this point unanswered. Examinations regarding the initialization in the context of topology, object properties and image quality will be part of Chapter 4.

4. Results and analysis

In this chapter the new method of network snakes is analyzed and evaluated. The objective is to point out to which extent the new method can facilitate the established aims and requirements given in Chapter 1. First, the goals of the analysis are stated to define the different relevant topics concerning the investigations and their relations to each other. In addition, a framework is specified for the analysis and evaluation. Second, the general contents of the analysis concerning the initialization requirements, the parameter control, the iteration behavior and the topology are implemented with exemplary synthetic data to emphasize the benefits and limitations of the proposed new method of network snakes. A special focus is on the introduction of the topology to analyze the contribution and effects to the other investigated contents. Third, the generality and usability is demonstrated with results and their analysis of a real application scenario regarding the delineation of field boundaries from high-resolution satellite imagery. Fourth, the transferability of the new method of network snakes is exemplified with the delineation of adjacent cells in medical image data discussing the derived results.

4.1. Goals of the analysis

The main goal of the analysis is to highlight the benefits and limitations of the proposed new method of network snakes developed in Chapter 3. The focus is on those topics which result from the newly introduced topology to the concept of parametric active contours resulting in network snakes. The interesting point to be analyzed is the question of what kind of potential from active contours can be tapped exploiting the topology during the optimization of the energy functional. Thus, the influence of the topology to the characteristics and behavior of parametric active contours achieved with the new method of network snakes is investigated and, in addition, the respective dependencies among each other are regarded. Taking up the goals of this thesis and their investigations concerning the state of the art in Section 2.1.4., the following topics are content of the analysis and evaluation of network snakes.

- Initialization:

Network snakes are based on the concept of parametric active contours. Hence, an initialization close to the true object boundary is required to enable the local optimization process. The aim of the analysis is to formulate rules, how a close initialization is defined and which requirements have to be considered. Furthermore, dependencies between the shape characteristics of the object of interest, the image characteristics and the initialization are content of the investigations. Particular attention is directed towards the relation of the initialization to the topology analyzing advances of the initialization process arising from the exploitation of the topology.

- Parameter control:

The minimization of the energy functional of network snakes is controlled by parameters representing the model of the object of interest within the image data. The influence of the different variables, especially the weight of the internal energy and the weight between internal and image energy, has to be examined when using network snakes. The aim is to derive general statements dependent on the object characteristics and to discover how robust the parameter control is affected by variations. Again, relations to the topology are of particular interest and, in addition, to the initialization and iteration behavior. The content of the analysis is to control the parameters not only based on the object model, but to consider the initialization requirements and topology in the process of parameter setting.

- Iteration behavior:

The optimization of the energy functional of network snakes is obtained by iterative processing. The aim is to analyze how fast the convergence of the contour network can be achieved and which parameters influence the minimization process. The derivation and verification of strategies is intended to enable a speed up of the iteration behavior. In addition, the connection of the iteration behavior to the initialization requirements of the contour network and to the parameter control during the energy minimization is the content of further

investigations. In particular, the dependency of the iteration behavior concerning the utilization of the topology is of interest to be analyzed.

- Topology:

The introduction of topology to parametric active contours is the main innovation of this thesis to enable the delineation of arbitrary degrees of nodes within a graph representing networks or adjacent objects. The question is to which extent network snakes can improve results or allow for coarser initializations of the contour. The aforementioned dependencies of the initialization, parameter control and iteration behavior have to be analyzed to evaluate the exploitation of the topology during the energy minimization process. In addition, the relation of the topology to the image data representing the object of interest is a prominent part of the examinations to point out the contribution of the topology to overcome disturbances or less concise and fragmented image features. Network snakes require a correct topology to be exploited during energy minimization. Consequently, an important point is the analysis of this assumption and the impact of a given wrong topology to the final result of the correct parts of the graph.

- Generality and transferability:

The goal of network snakes is the generality and transferability of the developed mathematical model. Thus, the applicability of the new model has to be tested with different synthetic and real application scenarios to evaluate this purpose. The aim is to analyze with exemplarily synthetic data whether the generality of the proposed new method can be assured. The transferability of network snakes is investigated with the application to different real image data to analyze and evaluate results of varying scenarios. Quality measures have to be derived with reference data to point out to which extent the proposed new method can improve specific applications compared to traditional solutions.

The listed goals concerning the analysis and evaluation of the new method of network snakes need different implementation strategies. The examination of every goal in a common process is impossible due to the extensive and complex problem and, thus, is divided into sub-questions. The goals of the analysis can be treated individually before a more comprehensive view is taken. At first, the more general questions concerning the initialization requirements, the parameter control and the iteration behavior are investigated independently of each other with synthetic data to simplify the analysis in a clearly defined framework (cf. Section 4.2.1. - 4.2.3.). Afterwards, the relations to the respective other goals to be analyzed are regarded with a special focus to the introduced topology. In addition, the contribution of network snakes exploiting the topology during energy minimization is examined and evaluated concerning the given quality of the topology using synthetic data (cf. Section 4.2.4.). Second, the generality and transferability of the proposed new method is applied to a real scenario: the delineation of field boundaries from high resolution satellite imagery (cf. Section 4.3.). The introduction and exploitation of the topology to the active contour models is a central point to be analyzed. Furthermore, the results regarding the initialization, the parameter control and the iteration behavior using synthetic data are verified with the real application scenario. The quality of the derived results of the application is evaluated with reference data yielding statements concerning the completeness, correctness and geometric accuracy. Third, the transferability is emphasized with a different application from the bio-medical sector delineating adjacent cells in microscopic cell imagery (cf. Section 4.4.). Again, the new method of network snakes is analyzed and evaluated regarding the more general questions mentioned above using this real application scenario. In addition, the derived results of the application are evaluated with reference data to obtain quality measures about completeness, correctness and geometric accuracy.

The analysis and evaluation of network snakes concerning the transferability to different real applications is carried out using the quality measures completeness, correctness and geometric accuracy. The *completeness* represents the part of the reference that matches the extraction within a specified buffer around the extraction result. The completeness $\in [0,1]$ is defined as

$$completeness = \frac{l_{ref_mat}}{l_{ref}}, \quad (52)$$

where l_{ref} defines the length of the reference and l_{ref_mat} defines the respective length of the matched reference. Both lengths are approximated with the number of nodes, which represent the contour parts of the graph. Obviously, the distance between neighboring nodes is equal to enable the calculation of the respective length of the reference and matched reference.

The *correctness* represents the part of the extraction which matches the reference within a specified buffer around the reference. The correctness $\in [0,1]$ is defined as

$$correctness = \frac{l_{ext_mat}}{l_{ext}}, \quad (53)$$

where l_{ext} defines the length of the extraction and l_{ext_mat} defines the respective length of the matched extraction. Again, both lengths are approximated with nodes of an equal distance, which represent the contour parts of the graph.

The *geometric accuracy* of the results is evaluated with the *root mean square* (rms) of the differences between reference and extracted result. The rms $\in [0, \text{buffer width}]$ is defined as

$$rms = \sqrt{\frac{1}{n} \sum_{i=1}^n d_{ext_ref}^2}, \quad (54)$$

where d_{ext_ref} defines the shortest distance between a matched node of the extraction to the reference, the parameter n is the number of matched nodes.

4.2. Synthetic examples

4.2.1. Analysis of the initialization requirements

The starting point of the optimization of the energy functional $E(C(s))$ defining network snakes is a given *initial* contour network. The initialization is a prerequisite for any parametric active contour models, since the minimization of the energy functional is solved with an iterative procedure (cf. Section 3.2.3). In addition, the concept of parametric active contours needs an initial contour *close* to the true object boundary, because the optimization of the energy functional considers only the local environment of the current contour position (cf. Section 2.2.). The question of what a close initial contour implies in this context has not been answered with general requirements in terms of minimum distances or similar specifications. In the literature, a comprehensive analysis of this problem so far does not exist, rather only partial solutions for overcoming the problem of sensitivity against the initialization or solutions to increase the capture range allowing for initializations farther away are discussed (cf. Section 2.1.3.2.). Thus, the initialization requirements concerning parametric active contours with a main focus on the proposed new method incorporating the topology to the model are analyzed in this section. There are dependencies between the initialization, the image characteristics compared to the modeled object characteristics, the parameter control of the energy functional and the topology of the objects of interest, which have to be incorporated in a comprehensive analysis afterwards.

The solution of the energy functional of network snakes utilizes the approximation of the derivatives with finite differences representing the internal energy (cf. Section 3.3.). Thus, the energy minimization process assumes *unit distances* between neighboring nodes representing the shape behavior of the contour. This prerequisite is solved in Section 3.4.1. where unit distances are obtained during the complete energy minimization process enabling a correct approximation of the derivatives with finite differences. Thus, this requirement of the initialization and processing is accepted and not further regarded during the analysis.

In addition, an appropriate *number* of nodes representing the object contours has to be ensured. Only a sufficient number of nodes can represent the shape characteristics of the contour due to the approximation of the derivatives of the internal energy with finite differences. The approximation of the object contour depends on the level of detail to be represented: parts with a high curvature need more nodes than relatively straight parts. A sufficient number of nodes is assumed to represent the initial contour and, thus, is not considered during the further analysis.

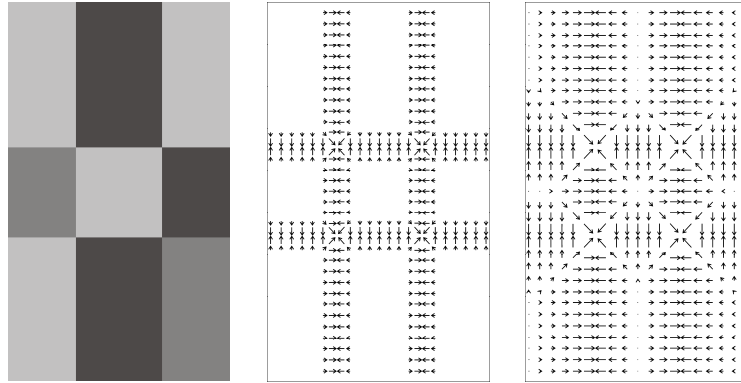


Figure 15: Synthetic example with different image energies: original image (left), gradient vectors (center) and distance vector field (right)

Evaluating the requirements which have to be fulfilled for the initialization, the point of a *close* initialization is the main but as well the most complex task to be analyzed in this section. The goal is to investigate if rules or boundary conditions can be defined to isolate the initialization problem. Taking an arbitrary synthetic example composed of homogeneous adjacent regions to ignore any disturbing influencing factors, an initial contour network will move to the closest image features. This fact can be expected regarding the mathematical definition of the image energy $E_{img}(C(s))$ defined in Section 2.1.2.1., because the image force pushes the contour parts to the closest object borders represented within the image. In Figure 15 a synthetic example is given as basis to exemplify the initialization requirements in this section. The derived image energy is based on the *distance potential force* (cf. Figure 15, right) computed from the edge map of the synthetic example (cf. Section 2.1.2.1), which significantly increases the capture range while preserving accurate image boundaries compared to traditional gradient vectors (cf. Figure 15, center). Both image energies are generated under the assumption of equal magnitudes of image gradients at the object borders to avoid disturbing effects. The aim is to symbolize exemplarily in Figure 15, how the contours will be attracted by the closest object boundaries in the image bridging uniform image parts.

Starting from an initial contour network such as the one given in Figure 16 (depicted in blue), each contour part moves step by step (depicted in white) to the expected correct result (depicted in red). This procedure illustrates the mathematical definition of the image energy $E_{img}(C(s))$ discussed in Section 2.1.2.1.: the utilized image energy of the distance potential force pushes each contour part to the closest object boundaries, when no disturbing image characteristics influence the movement. At the image borders, the optional constraint energy $E_{con}(C(s))$ is incorporated into the total energy functional to chain the open contour ends to the image borders and is allowed to move only along the borderline, i.e. the x or y coordinate is fixed.

Shifting the initial contour network to the left, a critical situation will be reached when an initial contour part is *exactly* located between two object borders represented within the image. The image force is neither able to push the contour to the correct object boundary nor to push the contour to any other boundary. In Figure 17 the right vertical contour composed of three contour parts defines the initial position (depicted in blue) *just before* the critical center between the two object boundaries. Thus, this contour as part of the common contour network moves again (depicted in white) to the expected correct result (depicted in red).

A given initial contour *beyond* the critical position will cause a wrong result. In Figure 18 the initialization is once more shifted to the left, whereby the center position between the two object boundaries represented in the synthetic image is passed. Consequently, the right vertical contour of the initial contour network (depicted in blue) moves step by step (depicted in white) to the wrong position (depicted in red). The topology-preserving energy (cf. Section 3.4.2.) is incorporated into the total energy functional to avoid merging of the contour parts at the left vertical image border conserving the initial topology. Obtaining the correct result is not possible, because the corresponding other vertical contour is too far away at the beginning of the optimization process.

The effect that the iteration behavior varies concerning the *speed* at different contour parts (cf. Figure 16 – Figure 18) is caused by the image energy used within the minimization process as displayed in Figure 15 on the right. Those parts of the vertical contours being closer to the as of yet not regarded horizontal object borders

within the image are less influenced by the proportion of the distance potential force which causes horizontal image energy forces. Thus, contour parts farther away from the perpendicular object borders are more affected and move faster to the respective object borders. Further details concerning the iteration behavior are discussed in Section 4.2.3. The horizontal contour parts connecting the vertical ones building the real network have not been considered so far because the above discussed investigations apply to only two separate contours as well. Thus, their initialization is identical to the required result at the object borders exercising no influence.

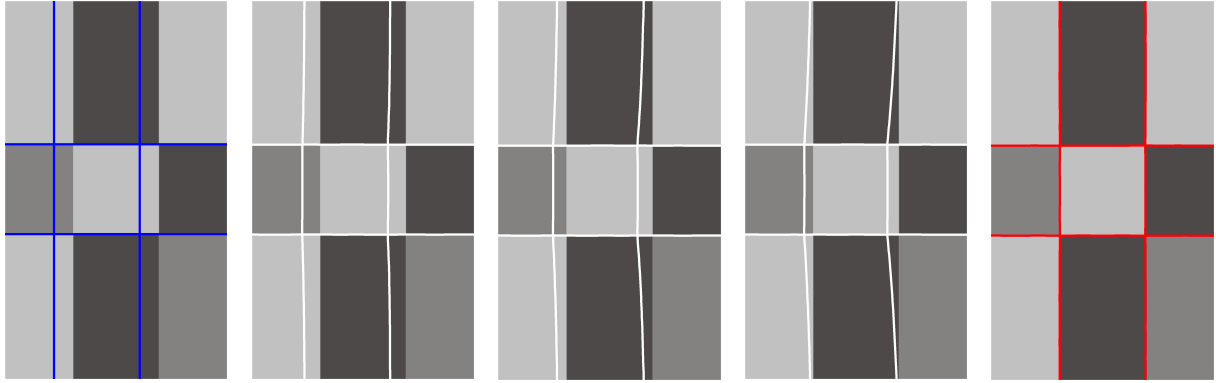


Figure 16: Correct initialization of network snakes: initialization (blue), optimization steps (white) and result (red)

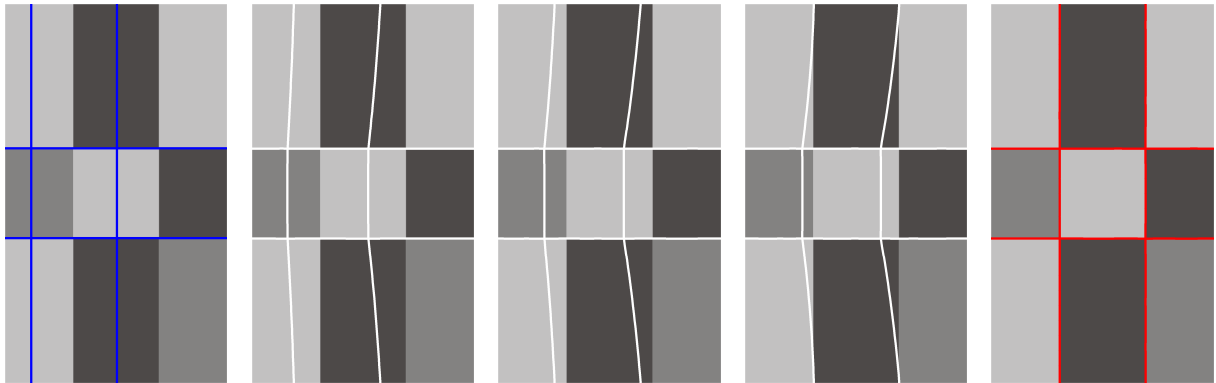


Figure 17: Critical initialization of network snakes: initialization (blue), optimization steps (white) and result (red)

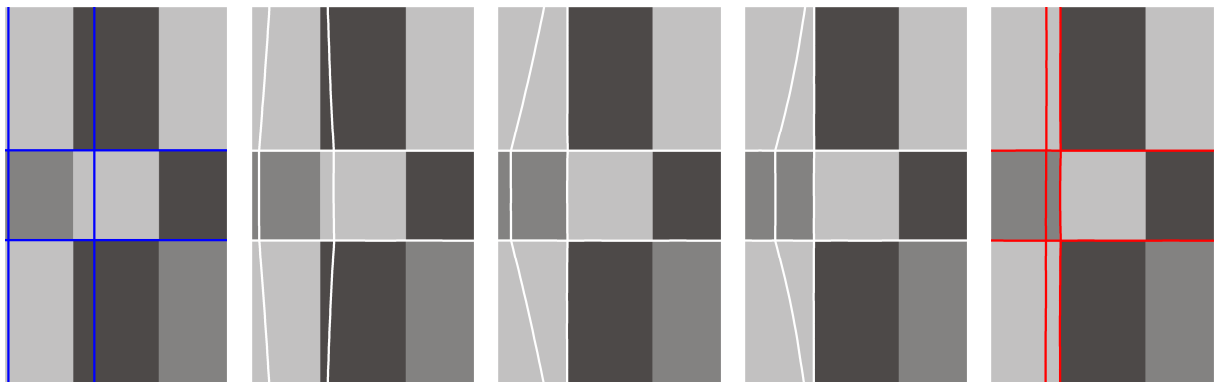


Figure 18: Wrong initialization of network snakes: initialization (blue), optimization steps (white) and result (red)

The analysis of the contribution of the *topology* incorporated in the new method of network snakes and, moreover, the exploitation of the topology is the aim of the main investigations. In Figure 19 the middle part of the right vertical contour is initialized beyond the critical position (depicted in blue), which would cause a wrong final result performing this contour part *separately* using traditional parametric active contours as demonstrated in Figure 18 with the right vertical contour. Network snakes consider the *complete network* simultaneously during the optimization of the energy functional and, in particular, exploit the connectivity of the individual contour parts. Consequently, the adjacent and correctly initialized contour parts guide the middle part step by step (depicted in white) to the assumed correct result (depicted in red). The internal energy $E_{int}(C(s))$ has a dominant weight compared to the image energy $E_{img}(C(s))$ of the total energy functional to control the network snake while exploiting the given initial topology. Clearly, the topology can only support the optimization when at least half of a contour within the contour network is initialized correctly. The optimization in Figure 19 illustrates that the new method of network snakes facilitates the compensation of wrongly initialized contour parts because the connectivity of the wrong part to the remaining correct parts of the network enables a correct optimization of the network.

Generating an increased critical initialization with *several* wrong initial contour parts within the complete network, the new method of network snakes detects the correct result as well (cf. Figure 20). Both wrongly initialized contour parts in the middle of the horizontal and vertical contour, respectively, (depicted in blue) move as part of the network step by step (depicted in white) to the correct result (depicted in red). The given correct topology conserves at the beginning of the minimization process together with the internal energy the topologically correct network, whereas the image energy pushes the wrongly initialized contour parts guided by the adjacent correct ones to the final result. In general, contour parts farther away from the object boundaries are more influenced by the internal energy, which is why the topology has such a great impact to the optimization process. Thus, the introduction and exploitation of the topology to the concept of parametric active contours enables weaker initialization requirements compared to the traditional concept.

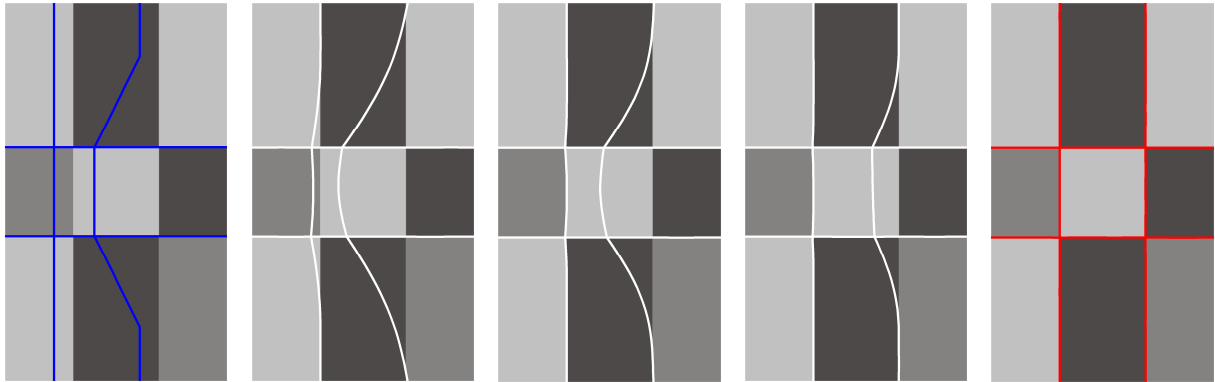


Figure 19: Initialization of network snakes exploiting the topology: initialization (blue), optimization steps (white) and result (red)

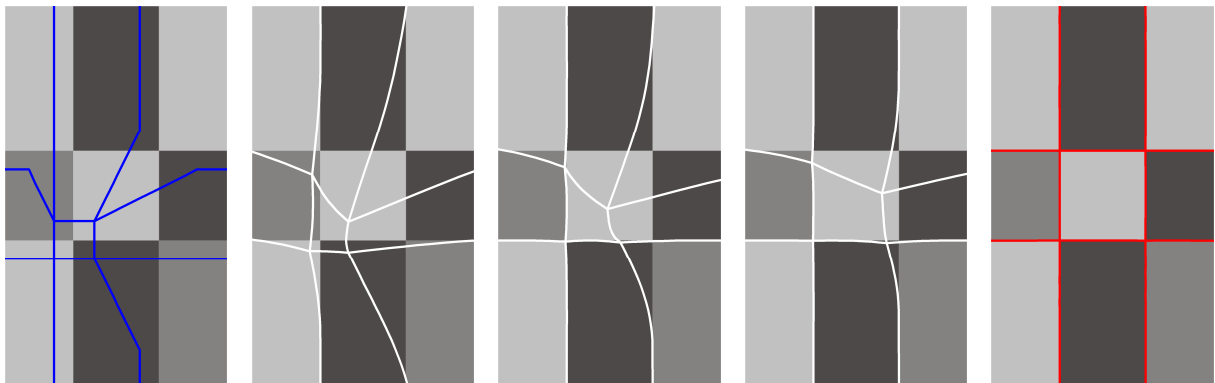


Figure 20: Critical initialization of network snakes exploiting the topology: initialization (blue), optimization steps (white) and result (red)

The analysis of the synthetic example taken in this section presumes equal magnitudes of image gradients to define a consistent distance potential field. Of course, critical situations such as displayed in Figure 17 will show a different result if one object border is represented in the image energy more distinctively. Thus, the influence of the object characteristics represented within the image can alter the established rules above. In addition, the control of the total energy functional $E(C(s))$ depends on the parameters enabling a varied modeling of the behavior of the contour network describing the objects of interest. Consequently, the initialization requirements are influenced by the parameters, too, details are discussed in Section 4.2.2.

Concluding the initialization requirements, the following rule can be established:

- The length of the contour parts, discretized by the number of nodes C_0, \dots, C_n , with shorter distances to the true object boundary has to be *larger* than of those contour parts with shorter distances to wrong contour parts:

$$\sum_{i=C_0}^{C_n} (d_{correct} < d_{wrong}) > \sum_{i=C_0}^{C_n} (d_{correct} > d_{wrong}) . \quad (55)$$

The parameter $d_{correct}$ is defined as the difference between the initial contour and the correct object boundary $d_{correct} = |C_{init} - O_{correct}|$, and the parameter d_{wrong} is defined as the difference between the initial contour and an arbitrary wrong object boundary $d_{wrong} = |C_{init} - O_{wrong}|$ for the coordinates x and y , respectively. The following conditions must be valid:

- The magnitude of the image energy is equal at every object boundary.
- The internal energy $E_{int}(C(s))$ has a larger weight compared to the image energy $E_{img}(C(s))$ of the total energy functional, i.e. the parameter κ is defined as $0 < \kappa < 1$.

It has to be noted, that the established rule above has a very theoretical background. Using real data and real application scenarios, the estimation of the required conditions could be difficult. Thus, the left part of Equation 55 must be guaranteed to be large enough to compensate in particular disturbing image characteristics and the uncertainty of how close the contour network is initialized to the true object boundary. But, the established rule defines conditions for the initialization and, most important, the introduction and exploitation of the topology to the concept of parametric active contours enables weaker initialization requirements.

4.2.2. Analysis of the parameter control

Parametric active contours are generally controlled by *parameters* to incorporate object knowledge concerning the shape behavior or movement of the object of interest during the optimization of the energy functional $E(C(s))$. The concept behind this is the coupling of the image energy $E_{img}(C(s))$ with the internal energy $E_{int}(C(s))$ in an energy minimization framework to delineate non-rigid curves from images or image sequences. The parameters controlling the proposed new method of network snakes comprise the image energy $E_{img}(C(s))$, the internal energy $E_{int}(C(s))$ and the optional constraint energy $E_{con}(C(s))$ and topology-preserving energy $E_{topo}(C(s))$ (cf. Section 3.4.3.). The four energy terms can be manipulated to optimize the respective function separately and, in addition, can be weighted against each other to control the influence of each energy term to the overall result. Investigations concerning the parameter control of traditional parametric active contours are very limited in the literature, which is why no sufficient basis can be provided as a starting point (cf. Section 2.1.3.2.). Often, the control of the parameters is only treated marginally and is only focused to particular applications.

The aim of the analysis accomplished in this section was to derive more general statements dependent on the object characteristics or, at least, to define indications for the parameter control. The problem of parameter setting cannot only be solved by a translation of the shape characteristics of the object of interest to the parameters, for example obtained by a specific setting for a specific curvature of the contour. The reason for this is the local minimization of the energy functional considering only the local environment in the image and, thus, the dependency on the *initialization*, which could be farther away and hamper the optimization. Consequently, the parameter setting does not only have to represent the shape characteristics of the object, but also must guarantee the detection of the object boundary in the image during the energy minimization process. The connections between the shape characteristics and the initialization conditions have to be analyzed in this section to give an estimation regarding the parameter control. Moreover, the introduction of the *topology* to the concept

of parametric active contours with the resulting possibilities and improvements has to be examined evaluating network snakes. The dependencies between the parameter control of the energy functional representing the modeled object characteristics compared to the image characteristics, the initialization requirements and the topology of the objects of interest have to be incorporated in a comprehensive analysis.

An additional important task to be investigated is the *robustness* of the parameter control affected by variations. The question is to what extent do parameter modifications alter the minimization process and, more relevant, alter the final result using network snakes. Again, relations to the topology are of particular interest for analyzing the impact of the proposed new method regarding the robustness of the parameter control. The content of the analysis is to control the parameters not only based on the object model, but to regard the initialization requirements and the topology in an integrated process.

The influence of the different variables is of different significance to the overall result during the minimization of the total energy functional $E(C(s))$ and, thus, the examination of the parameters is separated in terms of their relevance. The parameter k aims to weight the constraint energy compared to the other energy terms of the whole energy functional (cf. Equation 10). But, usual constraints such as the fixing of particular points or parts of a contour network entail the non-consideration of any other energy terms, for instance the chained end points of the synthetic examples in this chapter. Thus, the parameter k is set to $k = 1$ and any other weighting parameters are set to zero, if the constraint energy is considered. Accordingly, the introduction of the constraint energy can be done in general without any varying parameter control, which is why this optional energy is not further investigated in this section.

The *topology-preserving energy* $E_{topo}(C(s))$ is introduced to the total energy functional to preserve the given topology during the complete energy minimization process enabling their exploitation (cf. Section 3.4.2.). Within the topology-preserving energy $E_{topo}(C(s))$ the parameter d_{topo} monitors the distance between two neighboring contour parts (cf. Equation 51). The interesting point concerning the parameter control arises when object contours are close to each other where the distance is restricted by an upper limit of d_{max} with $0 < d_{topo} < d_{max}$. Thus, the definition of the spacing where the topology-preserving energy is activated is the only parameter to be controlled. The parameter d_{max} is set at the beginning of the minimization process to a specific value dependent on the application with no variations during the energy minimization process. The weight of the topology-preserving energy $E_{topo}(C(s))$ is set twice as large as the image energy $E_{img}(C(s))$ and the internal energy $E_{int}(C(s))$ to guarantee the predominance of the energy if activated. Thus, investigations regarding the topology-preserving energy $E_{topo}(C(s))$ are not accomplished, because the variation of any parameters is not necessary and, more important, the parameter setting of the optional energy has no influence on the performance of the image energy and internal energy concerning the shape behavior of the contour network.

The *internal energy* $E_{int}(C(s))$ in conjunction with the *image energy* $E_{img}(C(s))$ are the most prominent energy terms controlling the optimization of the energy functional $E(C(s))$ of the proposed new method of network snakes. In Figure 21 an arbitrary synthetic example composed of homogeneous adjacent regions to ignore any disturbing influencing factors is given as a basis to exemplify the investigations concerning the parameter control of network snakes. Different curvatures of the contour parts represent the overall specifications delineating non-rigid contours as part of a contour network. Again, the derived image energy is based on the distance potential force increasing the capture range as already used regarding the investigations of the initialization requirements in Section 4.2.1. The synthetic example in Figure 21 pictures the *ideal parameter setting* comprising the control of the internal energy and image energy. Starting from an arbitrary initial contour network complying with the defined initialization requirements in Equation 55 (depicted in blue), the contour network moves step by step (depicted in white) to the expected final result (depicted in red). The iterations are shown after 50, 150 and 400 steps to demonstrate the *relative* minimization behavior of network snakes. In this connection the absolute number of iterations is irrelevant, because here the aim is not to achieve fast iteration strategies, but rather to analyze the parameter control and the involved properties of network snakes. The ideal parameter setting represents the different object models of the contour parts and their shape characteristics in an optimal manner and defines the starting point regarding the analysis of the parameter control. The relevant parameters of the internal energy $\alpha(s)$ and $\beta(s)$, the step size γ and the parameter κ controlling the weight between internal energy and image energy (cf. Section 2.1.2.1. and Section 2.2.) are specified in the middle row of Table 2 - Table 4, respectively, to define the basis of parameter variations and the analysis of the robustness.

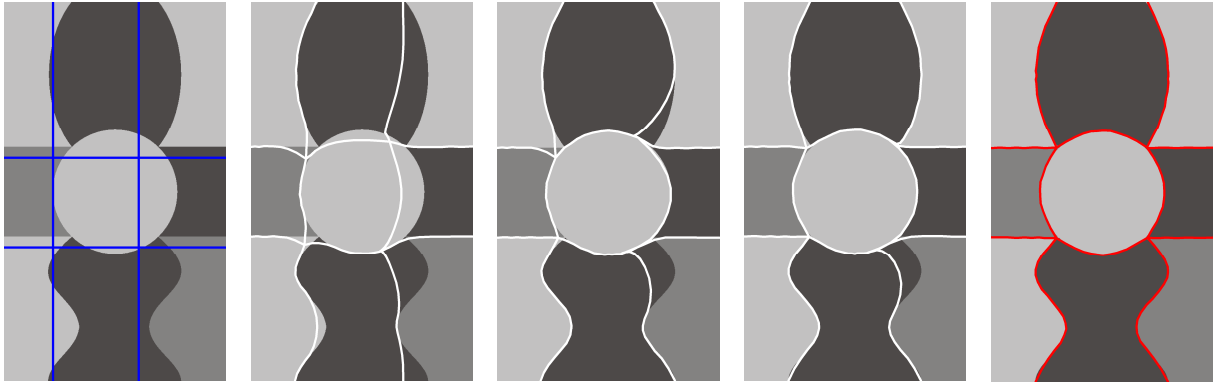


Figure 21: Ideal parameter control of network snakes: initialization (blue), optimization steps after 50, 150 and 400 iterations (white) and result (red)

The *internal energy* $E_{int}(C(s))$ is controlled by the parameters $\alpha(s)$ and $\beta(s)$ representing the modeled object knowledge about the shape behavior or movement of parametric active contours (cf. Section 2.1.2.1.). The parameter $\alpha(s)$ weights the first term of the internal energy to control the *elasticity* or *tension* of the curve, the parameter $\beta(s)$ weights the second term of the internal energy to control the *rigidity* of the curve (cf. Equation 9). The parameter γ defines the *step size* or *speed* of the contour network during the energy minimization. Regarding the investigations of the internal energy $E_{int}(C(s))$ the parameter γ is kept constant with a value enabling a natural behavior of the optimization process (details of the iteration behavior are discussed in Section 4.2.3.). The parameter κ weighting the internal energy *compared* to the image energy is set at the upper limit of the defined range for this parameter (cf. Section 4.2.1.) to enable a high image energy obtaining a fast iteration behavior. Concerning the analysis of the internal energy, the parameter κ is kept constant (cf. Table 2 and Table 3). Afterwards variations are accomplished to evaluate the dependencies between internal energy and image energy.

In Figure 22 different parameter settings of the internal energy $E_{int}(C(s))$ of network snakes are shown to demonstrate variations and their effects concerning the *relative* weight of the parameters α and β . Both parameters are set independently of s , which is a common procedure for applications without prior information about distinctive features at particular contour parts. The optimization result of network snakes using the ideal parameter setting of the relative weight between the parameters α and β is depicted in the center of Figure 22, the associated parameter values are listed in the middle row of Table 2 (cf. Figure 21 for the complete optimization procedure). The ideal parameter setting has been generated with tests to obtain an optimal object delineation. The aim at that point is not to define an ideal parameter setting for a specific object type, but to provide a basis for the following investigations. The ideal proportion between both parameters α and β is weighted with a considerable predominance of β , because the second term of the internal energy models the shape behavior more naturally in terms of the curvature of the contour compared to the first term weighted by α . In addition, the parameter α tends to shrink the contour, which is undesirable representing contour parts with high curvatures. Starting from the ideal parameter setting c) of the relative weight (cf. Table 2, middle row), parameter settings with *smaller proportions* are listed as parameter settings a) and b), the results of the optimized energy functional of network snakes are shown in Figure 22 on the left side. Obviously, the contour part with the highest curvature of the network can not be delineated correctly because the increasing parameter α hampers the necessary stretching of the contour part. Additionally, the parameter setting a) does not enable a precise localization of the both left nodes with a degree $\rho(C) = 4$ caused by the high value of the parameter α . On the other hand, *larger proportions* listed as parameter settings d) and e) of Table 2 and shown in Figure 22 on the right side cannot delineate contour parts with high curvatures because the increasing parameter β allows only for less curved contour parts. Thus, the relative parameter settings must represent the shape characteristics of the objects of interest correctly *and* must enable the detection of them during the energy minimization of network snakes.

In Figure 23 different parameter settings of the internal energy $E_{int}(C(s))$ of network snakes are shown to demonstrate variations and their effects concerning the *absolute* weight of the parameters α and β . For this purpose the ideal parameter setting c) of Table 3 is taken as starting point to vary the absolute parameter values of α and β keeping the relative weight between them constant. *Smaller absolute values* of the parameters α and β as defined in the parameter settings a) and b) result in incorrect delineations of the borderlines of the adjacent

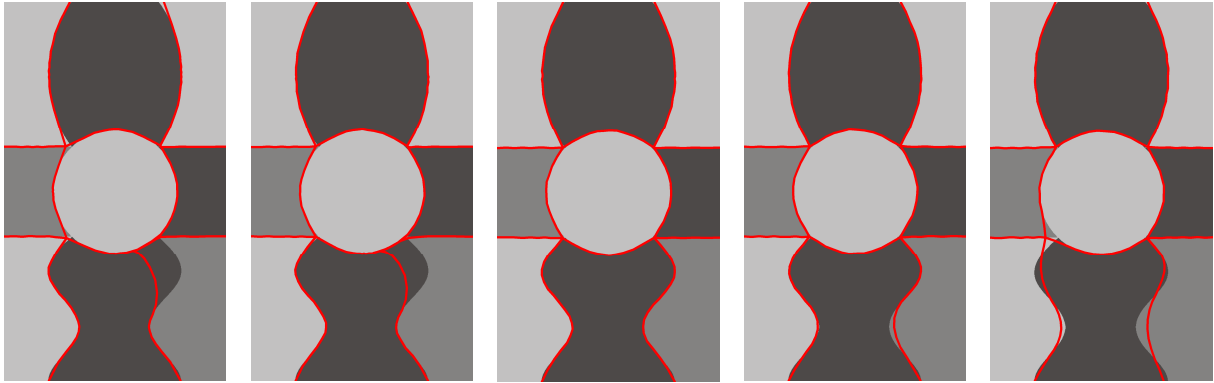


Figure 22: Results of different parameter settings a) - e) to control the internal energy $E_{int}(C(s))$ of network snakes (cf. Table 2): the ideal *relative* weight of the parameters α and β is displayed in the center

Parameters	α	β	γ	κ
parameter setting a	0.4	0.5	6.0	0.9
parameter setting b	0.2	1.0	6.0	0.9
ideal parameter setting c	0.1	2.0	6.0	0.9
parameter setting d	0.05	5.0	6.0	0.9
parameter setting e	0.01	10.0	6.0	0.9

Table 2: Parameters of Figure 22 to control the *relative* weight of the parameters α and β of the internal energy

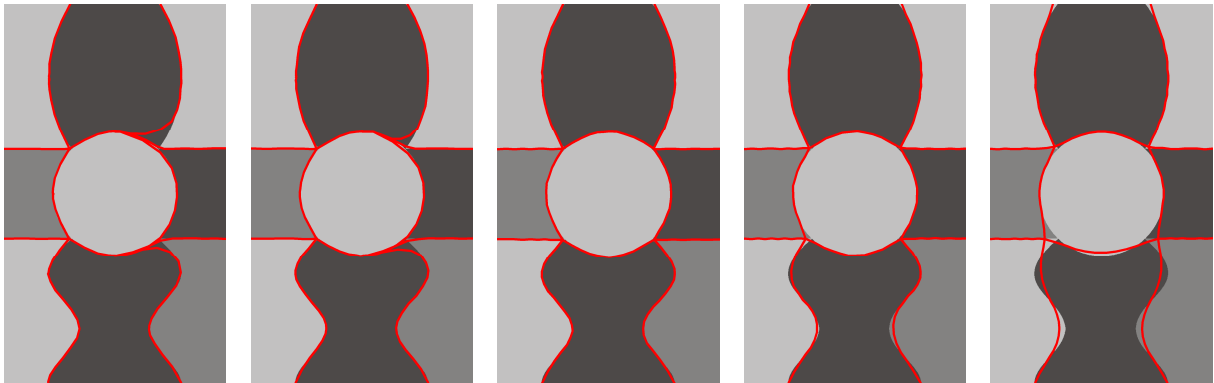


Figure 23: Results of different parameter settings a) - e) to control the internal energy $E_{int}(C(s))$ of network snakes (cf. Table 3): the ideal *absolute* weight of the parameters α and β is displayed in the center

Parameters	α	β	γ	κ
parameter setting a	0.025	0.5	6.0	0.9
parameter setting b	0.05	1.0	6.0	0.9
ideal parameter setting c	0.1	2.0	6.0	0.9
parameter setting d	0.25	5.0	6.0	0.9
parameter setting e	0.5	10.0	6.0	0.9

Table 3: Parameters of Figure 23 to control the *absolute* weight of the parameters α and β of the internal energy

regions. The reason for this is the small value of β , which allows for high curvatures of the contour resulting in a remaining of both right nodes with a degree $\rho(C) = 4$ at a wrong place on the boundary of the central round object (cf. Figure 23, left). The neighboring contour parts ending in the mentioned nodes are close to the object boundaries. Hence, the image energy shows no great influence anymore. The introduced topology can keep the contour parts together, but an exploitation of the topology supporting the optimization of the contour network is only possible if the internal energy conserves the topology in terms of a planar graph with a reasonable parameter control enabling a reasonable shape behavior of the contour network. *Higher absolute values* of the parameters α and β such as listed in the parameter settings d) and e) of Table 3 cannot delineate contour parts with high curvatures because the increasing parameter β allows only for less curved contour parts (cf. Figure 23, right). This fact is similar to the parameter settings d) and e) of the investigations concerning the relative weight of the parameters α and β (cf. Figure 22, right). In addition, the increasing parameter α intensifies this effect caused by a shrinking of the contour parts of the network. Thus, the absolute parameter settings regarding the internal energy must represent the shape characteristics of the objects of interest and, moreover, must enable an exploitation of the topology in terms of a planar graph using balanced parameter settings.

The energy minimization process of network snakes assumes unit distances between neighboring nodes C representing the contour during the energy minimization process to enable a correct approximation of the derivatives with finite differences (cf. Section 3.4.1.). A further point to be regarded when setting the parameters α and β to control the internal energy is the *absolute distance* between neighboring nodes C discretizing the contour network. The shape behavior of the contours is calculated using finite differences (cf. Equation 35) which leads to shape models dependent on the absolute distance between the nodes such as illustrated in Figure 24. Both discretizations represent the same object boundary (cf. Figure 24, depicted in red), but the different distances of the nodes result in different angles w_1 and w_2 . Thus, the absolute distance between neighboring nodes has to be incorporated when defining the parameters α and β to control the internal energy. Larger numbers of nodes defining a contour part, i.e. smaller distances of neighboring nodes, require in particular larger values of the parameter β to represent the shape characteristics of the object correctly. The synthetic examples of this section are discretized with a total number of 160 nodes (cf. Figure 21 - Figure 23 and Figure 25) giving an indication for the analyzed parameter settings.

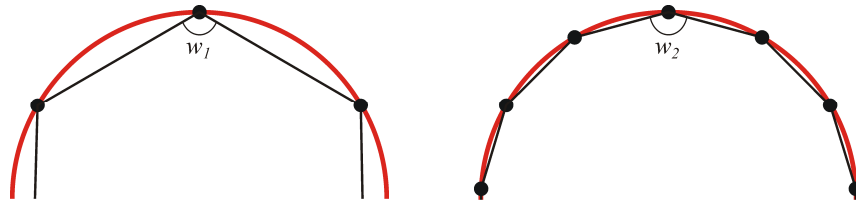


Figure 24: Influence of the absolute distance between neighboring nodes C to the parameter control of the internal energy

The *image energy* $E_{img}(C(s))$ is the second prominent energy term in conjunction with the *internal energy* $E_{int}(C(s))$ controlling the optimization of the energy functional $E(C(s))$ of the proposed new method of network snakes. The image energy is not controlled by internal conditions and, thus, is incorporated in the energy functional as a constant energy without the control of any parameters. The generation of the image energy offers several possibilities which can include the setting of parameters aiming at the derivation of an optimal description of the object of interest in the imagery (cf. Section 2.1.2.1.). The derived image energy concerning the investigations of the parameter control is based on the distance potential force obtaining an optimal object description within the imagery. The interesting point to be analyzed in this context is the control of the weight *between* the image energy and the internal energy, which is obtained with the parameter κ . In contrary to the examinations concerning the internal energy, now the parameter κ is varied keeping the other parameters of the energy functional constant. In Figure 25 results of network snakes with different parameter variations of the parameter κ are shown, the parameter settings are listed in Table 4, respectively. Again, the ideal parameter setting is listed in the middle row of Table 4 and the optimized network snake is displayed in the center of Figure 25. Parameter settings with *decreasing* weights of the image energy compared to the internal energy involving a small value of the parameter κ cause very smooth contour parts, but are more and more independent of the image information as shown in Figure 25 on the left. Parameter settings with *increasing* weights of the image energy compared to the internal energy listed as parameter settings d) and e) in Table 4 result in delineations which are close to the true object boundaries, but do not fit the shape model (cf. Figure 25, right).

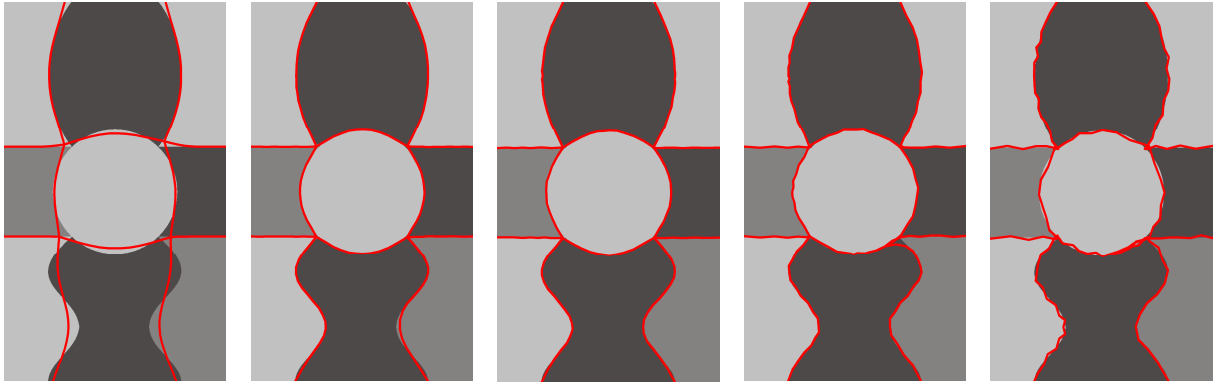


Figure 25: Results of different parameter settings a) - e) to control the weight between the internal energy $E_{int}(C(s))$ and the image energy $E_{img}(C(s))$ of network snakes (cf. Table 4): the ideal weight of the parameter κ is displayed in the center

Parameters	α	β	γ	κ
parameter setting a	0.1	2.0	6.0	0.1
parameter setting b	0.1	2.0	6.0	0.5
ideal parameter setting c	0.1	2.0	6.0	0.9
parameter setting d	0.1	2.0	6.0	2.0
parameter setting e	0.1	2.0	6.0	5.0

Table 4: Parameters of Figure 25 to control the weight of parameter κ between the internal energy $E_{int}(C(s))$ and the image energy $E_{img}(C(s))$

In addition, the preservation of the topology in terms of a planar graph cannot be sustained, since the influence of the internal energy preserving a meaningful shape behavior is dwindling. Thus, a parameter control with a too large image energy loses the possibility to exploit the topology during the energy minimization of network snakes.

Concluding the investigations regarding the parameter control, the following statements can be made:

- The parameter control of network snakes is dominated by the parameters α and β controlling the internal energy $E_{int}(C(s))$ representing the shape model of the object of interest and the parameter κ controlling the weight between the internal energy $E_{int}(C(s))$ and image energy $E_{img}(C(s))$. The setting of the parameters depends on the shape characteristics of the objects including their discretization in conjunction with the possibility to reach the object boundaries during the energy minimization of network snakes.
- The parameter control of network snakes must consider the uncertainty of the initialization to guarantee the detection of every part of the object boundaries differing from the ideal parameter setting defined by the shape characteristics resulting in decreasing values of the parameters α and β .
- The parameter control of network snakes must enable an exploitation of the topology in terms of a planar graph using balanced parameter settings by the use of a larger internal energy $E_{int}(C(s))$ compared to the image energy $E_{img}(C(s))$ accomplished with the weighting parameter κ with $0 < \kappa < 1$.
- The parameter control of network snakes is robust against small parameter variations, but larger changes lead to modified object models. Consequently, the parameter setting is an important task, particularly in overcoming blurry or disturbing image features and initializations of the contour network being farther away.

4.2.3. Analysis of the iteration behavior

The optimization of the total energy functional $E(C(s))$ of parametric active contours is obtained by an iterative processing introducing an additional *step size* γ to find the final solution (cf. Section 2.2.). Thus, network snakes start generally with an initial contour close to the true object boundary, because the optimization of the energy functional considers only the local environment of the current position of the contour (details of the initialization requirements are discussed in Section 4.2.1.). Similar to the parameter control of parametric active contours, investigations regarding the iteration behavior are very limited in the literature, which is why a starting basis in that context cannot be provided (cf. Section 2.1.3.2.).

The aim of this section is to analyze the iteration behavior of network snakes and to examine which factors influence the minimization process and how fast the convergence of the contour network can be achieved. In particular, the dependency on the initialization requirements of the contour network and the parameter control during the energy minimization is content of the investigations (cf. Section 4.2.1. and Section 4.2.2.). Initializations closer to the object boundary accelerate the iteration behavior because the image energy $E_{img}(C(s))$ exerts an increasing influence to the total energy functional $E(C(s))$. In addition, different parameter variations alter the iteration speed of network snakes, but the shape model of the object of interest has to be fulfilled during the minimization of the energy functional to consider the topological control of the contour network. The dependency of the iteration behavior concerning the utilization of the topology is of particular interest to be examined in this section to obtain statements regarding the impact of the topology. The goal of the analysis is the derivation and discussion of possible strategies to fathom a speed up of the iteration behavior.

As already mentioned, the question of the iteration behavior of network snakes concerning the *speed* is highly related to the initialization of the contour network and the parameter control. While the initialization cannot be affected methodically depending only on the application and the given prior starting point, the iteration behavior controlled by the parameters can alter the speed of the minimization. Continuing the investigations regarding the parameter control in Section 4.2.2., the step size γ is selected to analyze the influence on the behavior of network snakes. Again, the starting point is the initial contour network given in Figure 21 on the left complying with the defined initialization requirements in Equation 55 and being sufficiently far away to enable a comprehensive

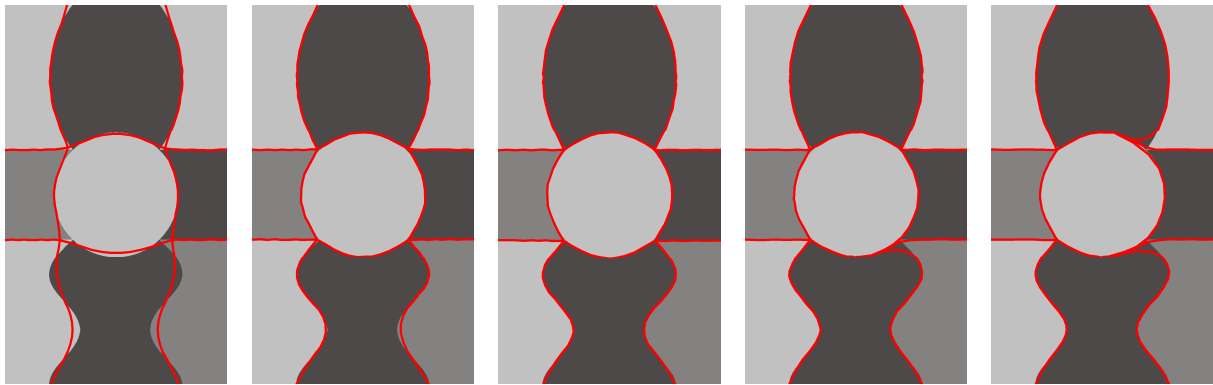


Figure 26: Iteration behavior of different parameter settings a) - e) to control the step size γ of network snakes (cf. Table 5): the ideal weight of the parameter γ is displayed in the center

Parameters	α	β	γ	κ
parameter setting a	0.1	2.0	1.0	0.9
parameter setting b	0.1	2.0	3.0	0.9
ideal parameter setting c	0.1	2.0	6.0	0.9
parameter setting d	0.1	2.0	9.0	0.9
parameter setting e	0.1	2.0	12.0	0.9

Table 5: Parameters of Figure 26 to control the step size γ of the energy functional of network snakes

analysis of the optimization process. In Figure 26, results of network snakes with different parameter variations of the step size γ are shown, the related parameter settings are listed in Table 5. Again, the ideal parameter setting is listed in the middle row of Table 5 and the optimized network snake is displayed in the center of Figure 26. In general, higher values of the step size γ result in a faster movement of the contours yielding in a faster iteration behavior (cf. Section 2.2.). However, the larger step sizes involve a wrong behavior during the optimization which inhibits the delineation of the correct object borders such as illustrated in Figure 26 on the right with the corresponding parameter settings d) and e) in Table 5. This fact becomes apparent compared to the investigations of the parameter control in Section 4.2.2. in terms of controlling the internal energy and image energy: points or parts of the contour network, which are highly influenced and pushed by the image energy, move very fast potentiated by a large step size γ . Thus, the involved shape behavior can differ from the shape model of the object of interest leading to a wrong object delineation such as depicted in Figure 26 on the right. The parameter variations concerning the step size γ are completed with decreasing values shown in Figure 26 on the left and listed in Table 5 with the parameter settings a) and b). In contrast to the findings described above, the contour network is now not able to reach the object boundaries throughout the optimization while the shape model is fulfilled at any time. Consequently, the step size γ cannot be used in an arbitrary increasing way to speed up the iteration behavior. Moreover, the shape model of the object has to be considered during the minimization of the energy functional to facilitate the exploitation of the topology in terms of a planar graph.

The main objective of the analysis in this section is the development and discussion of possible *strategies* to fathom a speed up of the iteration behavior considering the discussed conditions above concerning the parameter control. The results of the previous investigations give rise to change the parameters during the optimization of the energy functional to speed up the processing in conjunction with the preservation of the shape model enabling the exploitation of topology. In Figure 27 intermediate results after 750 iterations of different parameter variations concerning the step size γ are shown to represent their iteration behavior and speed. In this connection, the absolute number of 750 iterations is not the interesting point, but rather the relative number compared to the subsequent investigations. In Table 6 the corresponding parameter settings are listed starting with the ideal parameter setting a), the intermediate delineation is depicted after 750 iterations in Figure 27 on the left side. An additional column is given in Table 6 with the total number of iterations required for the minimization of the

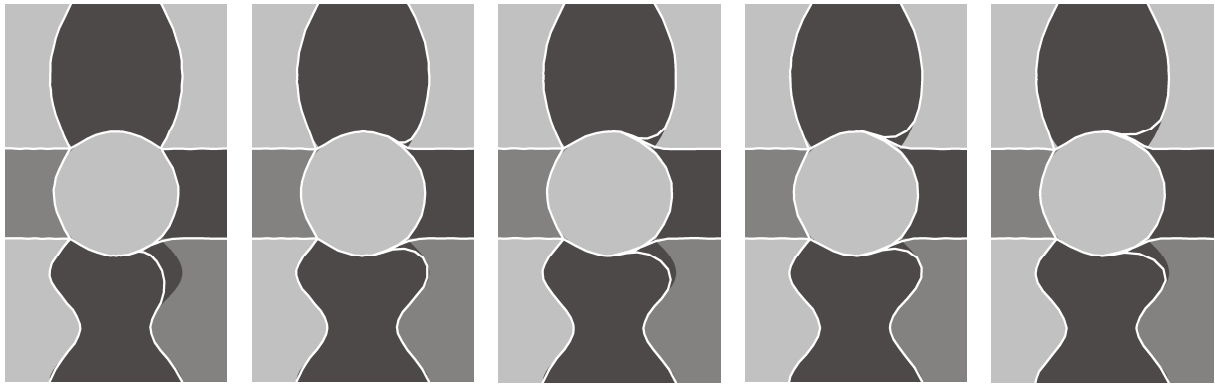


Figure 27: Iteration behavior of network snakes depicted after 750 iterations of different parameter variations concerning the step size γ

Parameters	α	β	γ	κ	total iterations
ideal parameter setting a	0.1	2.0	6.0	0.9	1500
parameter setting b	0.1	2.0	9.0	0.9	1150
parameter setting c	0.1	2.0	12.0	0.9	900
parameter setting d	0.1	2.0	15.0	0.9	850
parameter setting e	0.1	2.0	20.0	0.9	900

Table 6: Parameters of Figure 27 to control the iteration behavior of the energy functional of network snakes with a varying step size γ and the total number of required iterations

energy functional (final results of the parameter settings a) - c) are displayed in Figure 26 on the right side). The increasing step size γ does not cause a continuously faster minimization, a minimum of required iteration steps is derived with the parameter setting d) (cf. Table 6). However, a correct delineation of the object borders can not be guaranteed as already discussed before and shown in Figure 26.

The implication of the iteration behavior and the required total number of iterations is to use first the fastest parameter setting and change it when the intermediate result is close to the object boundary or when the object model is falsified. Two different strategies are presented in Figure 28: the first strategy starts with the fastest parameter setting with a step size $\gamma = 15$ changing after 500 iterations (depicted in white) to the ideal setting resulting in a total number of 1400 iterations to obtain the final result (depicted in red). Compared to the ideal parameter setting accomplished without a parameter variation, 1500 iterations are needed. Thus, the speed up of the minimization using the proposed first strategy is only moderate. The second strategy uses initially the parameter setting with a high image energy with $\kappa = 2$ given as parameter setting d) in Table 4. The parameter setting is already changed after 200 iterations (cf. Figure 28, right, depicted in white) to the ideal parameter setting resulting in a total number of 850 iterations to obtain the final result (depicted in red). Compared to the standard procedure and the first strategy, a significant speed up of the minimization of the energy functional of network snakes can be achieved. But, the question of when to change the parameter settings is difficult to answer generally. More importantly, the use of a partly high image energy compared to the internal energy can lead to a loss of the correct topology in terms of a planar graph as discussed in Section 4.2.1. Consequently, general strategies to speed up the minimization cannot be derived because the preservation of the shape model of the object of interest must be guaranteed to enable the exploitation of the topology during the optimization of the energy functional.

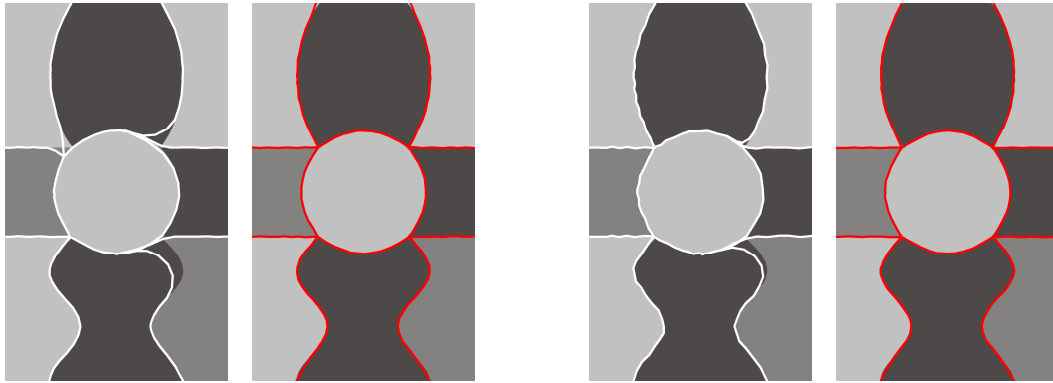


Figure 28: Two different strategies to speed up the iteration behavior of network snakes: starting with a step size $\gamma = 15$ (left, white) the final optimization is achieved after 1400 iterations (left, red); starting with $\kappa = 0.5$ (right, white) the final optimization is achieved after 850 iterations (right, red)

Concluding the iteration behavior of network snakes, the following statements can be made:

- The iteration behavior of network snakes is highly influenced by the parameters, which can be manipulated to control the behavior of the contour network during energy minimization.
- The step size γ can not be used in an arbitrary increasing way to speed up the iteration behavior because the shape model of the object has to be considered during the minimization of the energy functional to facilitate the exploitation of the topology in terms of a planar graph.
- Strategies to change the parameter settings during the minimization of the energy functional speed up the minimization process, but run the risk to break the rules concerning the shape model of the object. A falsified shape model during the optimization can result in wrong object boundaries.
- The exploitation of the topology in terms of a planar graph can only be enabled when the shape model of the object of interest is fulfilled during energy minimization obtained with a correct parameter setting. Thus, the speed up of the iteration behavior can only be accomplished moderately to preserve the possibility to facilitate the incorporated topology.

4.2.4. Analysis of the topology

The introduction of the *topology* to the concept of parametric active contours is the main innovation of this thesis. The benefit of the proposed new method of network snakes is the *exploitation* of the topology during the energy minimization process. The aim is to overcome poor or fragmented object representations within the imagery causing a non-purposive image energy $E_{img}(C(s))$ utilizing the topology of the objects of interest. Furthermore, objects could only be detectable exploiting the topology to enable initializations far away, because adjacent edges in the graph help to push every contour part to the respective object boundary due to their connectivity (cf. Section 1.1. and Section 3.2.2.). The question of to which extent the introduced topology of network snakes allows for coarser initializations of the contour network can only be answered by investigations of the impact of the topology to the final result accomplished in this section using the synthetic data introduced in the sections above. Investigations regarding less concise object characteristics within real image data in conjunction with the exploitation of the topology are made in Section 4.3. and Section 4.4.

The requirement of network snakes is a given topology which is assumed to be correct (cf. Section 3.2.4.). In addition, the preservation of the topology during the optimization process has to be ensured within the complete processing to avoid touching or overlapping contour parts changing the initial correct topology in terms of a planar graph. The second prerequisite has been solved with the introduction of the topology-preserving energy $E_{topo}(C(s))$ to the energy functional as defined in Section 3.4.2. Since the prerequisite assuming a given correct topology cannot always be guaranteed, the *influence* of a *wrong topology* is the first question to be analyzed in this section. In particular, the impact of a partly wrong topology to the result of the given adjacent correct parts of the graph is content of the investigations. Afterwards, the contribution of the topology in dealing with non-ideal object representations in the imagery, for example caused by *fragmented* object boundaries, is investigated to explore the interaction between the image energy $E_{img}(C(s))$ and the topology of network snakes.

The analysis of the topology must be seen in close connection to the analyses concerning the initialization requirements, the parameter control and the iteration behavior (cf. Sections 4.2.1. - 4.2.3.). Thus, the discussed results and evaluations of the new method given before are considered to initiate the examination of the topology. The established rule concerning the initialization requirements defines prerequisites for the initialization to enable weaker initialization conditions (cf. Section 4.2.1.). The investigations regarding the parameter control point out that only balanced parameter settings using a larger internal energy $E_{int}(C(s))$ compared to the image energy $E_{img}(C(s))$ enable the exploitation of the topology (cf. Section 4.2.2.). Similarly, the iteration behavior can only be accomplished with a moderately speed up to preserve the possibility exploiting the topology (cf. Section 4.2.3.). The reason is the fact that the exploitation of the topology in terms of a planar graph can only be enabled when the shape model of the object of interest is fulfilled during the energy minimization.

The analysis of the influence of a given *wrong topology* to the proposed new method of network snakes is done with two types of initializations: first, contour parts are *added* to the topologically correct contour network and, second, contour parts are *removed* from the topologically correct contour network. In Figure 29 one additional contour part is *added* to the initial network at the center on the right side (depicted in blue). This example is chosen to provide a comparison to the ideal parameter setting with a given correct topology shown in Figure 21. The optimization steps of the contour network are depicted after 50, 150 and 400 iterations to demonstrate the iteration behavior exploiting the wrong topology (cf. Figure 29, depicted in white). The middle contour part of the right vertical contour is influenced marginally, because the additional node with the degree $\rho(C) = 3$ cause a separation of the specific contour part at this point concerning its shape. This fact is visible during the first iteration steps at the node represented by a bend, but the final result of the optimization represents the expected object delineation correctly plus the surplus contour part (cf. Figure 29, depicted in red). Compared to the final result exploiting the correct topology shown in Figure 21, the additional wrong contour part does not influence the adjacent correct contour parts of the network. Obviously, the inserted wrong contour part remains wrong after the optimization process because the network snakes exploit the topology during the minimization precluding a topology change. The contour part stays in the middle between the two horizontal object borders, since the initialization was located exactly between the two borders preventing a movement to one object boundary caused by the image energy.

In Figure 30 a further wrong contour part is added to the network to create once more a wrong initial topology containing two surplus contour parts (depicted in blue). In contrast to the first added wrong contour part presented in Figure 29, the second surplus contour part at the bottom connects two correct parts of the network.

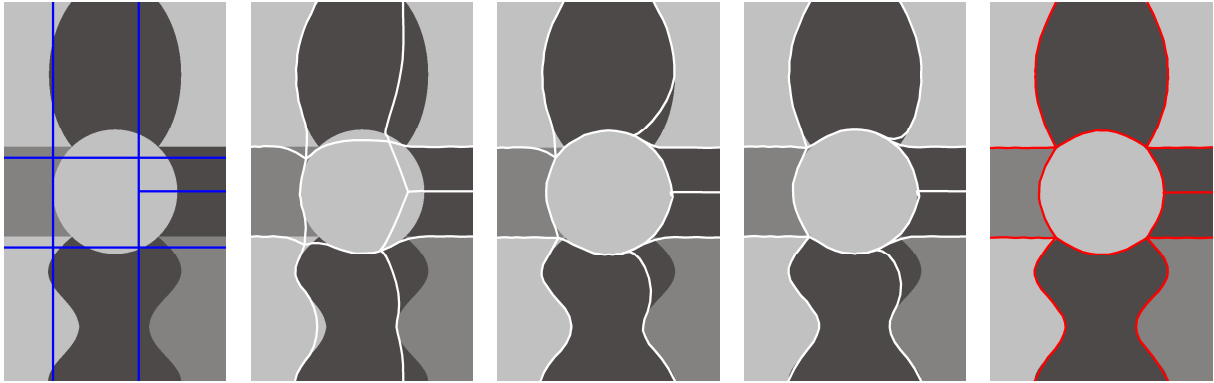


Figure 29: Optimization of network snakes exploiting a wrong topology with one surplus contour part: initialization (blue), optimization steps (white) and result (red)

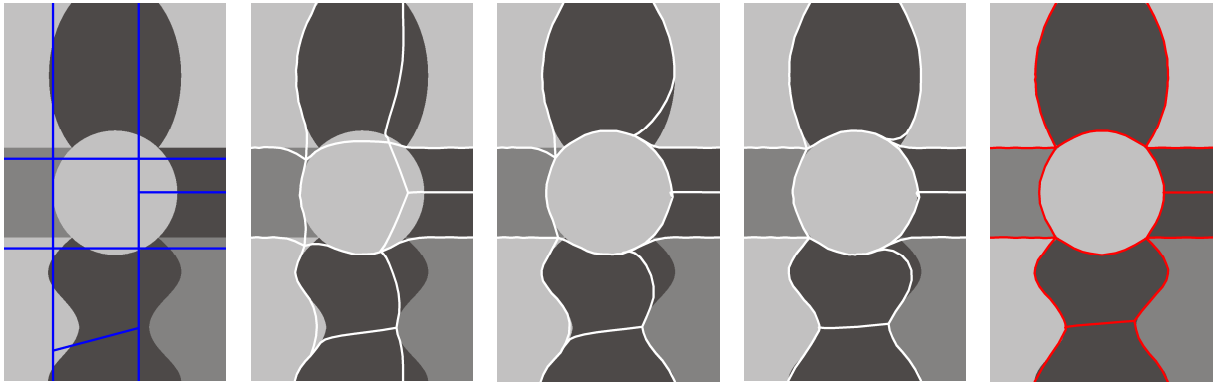


Figure 30: Optimization of network snakes exploiting a wrong topology with two surplus contour parts: initialization (blue), optimization steps (white) and result (red)

Again, the optimization steps of the energy minimization process of network snakes are depicted after 50, 150 and 400 iterations to demonstrate the iteration behavior exploiting the wrong topology (cf. Figure 30, depicted in white). The influence of the additional wrong contour part to the adjacent correct parts of the network is once more relatively insignificant, even though the shape model of both vertical contours at the bottom is split. Again, the final result delineates the object borders correctly, and the surplus contour parts move to the minimum without the presence of a related object border (depicted in red). Consequently, the introduction of surplus contour parts to a correct initial topology does not influence the adjacent correct contour parts of the network in the final result. This statement involves a balanced parameter setting as discussed in Section 4.2.2. and exemplarily illustrated in the respective Figure 21.

The second point to be investigated regarding the exploitation of a given wrong topology when optimizing network snakes is the *removal* of contour parts from the initial correct topology. In Figure 31 the top contour part of the right vertical contour is eliminated leading to an incomplete representation of the topology of the objects of interest. Starting the optimization of the contour network it is apparent that the missing contour part results in a missing delineation of the respective object boundary as shown within the optimization steps after 50, 150 and 400 iterations (cf. Figure 31, depicted in white). Compared to the optimization exploiting the correct topology given in Figure 19, the adjacent contour part in the middle of the vertical contour is not able to reach the true object boundary. The topology-preserving energy $E_{topo}(C(s))$ prevents a merging with the left contour part, but the final result of the network comprises not only one missing but in addition two wrong contour parts (Figure 31, depicted in red). The exploitation of the topology enables the delineation of wrongly initialized contour parts due to the connectivity to adjacent correctly initialized contour parts as defined in Section 4.2.1. concerning the initialization requirements. But, the length of the contour parts with shorter distances to the true object boundary has to be larger than that of the contour parts with shorter distances to a wrong boundary as

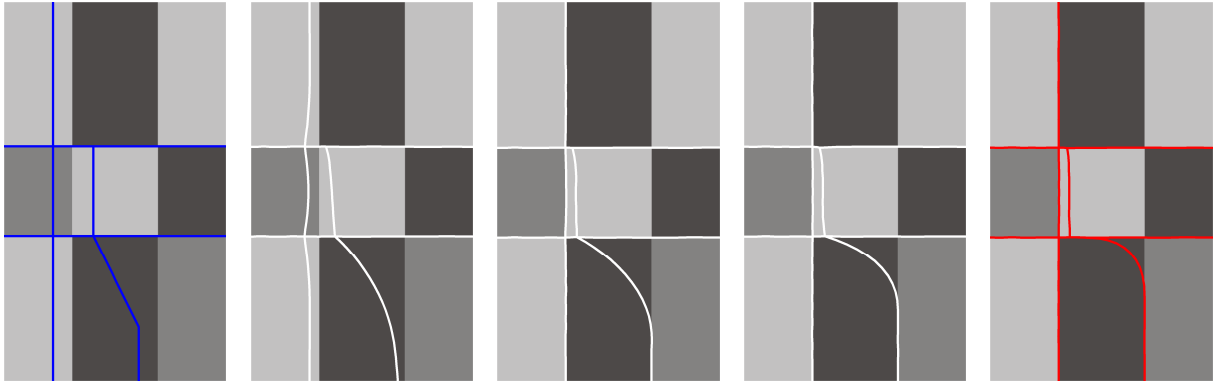


Figure 31: Optimization of network snakes exploiting a wrong topology with one missing contour part: initialization (blue), optimization steps (white) and result (red)

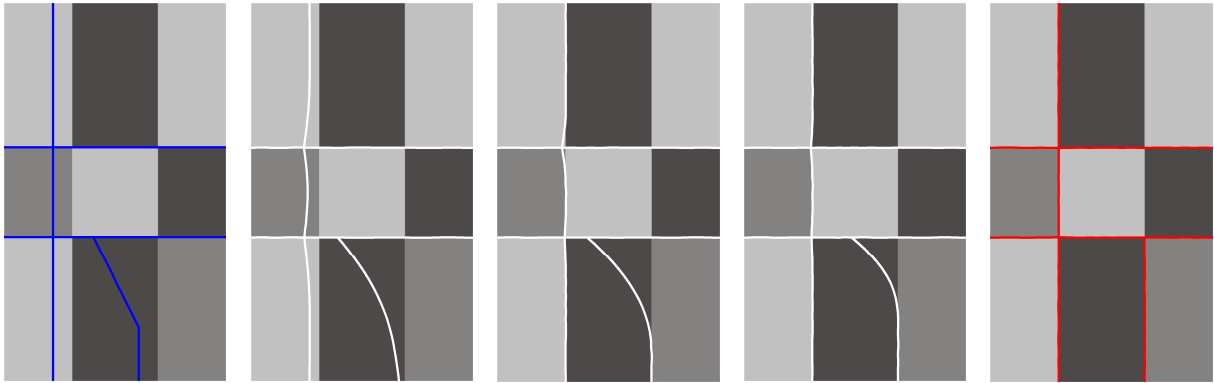


Figure 32: Optimization of network snakes exploiting a wrong topology with two adjacent missing contour parts: initialization (blue), optimization steps (white) and result (red)

defined in Equation 55. This condition is not fulfilled concerning the right vertical contour initialized in Figure 31 and, thus, the missing top contour part influence the correct optimization of the adjacent contour parts. However, missing contour parts affect adjacent ones only in that case adversely, if they are wrongly initialized such as the middle contour part in Figure 31. The force of attraction caused by the image energy keep the middle part at the left object boundary and, thus, the connected bottom part at the node of degree $\rho(C) = 4$, too. Consequently, the requirement of a given correct topology is not only essential to detect the complete network due to the fixed topology, but the exploitation of the topology enables the correct delineation of wrongly initialized contour parts.

In Figure 32 a second contour part is removed from the initial correct contour network (depicted in blue), adjacent to the first removed part discussed above. The missing contour part in the middle of the right vertical contour affects in particular the behavior of the adjacent vertical contour part at the bottom, because the further adjacent horizontal parts are already located at the object boundaries. In contrast to the investigations above, the contour part at the bottom now moves to the correct object boundary (Figure 32, depicted in white). The reason for this fact is the same as argued above for the failure: the length of the contour pieces with shorter distances to the true object boundary is larger, which is why the adjacent missing contour part has no adverse effect. Obviously, the placement of the initialization is just an example, but the behavior demonstrates the established rules concerning the iteration behavior in conjunction with the exploitation of the topology. The final result shows the correct delineation using network snakes, even though the initial missing contour parts lead to a gap in the network at the position of the respective object boundaries (Figure 32, depicted in red).

All analysis carried out in this section above and in the sections before are based on *ideal object representations* within the image to define a clear framework for the investigations focusing only on the respective contents of

interest. However, the assumption of given ideal object boundaries can not be ensured, in particular when using real application scenarios (cf. Section 4.3. and Section 4.4.). Thus, the second goal examined in this section is the impact of the *topology* to deal with poor or *fragmented object representations* in the image. The aim is to point out to which extent the new method can overcome with a non-purposive image energy $E_{img}(C(s))$ exploiting the incorporated topology in the energy functional. In Figure 33 a fragmentation of the synthetic example is accomplished by randomly cutting holes out of the object representation. In that case, the fragmented edge image is the input for the distance map. Starting from an arbitrary initial contour network (depicted in blue) considering the defined initialization requirements (cf. Section 4.2.1.), the contour network moves step by step (depicted in light gray) to the correct final result (depicted in red). The iterations are shown after 50, 150 and 300 steps to demonstrate the behavior of the contour network. Contour parts, which are directly influenced by object boundaries and, thus, are represented with attracting forces in the image energy, move faster to the object boundaries compared to those parts, where the holes cause a neutral image energy. Since the synthetic example is only slightly fragmented, the concerned parts in the contour network can be delineated successfully as result of the internal energy $E_{int}(C(s))$ and the incorporated shape model in the energy functional. Points of special interest are the nodes with a degree $\rho(C) \neq 2$, in particular in the synthetic example in Figure 33 the four nodes with a degree $\rho(C) = 4$. The introduced topology is the crucial factor enabling the delineation of those parts of the object boundaries compared to traditional parametric active contours. As already emphasized in Section 3.3., nodes with a degree $\rho(C) = 4$ can only be delineated correctly using network snakes. Moreover, non-ideal object representations in the image increase the problem to detect object parts with multiple terminating contours using the traditional concept, which points out the impact of network snakes to overcome with fragmented object representations.

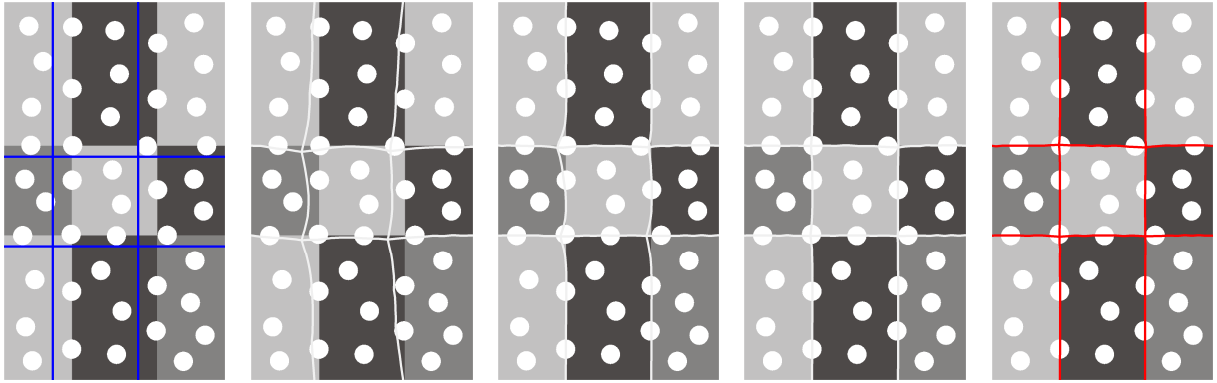


Figure 33: Impact of the topology to slightly fragmented object representations in the imagery, white blobs represent holes in the image energy: initialization (blue), optimization steps (light gray) and result (red)

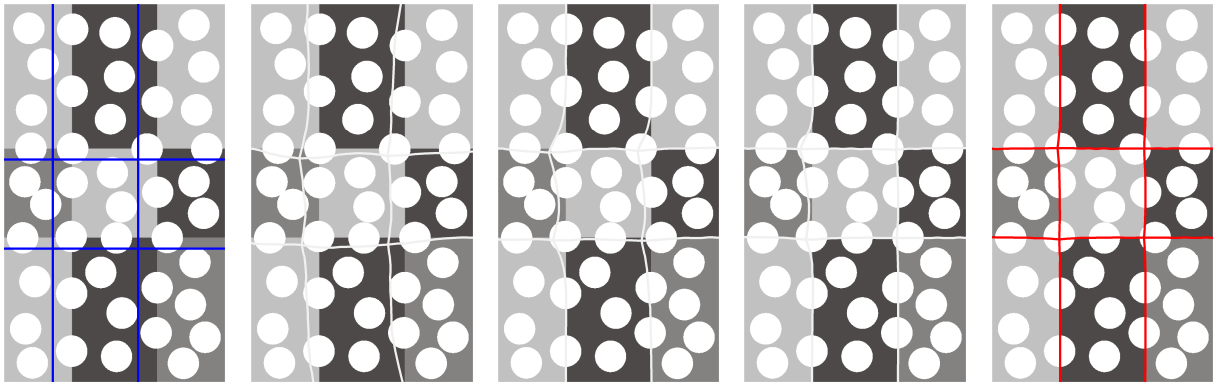


Figure 34: Impact of the topology to strongly fragmented object representations in the imagery, white blobs represent holes in the image energy: initialization (blue), optimization steps (light gray) and result (red)

In Figure 34 the fragmentation of the object representation is increased through larger holes in the imagery and, thus, with an increasing non-purposive image energy $E_{img}(C(s))$. Again, the initial contour network (depicted in blue) moves step by step (depicted in light gray) to the expected final result (depicted in red). The iterations shown after 50, 150 and 300 steps demonstrate the different behavior of the contour network during the optimization compared to Figure 33. The parts of the object contours causing attracting forces in the image energy are reduced, which lead to a slower movement of the contour network. In particular, the parts with a neutral image energy retard the optimization being dependent on the adjacent contour parts with attracting image forces. The internal energy $E_{int}(C(s))$ and the topology keep the contour parts and their initial structure together presenting a relatively good delineation of the assumed object contours. The delineation within the holes in the image can only be accomplished based on the defined shape model, which leads to slightly curved object contours, particularly in the vicinity of the nodes with a degree $\rho(C) = 4$ (cf. Figure 34). Both examples given in Figure 33 and in Figure 34 point out that fragmented object representations can be compensated using network snakes and, in addition, that the topology has an important impact to delineate contour parts in the vicinity of nodes with a degree $\rho(C) \neq 2$.

Concluding the analysis of the topology introduced with the new method of network snakes, the following statements can be made:

- An initial correct topology is required to delineate the complete network correctly due to the fixed topology, initial missing contour parts lead to an omission of the respective object boundaries.
- An initial wrong topology caused by additional contour parts does not influence the adjacent correct contour parts of the network.
- An initial wrong topology caused by missing boundaries can result in wrongly delineated adjacent contour parts due to the failed exploitation of the topology, if the adjacent contours are incorrectly initialized.
- The exploitation of the topology is related to the initialization requirements; the parameter control and the iteration behavior requiring a balanced parameter setting.
- The exploitation of the topology enables the correct delineation of object parts in the vicinity of nodes with a degree $\rho(C) \neq 2$, even though fragmented and weak object representations hamper a purposive image energy $E_{img}(C(s))$.

4.2.5. Discussion of the results

The aim of this chapter is the analysis and evaluation of the proposed new method of network snakes to highlight the benefits and limitations. A focus is on those topics resulting from the newly introduced topology to the concept of parametric active contours. The particular investigations defined at the beginning of this chapter concerning the initialization requirements, parameter control, iteration behavior, topology, generality and transferability are divided into two main parts.

The analysis of network snakes using *synthetic data* aims at results evaluating the general and methodical impact of the new method. The choice of the utilized two synthetic examples and the respective used initializations guarantee both a simplification of the investigations to point out the obtained results and a comprehensive significance of them. This fact is very important when discussing the proposed new method of network snakes because the transferability of the results to real application scenarios requires rules as clear as possible to define a framework for their utilization and evaluation.

The individual results of the analyses concerning the initialization requirements, parameter control, iteration behavior and topology emphasize that not only individual rules can be defined to control network snakes but, in addition, that there is a high dependency between them. In particular, the introduction and exploitation of the topology provides the opportunity to solve problems with more complex conditions delineating networks or the boundaries between adjacent objects. The requirement of a given topology to initialize the minimization process of the energy functional implies *additional costs* regarding the overall problem, but *benefits* the achievable results. This becomes apparent regarding the initialization requirements: the exploitation of the topology allows weaker rules concerning the initial contour network enabling wrongly initialized contour parts to attain the correct object boundaries utilizing the connectivity to the whole network (cf. Section 4.2.1.). In addition, the exploitation of the topology emphasizes the *dependency* on the parameter control as well as to the iteration behavior to guarantee the preservation of the topology in terms of a planar graph during the optimization of the

contour network (cf. Section 4.2.2. and Section 4.2.3.). The important point in this context is the fact that the parameter control can not just be defined dependent on the shape characteristics of the object of interest, but has to consider the uncertainty of the initialization to guarantee the detection of every part of the object boundaries during the optimization process.

The exploitation of the topology turns out to be a powerful enhancement of active contour models delineating networks or boundaries of adjacent objects. The combination of the *image energy* representing the object in the real world, the *internal energy* representing the shape characteristics of the object and the *topology* representing the structure of the object scene together in *one* energy minimization framework models the object representation in a very holistic manner. Thus, the developed method of network snakes enables for the first time a generally and methodically motivated solution with a clear mathematical basis for delineating the defined object class of networks. On the other hand the exploitation of the topology assumes a given correct initial topology. Missing or surplus contour parts in the network lead to missing or surplus delineations of the respective object boundaries caused by the fixed topology (cf. Section 4.2.4.). A concept to involve a correction of the topology *simultaneously* with the exploitation of the topology during the energy minimization does not exist at present.

The provided synthetic examples utilized in this section ensure an optimal object representation in the image resulting in an ideal image energy to clarify the investigations and achieved results. The impact of topology to overcome with fragmented or less concise image features is investigated in terms of *fragmented synthetic image data* simulating a non-purposive image energy $E_{img}(C(s))$. The introduction of the topology to the concept of parametric active contours incorporated in *one* energy functional turns out to be the crucial point to *overcome* fragmented object representations, in particular in the vicinity of nodes with a degree $\rho(C) \neq 2$. A question that at this point has not been answered concerning the analysis of network snakes is the impact of the topology to overcome poor object representations or disturbances contained in *real* image data, which is investigated in the following Section 4.3. and Section 4.4.

4.3. Delineation of field boundaries

4.3.1. Model, strategy and initialization

In this section the proposed new method of network snakes is applied to a *real* application scenario regarding the delineation of *field boundaries* from high-resolution optical satellite imagery. A second example, the delineation of adjacent biological cells in microscopic cell imagery, is discussed in the following Section 4.4. to point out the applicability of the new method to different real scenarios.

Regarding the defined goals at the beginning of this chapter, two points have not been investigated so far: the first point is the analysis of the *generality and transferability* of the proposed new method of network snakes. The generality has been identified with different synthetic examples and investigations in the previous section, but is extended in terms of real applications in this section. The transferability of the proposed new method of network snakes is a very important point because the new method aims at a general solution not only being developed for a specific application, but to delineate arbitrary networks and the boundaries of arbitrary adjacent objects. The analysis and evaluation of the new method concerning the transferability to different applications is derived with the defined quality measures completeness, correctness and geometrical accuracy (cf. Section 4.1.). The second point that has so far not been investigated is the contribution of the *topology* concerning its impact to overcome disturbances or less concise object feature represented in *real* imagery. The question is to which extent the topology can support the energy minimization process to deal with poor or fragmented object representations and disturbances contained in the image data. The goal is to investigate the influence of the topology when an optimal object representation in the image can not be guaranteed. In addition, the rules and statements derived in the previous Section 4.2. concerning the initialization requirements, parameter control, iteration behavior and topology are considered to analyze the transferability to real application scenarios.

The aim of the analysis of network snakes concerning the delineation of field boundaries is to describe a complete process achieving the final results. The *strategy* is divided into two main parts: first, a segmentation is carried out in a coarse scale ignoring small disturbing structures and thus exploiting the relative homogeneity of

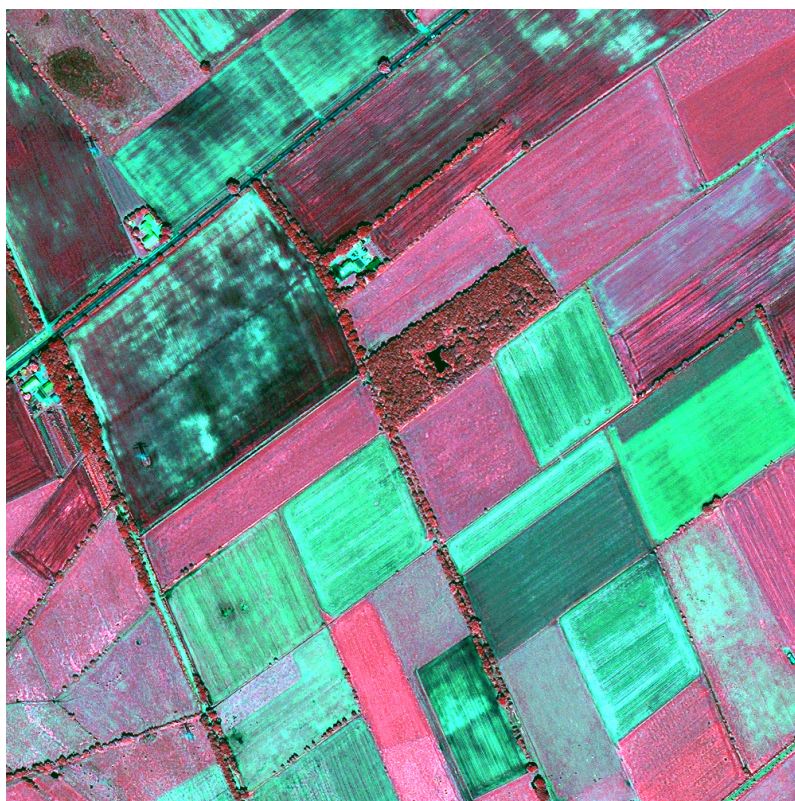


Figure 35: IKONOS CIR-image (1000×1000 pixel)

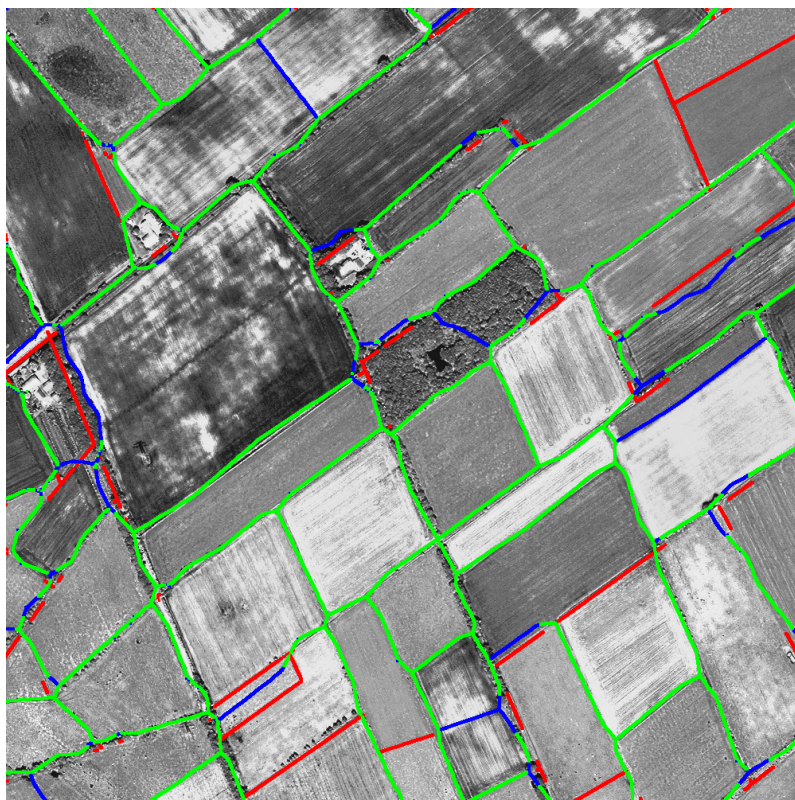


Figure 36: Evaluation of the initial segmentation: correctly segmented initial field boundaries (green), missing initial boundaries (red) and falsely segmented boundaries (blue)

the vegetation within each field. The objective is to obtain a topologically correct result, even if the geometrical correctness is not very high. Second, the new method of network snakes is used to improve the accuracy starting from the initial segmentation result and exploiting the derived topology. It must be emphasized that the strategy using a preliminary segmentation to derive the initialization and the topology is only one possibility to start the optimization process. Alternative approaches given in the literature have been discussed in Section 2.3.2., further opportunities could be the prior utilization of available GIS-data or preceding processes to predict field boundaries. The important point in this context is to analyze the new method of network snakes with real data including a *real initialization*. Regarding the specific application of extracting field boundaries, the question is how the proposed new method of network snakes can improve results of this kind of application.

The *model* of field boundaries is briefly described to provide both the basis for the initialization accomplished with a preliminary segmentation and the shape model utilized for the new method of network snakes. The *field* is divided into *field boundaries* and *field area* enabling the exploitation of different characteristics of the object leading to the same result. The field boundary is an elongated vegetation boundary, which is modeled as a relatively straight line or edge in the image. The field is a vegetation region, which is represented as a relatively homogeneous area concerning its spectral characteristics. The main problem causing the difficulty modeling and extracting field boundaries is the fact that the features describing the object of interest can strongly vary within a field. In Figure 35 a typical example of an IKONOS CIR-image is shown with a ground resolution of 1.0 m, displayed is a part of 1000×1000 pixel in Northern Germany.

The preliminary *segmentation* to initialize the new method of network snakes is demonstrated by taking the example in Figure 35. The segmentation exploits the modeled characteristics described above and is accomplished with a combination of a region- and edge-based approach. A multi-channel region growing is carried out using all available channels with a resolution of a few meters. Neighboring pixels are aggregated into one and the same region, if the difference in color does not exceed a predefined threshold. In addition, extracted edges, evaluated concerning their length and straightness, are introduced into the region growing process to restrict the growing at supposed field boundaries. The result of the initial segmentation process is compared to manually derived reference data in a 10 pixel wide buffer to evaluate the initialization concerning completeness, correctness and geometric accuracy (cf. Section 4.1.). The choice of a 10 pixel buffer equivalent to 10 m is made because the detection of field boundaries requires a minimum accuracy dependent on the application and its usability. A further reason is the provided satellite image data concerning its resolution and possible contained disturbances.

In Figure 36 the evaluation is superimposed onto the intensity channel: correctly segmented initial field boundaries are depicted in green, missing initial boundaries are depicted in red and falsely segmented boundaries are depicted in blue. The initial segmentation obtains a completeness of 79 %, a correctness of 83 % and the geometric accuracy as expressed in the horizontal root mean square value is 4.9 pixel equivalent to 4.9 m (cf. Table 7, upper row). The segmentation reflects a typical result concerning the completeness and correctness; only few initial boundaries are missing or are too much. For example, one field is in the state of being harvested causing a wrong and additional initial boundary, because it fulfills the model of field boundaries (cf. Figure 36 on the right). Missing boundaries are often the result of weak contrast between adjacent fields (cf. Figure 36 on the upper right). In addition, some segmented initial boundaries are too far away not being contained in the buffer of 10 pixel. However, the focus in the context of the analysis of network snakes is not the completeness or correctness, but to achieve a *real initialization* to evaluate the transferability of the new method to real application scenarios.

4.3.2. Results and evaluation of the delineation of field boundaries

The result of segmentation is the basis to initialize the proposed new method of network snakes (cf. Figure 37, depicted in blue). The contour network consists of 120 contour parts represented by 1850 nodes with a distance of about 6 pixels between neighbored nodes. The contour parts are connected by 101 nodes with a degree $\rho(C) \neq 2$, those points of the contour network which are of a particular interest for network snakes. The end points of the contour network with a degree $\rho(C) = 1$ are chained to the image borders and are allowed to move only along the borderline. Network snakes are used to improve the geometric accuracy of the field boundaries exploiting the image energy, the internal energy and the topology in a simultaneous optimization of the contour network. The image energy used for the delineation is derived from the standard deviation of the intensity channel of the CIR-image within a quadratic mask, because high values typically belong to field boundaries.

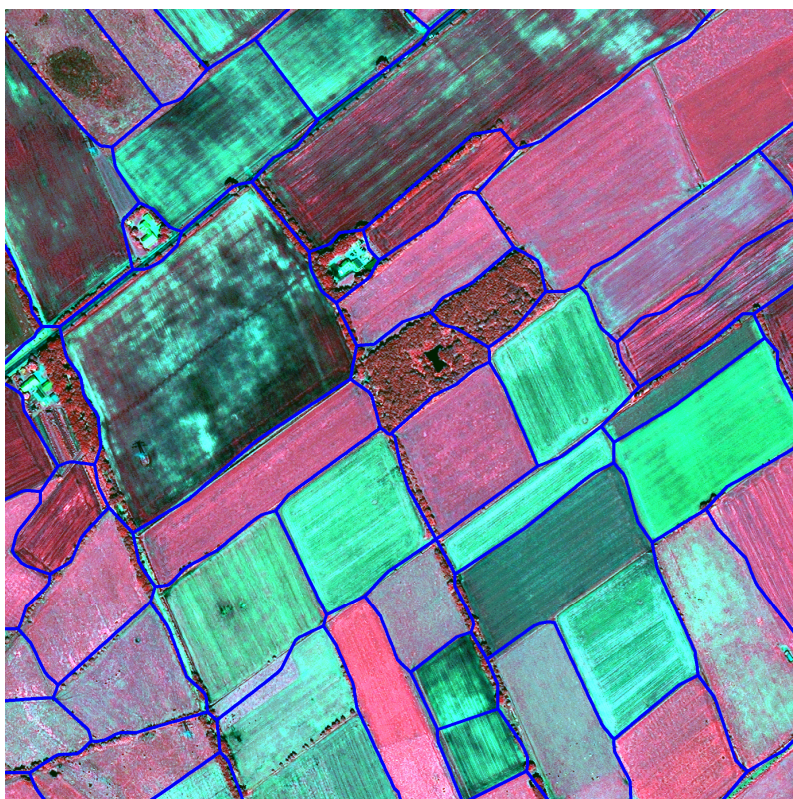


Figure 37: Initialization for network snakes using the initial segmentation

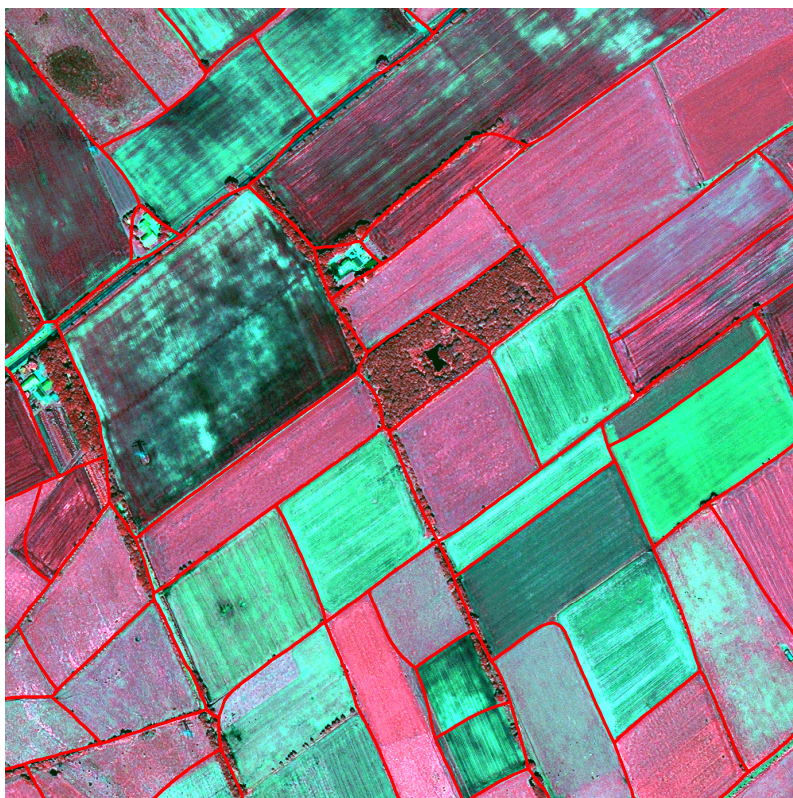


Figure 38: Final result of the delineation of field boundaries using network snakes

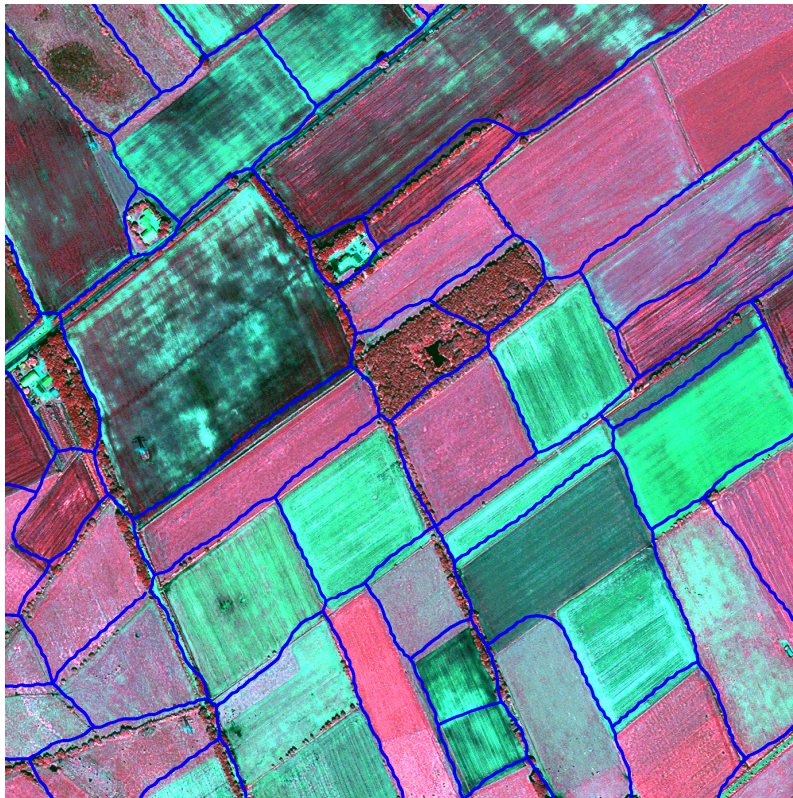


Figure 39: Initialization for network snakes using shifted segmentation

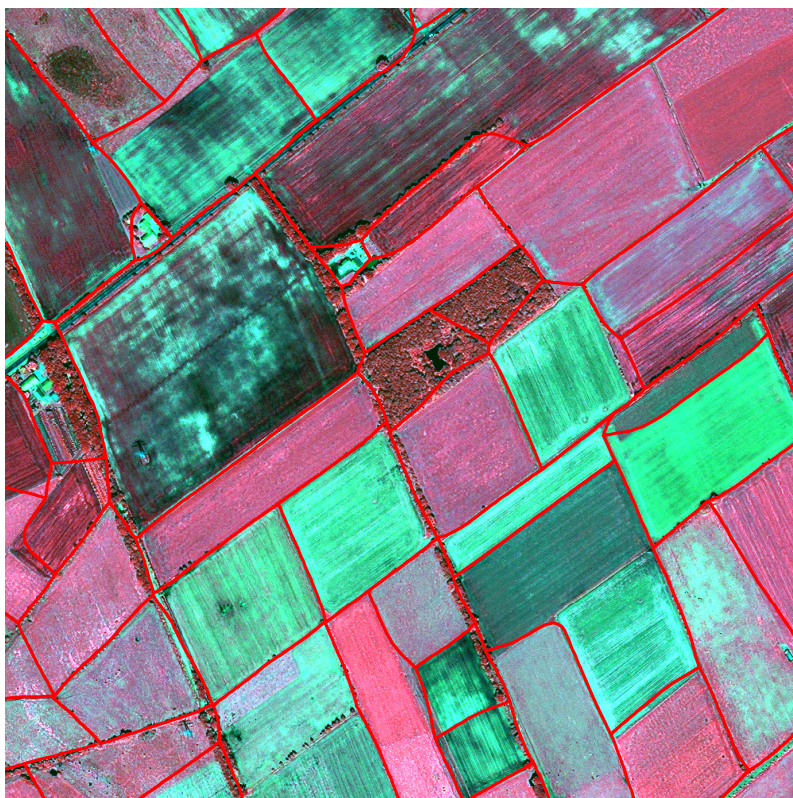


Figure 40: Final result of the delineation of field boundaries initialized with shifted segmentation

The used image energy is inverted before introducing it into the energy functional to fulfill the aim of energy minimization. The parameters for the internal energy are derived from the defined model of field boundaries and their shape characteristics. In addition, the parameter setting considers the accomplished investigations concerning the initialization requirements, parameter control, iteration behavior and topology (cf. Section 4.2.). Since the objects to be delineated are rather straight, the parameter β is set to a large value compared to α (cf. Section 4.2.2. for a detailed discussion). Both parameters are kept constant for the whole contour network, even though corners are possible within a contour part. In general, the parameter control used for the optimization of field boundaries is much more robust as the investigations of the synthetic examples in Section 4.2.2. would let assume. The reason is the fact that in contrast to the synthetic example fulfilling a large variety of curvatures and critical initialization conditions, the shape model of the field boundaries is more restricted to represent only rather straight object contours.

Starting from the initialization shown in Figure 37 (depicted in blue) the contour network moves step by step to the final result shown in Figure 38 (depicted in red). Again, the final result is compared to the reference data within a buffer of 10 pixel: the completeness increases to 83 %, the correctness to 87 % and the geometric accuracy improves about 36 % to 3.6 pixel or 3.6 m (cf. Table 7). The refinement is rather good, because the geometric accuracy achieves a quality which comes close to the original resolution of the provided IKONOS color channels of 4 m. Furthermore, the improvement of the completeness and correctness represents an enhancement of the field boundaries, which are contained in the buffer of 10 m and, thus, are usable for this specific application compared to the initial segmentation.

If the initialization had been worse but had still satisfied the defined initialization requirements (cf. Section 4.2.1.), the quality measures after applying network snakes would have been more or less the same, which emphasizes the robustness of network snakes against the initialization to a certain extent. The segmentation used as real initialization to start the optimization process (cf. Figure 37) is exemplarily shifted to the top to vary the initialization conditions as shown in Figure 39 (depicted in blue). Again, the contour network moves step by step to the final result presented in Figure 40 (depicted in red). The completeness of 47 % and the correctness of 48 % of the shifted initialization are considerably worsened compared to the correct initialization (cf. Table 8). But, the optimization using network snakes improves both quality measures to nearly identical values compared to the results obtained with the original initial segmentation. In addition, the geometric accuracy improves about 55 % to 3.8 pixel or 3.8 m using the shifted initialization, which is more or less the same compared to the geometric accuracy using the correct initialization. Problems occur for example at the boundaries of the small forest (cf. Figure 40, center), because there is no supporting image information pushing the shifted initial contours to the correct object boundaries. However, the results demonstrate that a moderately shift of the initialization can be compensated using network snakes. A detail is shown in Figure 41 and Figure 42 to point out the robustness of network snakes concerning the initialization, which again confirms the investigations accomplished in the previous Section 4.2.1. using the synthetic examples. Starting from different initializations (depicted in blue) the contour network moves step by step (depicted in white after 10, 50 and 100 iterations and superimposed to the image energy) to the same final result (depicted in red).

Quality measures	completeness	correctness	rms
initial segmentation	79 %	83 %	4.9 pixel
using network snakes	83 %	87 %	3.6 pixel

Table 7: Quality measures before and after the optimization with network snakes

Quality measures	completeness	correctness	rms
shifted segmentation	47 %	48 %	5.9 pixel
using network snakes	73 %	78 %	3.8 pixel

Table 8: Quality measures before and after the optimization with network snakes initialized with shifted segmentation

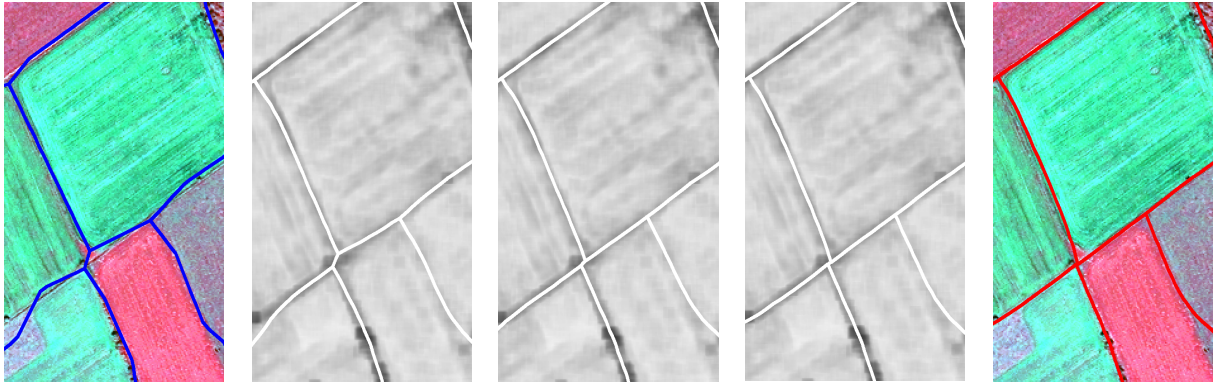


Figure 41: Detail of the utilization of network snakes shown in Figure 37 and Figure 38 using the correct initial segmentation: initialization (blue), optimization steps superimposed to the image energy after 10, 50 and 100 iterations (white) and final result (red)

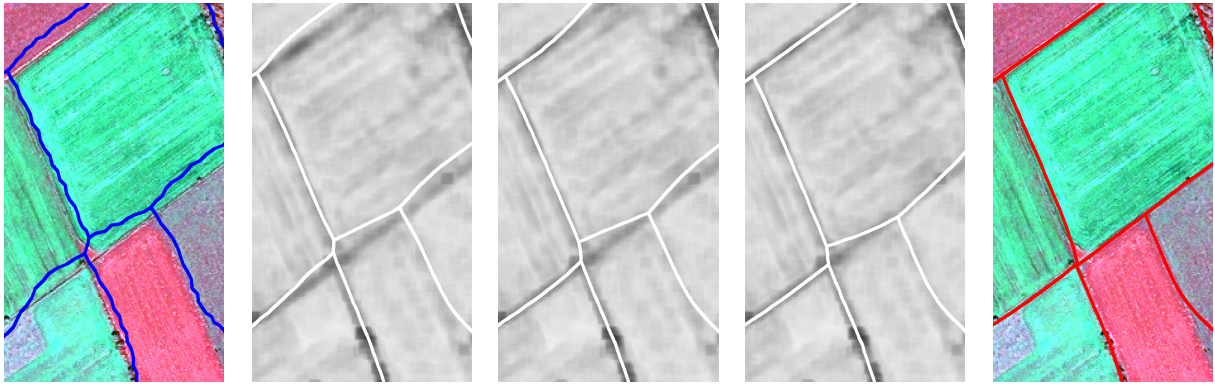


Figure 42: Detail of the utilization of network snakes shown in Figure 39 and Figure 40 using the shifted initial segmentation: initialization (blue), optimization steps superimposed to the image energy after 10, 50 and 100 iterations (white) and final result (red)

In Figure 43 and Figure 44 details of the minimization process are shown to demonstrate and analyze the functionality of network snakes in more detail. Starting from the initialization (depicted in blue) the contour network moves step by step (depicted in white after 10, 50 and 100 iterations and superimposed to the image energy) to the final result (depicted in red). In Figure 43 the nodes with a degree $\rho(C) = 3$ in conjunction with the contour parts in between behave as expected when optimizing the energy functional to delineate the boundaries of the fields. Even though the image energy does not represent the object boundaries very precisely due to rows of trees or other disturbances, and although other parts of the boundaries are only partly visible, the new method of network snakes enables a good and smooth delineation of the object boundaries. The shape characteristics included in the internal energy allow for corners within a contour part as for example illustrated in Figure 43 on the bottom right. Thus, the adjacent missing boundary at the corner in the initialization of the contour network has only a marginal influence at that point (cf. Figure 38, bottom right, too). This result confirms the investigations regarding missing contour parts in a network of Section 4.2.4. Furthermore, surplus contour parts such as the one within the forest (cf. Figure 38, center) do not influence the optimized result as concluded concerning the investigations of the topology using synthetic data.

Similar results can be seen in Figure 44, where the delineation of the field boundaries works well in the most cases. Yet the imprecision of the image energy to be compensated by the internal energy and topology has a limit as demonstrated in the upper part of Figure 44. The exact boundary between the adjacent fields is not detectable and, in addition, there are no neighboring precise boundary representations in the image energy providing a final result which does not vary within the image information. A further interesting point to be analyzed is the

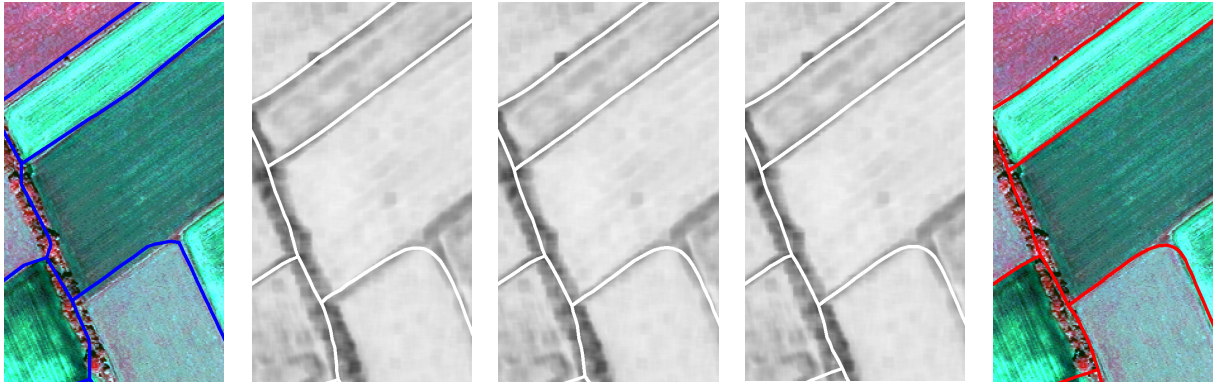


Figure 43: Detail of the utilization of network snakes shown in Figure 37 and Figure 38 to demonstrate the general functionality: initialization (blue), optimization steps superimposed to the image energy after 10, 50 and 100 iterations (white) and final result (red)

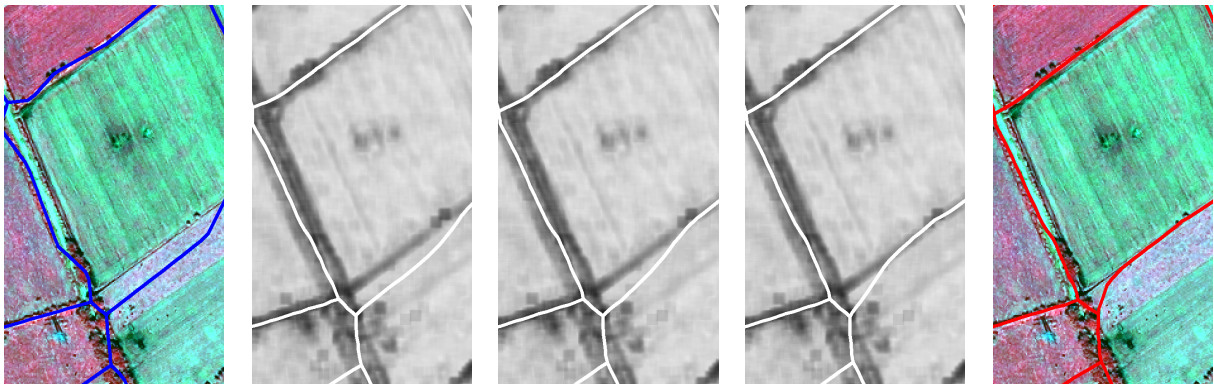


Figure 44: Detail of the utilization of network snakes shown in Figure 37 and Figure 38 to demonstrate the general functionality: initialization (blue), optimization steps superimposed to the image energy after 10, 50 and 100 iterations (white) and final result (red)

given topology which is assumed to be correct. At the right border of Figure 44 (bottom) one horizontal initial boundary is far away from the field boundary to be detected. During the optimization the contour moves to the expected field boundary, but the node with a degree $\rho(C) = 3$ remains in the wrong position. The reason is that the node is located within a distinctive minimum of the image energy. The internal energy allows for this curved shape behavior and the neighboring contour part on the left is not connected to this node due to the wrong initial topology. The solution of the problem would be to merge the two nodes with a degree $\rho(C) = 3$ to only *one* node with a degree $\rho(C) = 4$, but this decision is very hard to come to without the incorporation of additional information. For example, the nodes with a degree $\rho(C) = 3$ being very close to each other displayed in the center of Figure 44 are not allowed to merge because the left and right field boundary terminate at different positions at the vertical boundary.

4.3.3. Discussion of the results

The goal of this section is to analyze the generality and transferability of the proposed new method of network snakes and to investigate the contribution of the topology concerning its impact to overcome disturbances or less concise image feature represented in real image data. It has been demonstrated that the use of network snakes to delineate field boundaries from high-resolution optical satellite imagery leads to very promising results. The reason is the combination of the image energy, the internal energy and the topology in one comprehensive model to deal with complex real application scenarios. The important point to be highlighted is the utilization of the developed new method of network snakes with a complete processing of *real* data. Moreover, the investigation

of the introduced *topology* to the concept of parametric active contours emphasizes that fragmented and poor object representations within the image causing a non-purposive image energy $E_{img}(C(s))$ can be compensated using network snakes. In addition, the incorporated internal energy $E_{int}(C(s))$ enables the delineation of smooth object boundaries as represented in the shape model of field boundaries even if the image energy does not support a precise localization. On the other hand, only a given correct topology can be exploited correctly, because a modification of the initial topology is not possible during the optimization.

4.4. Delineation of cells

4.4.1. Model, strategy and initialization

In this section the developed new method of network snakes is applied to a second *real* application scenario to point out the applicability to different areas delineating adjacent objects and networks in a variety of applications. The aim is to demonstrate the utilization and impact with an example from the bio-medical area of research delineating *adjacent biological cells* in microscopic cell imagery. As already discussed at the beginning of the previous Section 4.3. concerning the delineation of field boundaries, the goal is the investigation of the *generality and transferability* of network snakes and the analysis of the contribution of the *topology* to overcome poor or weak object representations causing a poor *image energy*.

The aim of the analysis of network snakes concerning the delineation of biological cells is once more to describe a complete process achieving the final results. Again, the *strategy* is divided into two main parts, but regarding this application, the availability of multi-channel fluorescence labelings enables the exploitation of different image types. Each cell nucleus is located within the associated cell membrane, which allows for the taking of this information as seed point to derive the topology delineating the boundaries of adjacent cells. This strategy is reasonable because the cell nuclei are well defined against the background and, thus, are much easier to detect than the boundaries of the cytoplasm. First, a segmentation of the cell nuclei is accomplished to derive the initialization in the first channel, an exemplary image part with 200×200 pixel is shown in Figure 45 on the left. The objective is to obtain a topologically correct result utilizing the nuclei, even if the geometrical correctness of the derived cell boundaries is not very high. Second, the new method of network snakes is used to optimize and improve the accuracy using the second channel representing the cytoplasm; an example is shown in Figure 45 on the right. This strategy is well-known in the literature detecting and tracking cells, because the machine-dependent artifacts like noise and typical object characteristics like homogeneous areas in the intensity distribution at cell boundaries cause major difficulties using only one image channel. The goal in this context is to analyze the new method of network snakes with real data including a *real initialization* to demonstrate the transferability to bio-medical applications.

The *model* of cells including their nuclei is briefly described to provide both the basis for the initialization accomplished with a preliminary segmentation using the first channel, and the shape model utilized for the new method of network snakes utilizing the second channel. Cell nuclei are represented within the first channel as light blobs with varying intensity distributions, which are well-defined against the relatively dark and homogeneous background. Cells and their boundaries are pictured in the microscopic imagery with stained cytoplasm, which fluoresced during the data capture. In contrast to the first channel, the representation of the adjacent cells and their borders in the second channel is very blurry and weak with heterogeneous features defining the cell borders. The cells are characterized as relatively compact objects with smooth shapes representing the object contours.

The preliminary *segmentation* of the cell nuclei to initialize the new method of network snakes is demonstrated taking the example in Figure 45 on the left. The detection of the nuclei is accomplished by means of a segmentation of the relative homogeneous background utilizing a region growing algorithm. Subsequently, a skeleton is computed to yield a coarse initial network representing the boundaries between adjacent cells (cf. Figure 46 on the left, depicted in blue). Obviously, the detection of all cell nuclei leads to a correct topology, whereas the geometrical accuracy is so far not considered. The result of the initial segmentation process is compared to manually derived reference data in a 10 pixel wide buffer to evaluate the initialization concerning completeness, correctness and geometric accuracy (cf. Section 4.1.). The choice of a 10 pixel buffer is equivalent

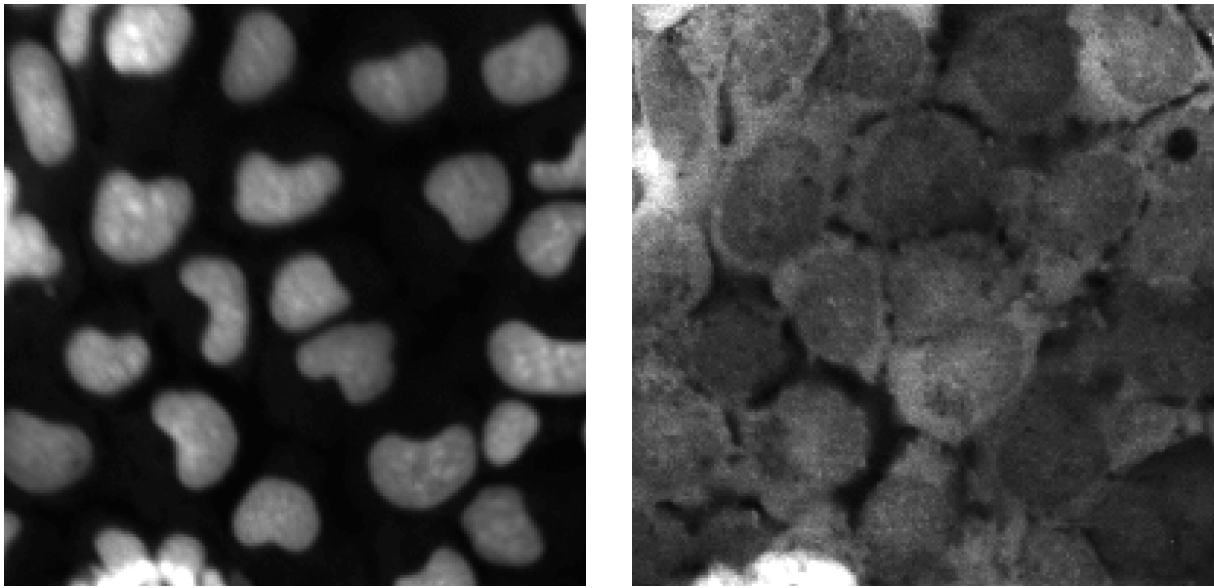


Figure 45: Cell nuclei and microscopic cell imagery (200×200 pixel)

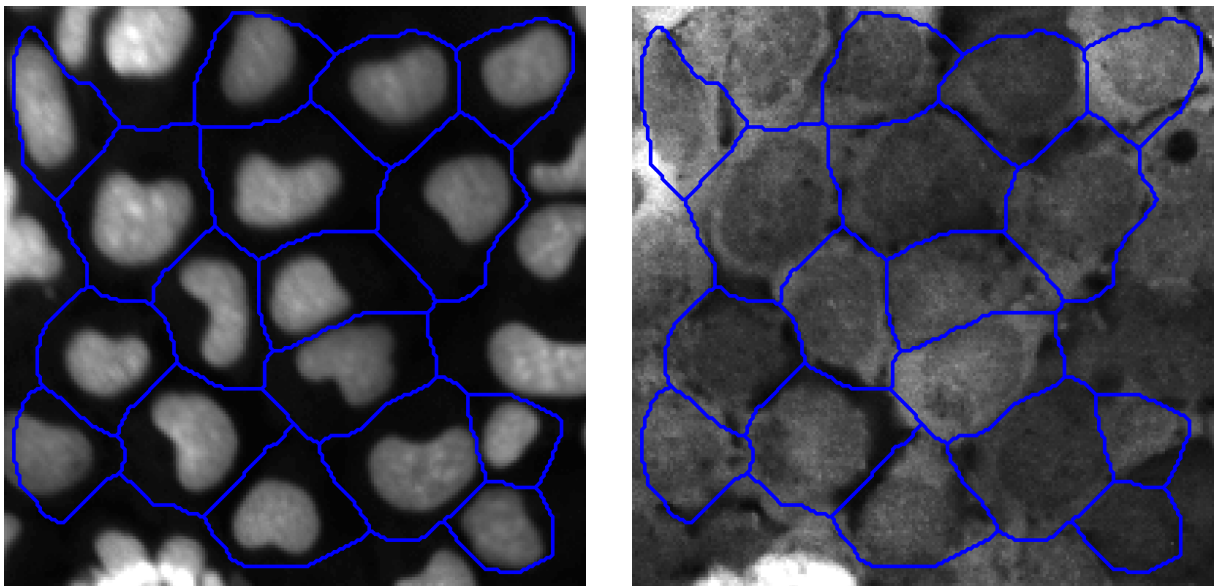


Figure 46: Cell nuclei with derived initialization (depicted in blue) and superimposed to the microscopic cell imagery

to approximately 1.5 micrometers. Thus, the requirement of a minimum accuracy for the usability of cells is guaranteed considering the provided resolution and noise within the image. All cell nuclei are detected correctly, which leads to computed quality measures concerning the completeness of 100 % and concerning the correctness of 100 %. The geometric accuracy as expressed in the horizontal root mean square value is 3.1 pixel (cf. Table 9, upper row). The derived initial results are obviously very promising concerning the completeness and correctness, but the accuracy of the delineation of the cell boundaries can be improved.

4.4.2. Results and evaluation of the delineation of cells

The result of the segmentation derived with the cell nuclei is the starting point to initialize the new method of network snakes to optimize the contour network (cf. Figure 47, depicted in blue). The contour network consists of 48 contour parts represented by 1500 nodes with a distance of about 1 pixel between neighbored nodes. The contour parts are connected by 32 nodes with a degree $\rho(C) = 3$. End points with a degree $\rho(C) = 1$ are not contained in the contour network, because only cell nuclei which could be detected completely are used to derive the initialization. The image energy used for the delineation is the image intensity itself, because the boundaries of cells are at least partly represented by low values of the stained cytoplasm in contrast to the cell substance. The parameters for the internal energy are derived from the defined model of adjacent biological cells and their shape characteristics. In addition, the results of the investigations using the synthetic examples regarding the initialization requirements, parameter control, iteration behavior and topology accomplished in Section 4.2. are considered in the parameter control. The objects of interest to be delineated have a specific range of curvature, which is why the parameter β is set to a large value compared to α , but is not set to such a large value compared to the delineation of mostly straight field boundaries (cf. Section 4.3.2.). The parameters of the internal energy are set to be constant for the whole contour network, because the different contour parts of the cell boundaries are modeled identically. The derived topology from the cell nuclei of the first channel is explicitly contained in the mathematical model of network snakes to be exploited during energy minimization.

Starting from the initialization shown in Figure 47 (depicted in blue), the contour network moves step by step to the final result shown in Figure 47 (depicted in red). Again, the final result is compared to the reference data: obviously, the completeness and correctness are kept constant at 100 %, but the geometric accuracy increases to 2.9 pixel (cf. Table 9, second row). The improvement of the complete network is only moderate, because the optimization works well in the center of the example, but works poorly at the borders of the image. This fact

Quality measures	completeness	correctness	rms
initial segmentation	100 %	100 %	3.1 pixel
using network snakes	100 %	100 %	2.9 pixel
initial segmentation (without border)	100 %	100 %	3.0 pixel
using network snakes (without border)	100 %	100 %	2.2 pixel

Table 9: Quality measures before and after the optimization with network snakes

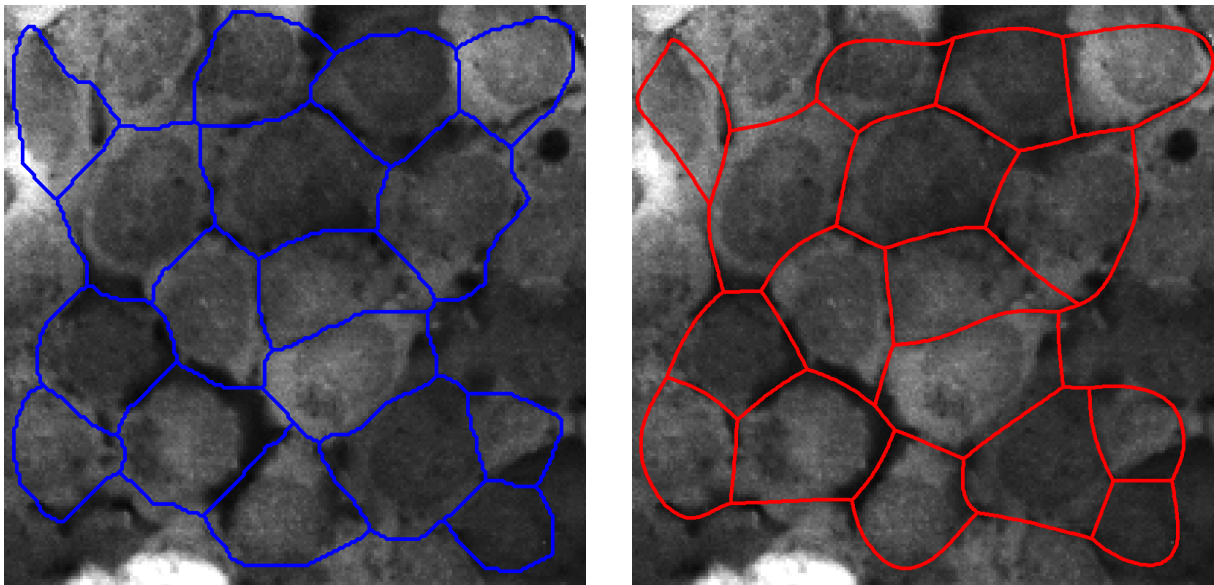


Figure 47: Initialization (blue) and final result of the delineation of cells using network snakes (red)

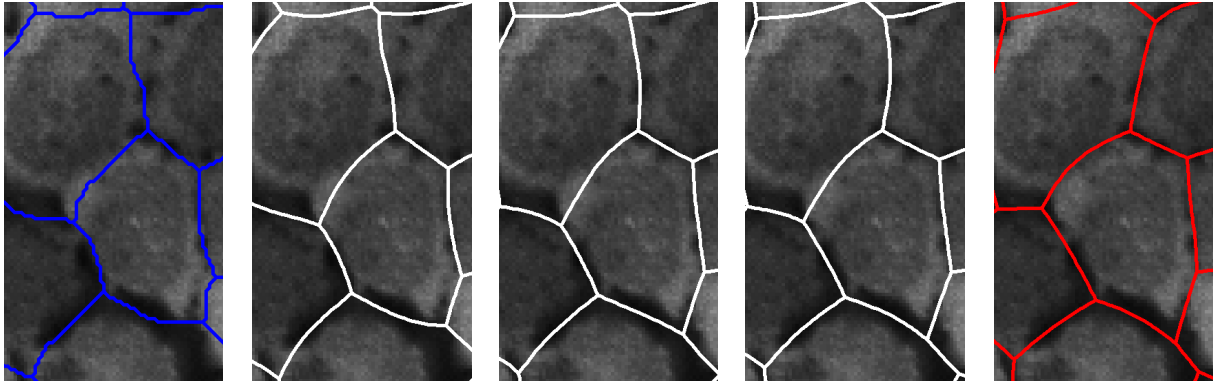


Figure 48: Detail of the utilization of network snakes shown in Figure 47 to demonstrate the general functionality: initialization (blue), optimization steps superimposed to the image energy after 20, 100 and 200 iterations (white) and final result (red)

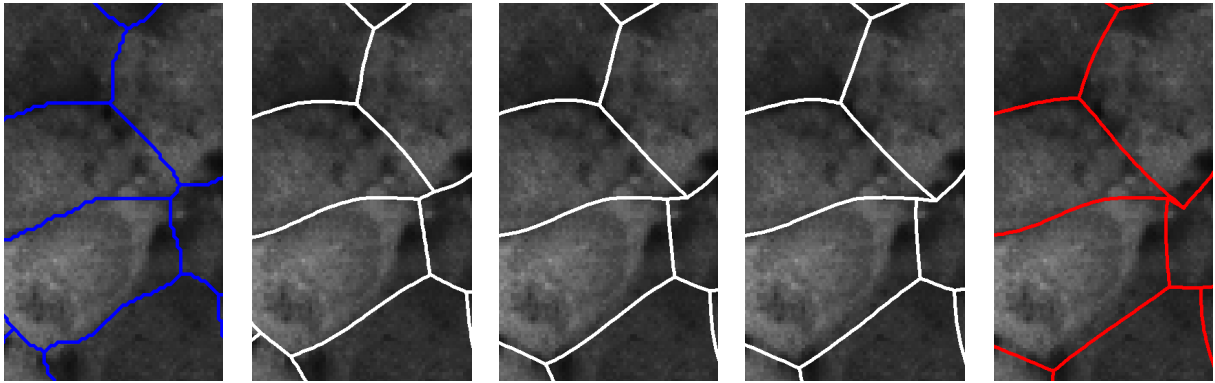


Figure 49: Detail of the utilization of network snakes without the utilization of the topology-preserving energy: initialization (blue), optimization steps superimposed to the image energy after 20, 100 and 200 iterations (white) and final result (red)

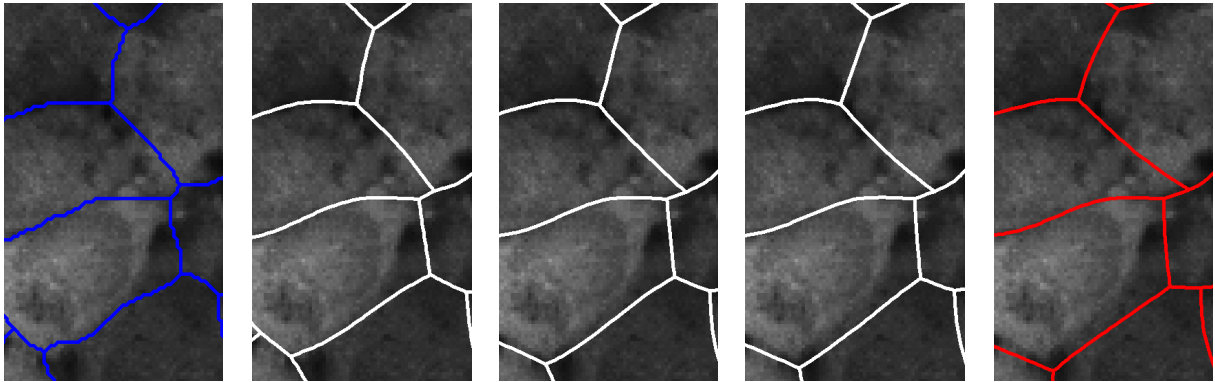


Figure 50: Detail of the utilization of network snakes shown in Figure 47 utilizing the topology-preserving energy: initialization (blue), optimization steps superimposed to the image energy after 20, 100 and 200 iterations (white) and final result (red)

is confirmed regarding only the quality measures in the center of the example excluding the border area: the initial geometric accuracy with 3.0 pixel is similar compared to the complete initialization (cf. Table 9, third row), but after the optimization using network snakes the accuracy increases to 2.2 pixel (cf. Table 9, bottom). The different improvement of the cells concerning the whole example and the center area is well-founded caused by the exploitation and impact of the topology. In particular, noisy image data or weak object representations in the image energy point out the benefit of the introduced topology to the new energy functional of network snakes. The topology keeps the structure of the object scene during the optimization, even though only parts of the object contours are represented concisely within the imagery. Cells which are located at the border of the scene are only connected at one side to the network leading to a shrinking of the outer contour parts of the object (cf. Figure 47 on the right side). In Figure 48 the general functionality of network snakes delineating cells is shown in more detail to point out the contribution of the method. Starting from the initialization (depicted in blue) the contour network moves step by step (depicted in white after 20, 100 and 200 iterations and superimposed to the image energy) to the final result (depicted in red).

In Figure 49 and Figure 50 further details of the minimization process are shown to demonstrate the functionality of network snakes and, in addition, to analyze the impact of the topology. Starting from the initialization (depicted in blue) the contour network moves step by step (depicted in white) to the final result (depicted in red). Figure 49 and Figure 50 show the same part of the contour network, but only in Figure 50 the additional topology-preserving energy $E_{topo}(C(s))$ is considered (cf. Section 3.4.2.). In contrast, the part of the example shown in Figure 49 does not include the topology-preserving energy. Thus, the two neighbored nodes, which are close to each other located on the right side, move around each other and change the correct initial topology in terms of a planar graph leading to a wrong result. The example demonstrates the impact of the utilization and preservation of the topology. The other depicted contour parts of the network move to the correct boundaries of the cells, even though the object representation within the image energy is not very distinct.

4.4.3. Discussion of the results

In this section a second real example was demonstrated to analyze and highlight the *transferability* of network snakes to further and different application scenarios. The delineation of biological cells is based on completely different image data characterized with different image features compared to remotely sensed imagery used for the delineation of field boundaries. The microscopic images include in general noise caused by the data capture process leading to a representation of the object boundaries with only weak features. The investigation of the new method of network snakes identifies the impact of the introduced and exploited topology to the concept of parametric active contours to overcome poor object representations in the images. Moreover, the utilization of the topology emphasizes the improvement of the obtained results in the center of the shown example where the cells are completely contained in the network. The proposed topology-preserving energy demonstrates the usability applied to real scenarios to preserve the initial given topology. A further important point is the shape behavior of the contour network representing the modeled object boundaries of the cells with the internal energy to overcome weak and frayed object representations in the image.

5. Discussion and outlook

In this chapter the developed new method of network snakes is discussed considering the stated goals of the thesis to give a concluding evaluation of the proposed new method and its impact. In addition, unsolved problems are highlighted to emphasize further questions and to point out possible future research.

5.1. Discussion

The main goal of the thesis was the development of a new method of active contour models, which enables the delineation of arbitrary graphs representing *networks* or the *boundaries between adjacent objects*. The presented new method of *network snakes* solves this task with the introduction of a clearly defined mathematical model based on the concept of parametric active contours. Hence, the well-known active contour models as an important method in computer vision are enhanced to a new object class.

Three sub-goals of the thesis have been defined at the beginning, which are discussed in the following concerning their realization:

- Development of a new method of active contour models, which optimizes graphs consisting of nodes of an arbitrary degree to enable the delineation of open contours, closed contours and any networks:

Both concepts of active contour models, parametric active contours and geometric active contours, are originally only defined for single closed object boundaries. The goal to optimize graphs representing nodes with arbitrary degree requires the introduction of topology to active contours models. The explicit representation of topology is only possible in the mathematical model of parametric active contours, which is why the developed new method is based on this concept. For the first time, a solution is provided in this thesis which enables the optimization of arbitrary graphs with a clearly defined mathematical model. The new method has been demonstrated with a synthetic example to point out the innovation of the proposed solution and, in addition, to picture the contribution of network snakes compared to traditional solutions. However, the concept of parametric active contours requires an initial contour to start the optimization process. Depending on the application, initial segmentations can be used as demonstrated with both real application scenarios or, alternatively, other available prior information can be utilized, for example derived from a GIS.

- Development of a new method of active contour models, which segments imagery without gaps or overlaps to enable the delineation of adjacent objects or networks:

The goal to segment imagery without gaps or overlaps has the identical solution, because the boundaries between adjacent objects represent a network, too. Thus, network snakes are a suitable method to partition an image into multiple, non-overlapping regions. In addition, the main impact of traditional parametric active contours bridging the gap between low-level feature extraction and high-level geometric representation of objects can be applied to segmentation tasks not only being suitable for single objects. The incorporation of topological knowledge to the total energy functional resulting in network snakes enhances the traditional concept to arbitrary object types combining image data with modeled object knowledge concerning the shape behavior.

- Development of a new method of image segmentation and object delineation with a high generality and transferability to enable its applicability for a variety of tasks:

The new method of network snakes is developed with a clearly defined mathematical model to guarantee its generality and transferability to a large variety of applications delineating networks and the boundaries between adjacent objects. The incorporation of any constraint and, thus, the limitation of the method to only particular applications is consciously avoided. In contrast, a method is presented in the thesis which enables a free optimization of the whole network incorporating a complete shape control of all contour parts. This goal is tackled methodically by analyzing synthetic examples to provide a comprehensive investigation of the impact. Moreover, the transferability is demonstrated with the analysis of real application scenarios

concerning the delineation of field boundaries from optical satellite images and the delineation of adjacent biological cells in microscopic cell images to point out the applicability to a large variety of different applications.

In addition to the defined goals reached with the developed new method of network snakes, a further important point is of interest: the aim of the thesis was not just to enable the optimization of nodes with arbitrary degree to delineate networks and the boundaries between adjacent objects, but was also to introduce and exploit the topology explicitly during the optimization. The integrated optimization of networks or boundaries of adjacent objects allows to deal with poor or fragmented object representations, in particular in the vicinity of nodes with a degree $\rho(C) \neq 2$. Furthermore, the exploitation of the topology enables weaker initialization requirements starting the minimization of the energy functional. Consequently, the main impact of network snakes is the combination of the image energy representing the objects in the real world, the internal energy incorporating the shape characteristics, and the topology representing the structure of the scene in one comprehensive energy functional.

The analysis of network snakes with synthetic examples provides rules and statements concerning the initialization requirements, the parameter control, the iteration behavior and the incorporated topology. Thus, a complete framework is given and discussed to apply network snakes to a variety of real scenarios. The accomplished investigations enable a basis to transfer the new method to arbitrary applications delineating networks and the boundaries of adjacent objects from a methodical and theoretical point of view. The usability of network snakes has been successfully demonstrated with the delineation of field boundaries from satellite images and the delineation of biological cells from microscopic cell images. Consequently, the important criterion concerning the generality and transferability of the developed new method has been highlighted and, in addition, the impact of network snakes to numerous further applications of this object class can be expected. The obtained results delineating field boundaries and biological cells demonstrate that network snakes can improve the geometric accuracy of these applications considering and exploiting their topological characteristics. In addition, the incorporated shape model into the minimization process enables smooth object delineations even though the object is only represented with poor features in the image.

One general limitation of active contour models are open contour ends. The new mathematical definition of network snakes enables a complete shape control up to the end points of open contours, but the internal energy representing the shape characteristics causes generally a contour shrinking due to the approximation of the derivatives with finite differences. Approaches to preserve the contour length or to fix the end points are a possible solution, but a mathematically clear and general approach is not given yet. Thus, the treatment of end points within a contour network has to be done depending on the specific application. For example, concerning the delineation of field boundaries, the contour ends at the image borders were chained to allow for movement only along the borderline.

5.2. Outlook

The discussion of the method of network snakes above emphasizes the impact of the new developments to optimize arbitrary networks and the boundaries of adjacent objects. Two main points are of special interest for possible future research: the first point concerns the given rigid topology and the question of whether a change in the topology can be introduced to the proposed mathematical model. The second point deals with the question of whether an internal evaluation of the contour network can provide the derivation of quality measures regarding the optimized results.

The introduction of the topology to the concept of parametric active contours is the main innovation of the new method of network snakes. The investigations concerning the exploitation of the topology points out that coarser initializations of the contour network or less concise or fragmented object features within the image can be compensated utilizing the given initial topology. The concept of parametric active contours includes an explicit representation of contours in their parametric form during the deformation process resulting in rigid topology. This fact involves two requirements: first, the initial topology is assumed to be correct and, second, the given topology must be preserved in terms of a planar graph during the optimization process. The second point has been fulfilled with the incorporation of the topology-preserving energy $E_{topo}(C(s))$ to the total energy functional. The first point requires a high demand regarding the given initial topology to be utilized during the optimization. The effects of missing or surplus contour parts in the network have been analyzed: surplus contours do not

influence neighboring correct contour parts significantly, but missing contours in the network can cause adverse effects. The question which arises from the investigations is whether surplus or missing contour parts can be deleted or added, respectively. The crucial point is the issue of whether the exploitation of the rigid topology can be combined with the detection of topology errors and their elimination in one optimization process. This is up to now an unsolved problem and requires additional information during the optimization, which has to be derived from the available data to be introduced to the energy functional. The main problem is the fact that for example two converging nodes with a degree $\rho(C) \neq 2$ cannot just be merged to only one node deleting the contour part in between, if they are close to each other. Similarly, the introduction of new contour parts requires a significant evidence, which has so far not been incorporated in the energy functional. The development of strategies and approaches to introduce the possibility to change the topology in conjunction with their exploitation is a challenging task for future research.

The second interesting point for possible further investigation is the question of whether an internal evaluation of the contour network can provide quality measures concerning the optimized results. Systems containing a self-diagnosis are presented for example in [FÖRSTNER AND LÄBE 2003] and [HINZ AND WIEDEMANN 2004], where the internal evaluation is based on redundant information. The question of internal evaluation is related to the above discussed problem of the rigid topology. A statement concerning the quality of a contour part during the optimization of the network can provide evidence to delete a contour part changing the topology. Yet decisions in this context could be deceptive: for example, the utilization of the image information to provide a new assessment criterion regarding a contour part could lead to a wrong decision. Active contour models have the advantage compared to other methods of combining image energy terms with internal energy terms and, thus, delineating a contour correctly even though the image information is non-purposive. The introduction of the topology improves this characteristic because network snakes enable a larger independence of the image information exploiting the topology. Consequently, the utilization of the image information during the optimization to derive quality measures of the contour parts of the network is difficult. In addition, an internal evaluation requires redundant information which causes a modification of the proposed method of network snakes to derive that independent information, which up to now has not been considered. The complexity of an internal evaluation of network snakes to provide quality measures or to give evidence to change the topology is a challenging task for further research with the aim of developing strategies to improve the general methodology.

The unsolved problems discussed above can be treated in future research to enhance the new method of network snakes. However, the goals stated at the beginning of this thesis have been solved with the introduction of the novel mathematical model to the energy minimization concept of active contour models. The incorporation of image features, shape models and topology in one common minimization framework turns out to be a powerful method to cope with complex questions of object delineation from imagery. Network snakes are an important contribution to delineate the object class of networks and boundaries of adjacent objects that are applicable to a large variety of tasks.

References

- ABE, T. AND MATSUZAWA, Y. (2000): Multiple Active Contour Models with Application to Region Extraction. In: *Proceedings International Conference on Pattern Recognition*, pp. 626-630
- AMINI, A. A., WEYMOUTH, T. E. AND JAIN, R. C. (1990): Using Dynamic Programming for Solving Variational Problems in Vision. *IEEE Transactions on Pattern Analysis and Machine Intelligence* 12(9), pp. 855-867
- APLIN, P. AND ATKINSON, P. M. (2004): Predicting Missing Field Boundaries to Increase Per-Field Classification Accuracy. *Photogrammetric Engineering & Remote Sensing* 70(1), pp. 141-149
- AUBERT, G. AND BLANC-FERAUD, L. (1999): Some Remarks on the Equivalence between 2D and 3D Classical Snakes and Geodesic Active Contours. *International Journal of Computer Vision* 34(1), pp. 19-28
- AUERNHAMMER, H. (2001): Precision Farming - the Environmental Challenge. *Computers and Electronics in Agriculture* 30(1-3), pp. 31-43
- BAILLOEUL, T., PRINET, V., SERRA, B., MARTON, P., CHEN, P. AND ZHANG, H. (2005): Digital Map Refinement from Knowledge-Driven Active Contours and Very High Resolution Optical Imagery. *Photogrammetric Fernerkundung Geoinformation* 6/2005, pp. 511-522
- BALLARD, D. H. AND BROWN, C. M. (1982): *Computer Vision*. Prentice Hall, 544 p.
- BAMFORD, P. AND LOVELL, B. (1998): Unsupervised Cell Nucleus Segmentation with Active Contours. *Signal Processing* 71(2), pp. 203-213
- BLAKE, A. AND ISARD, M. (1998): *Active Contours*. Springer, 352 p.
- BORGEFORS, G. (1984): Distance Transformations in Arbitrary Dimensions. *Computer Vision, Graphics, and Image Processing* 27(3), pp. 321-345
- BOSCOLO, R., BROWN, M. S. AND MCNITT-GRAY, M. F. (2002): Medical Image Segmentation with Knowledge-Guided Robust Active Contours. *Radio Graphics* 22(2), pp. 437-448
- BRESSON, X., VANDERGHEYNST, P. AND THIRAN, J. (2006): Multiscale Active Contours. *International Journal of Computer Vision* 70(3), pp. 197-211
- BRIGGER, P., HOEG, J. AND UNSER, M. (2000): B-Spline Snakes: A Flexible Tool for Parametric Contour Detection. *IEEE Transactions on Image Processing* 9(9), pp. 1484-1496
- BRONSTEIN, I. N., SEMENDJAJEW, K. A., MUSIOL, G. AND MÜHLIG, H. (2005): *Taschenbuch der Mathematik*, Vol. 6. Harri Deutsch, 1195 p.
- BURGHARDT, D. AND MEIER, S. (1997): Cartographic Displacement Using the Snakes Concept. In: W. Förstner and L. Plümer (eds.), *Semantic Modeling for the Acquisition of Topographic Information from Images and Maps*, Birkhäuser, pp. 59-71
- BURGHARDT, D. (2005): Controlled Line Smoothing by Snakes. *GeoInformatica* 9(3), pp. 237-252
- BUTENUTH, M. AND HEIPKE, C. (2005): Network Snakes-Supported Extraction of Field Boundaries from Imagery. In: W. Kropatsch, R. Sablatnig and A. Hanbury (eds.), *Pattern Recognition, Lecture Notes in Computer Science* 3663, Springer, pp. 417-424

- BUTENUTH, M. AND JETZEK, F. (2007): Network Snakes for the Segmentation of Adjacent Cells in Confocal Images. In: A. Horsch, T. M. Deserno, H. Handels, H.-P. Meinzer and T. Tolxdoff (eds.), *Bildverarbeitung für die Medizin 2007, Informatik aktuell*, Springer, pp. 247-251
- BUTENUTH, M., GÖSSELN, G. V., TIEDGE, M., HEIPKE, C., LIPECK, U. AND SESTER, M. (2007): Integration of Heterogeneous Geospatial Data in a Federated Database. *ISPRS Journal of Photogrammetry & Remote Sensing* 62(5), pp. 328-346
- BUTENUTH, M., STRAUB, B.-M., HEIPKE, C. AND WILLRICH, F. (2003): Tree Supported Road Extraction from Aerial Images Using Global and Local Context Knowledge. In: J. L. Crowley, J. H. Piater, M. Vincze and L. Paletta (eds.), *Computer Vision Systems, Lecture Notes in Computer Science* 2626, Springer, pp. 162-171
- BUTENUTH, M. (2007): Segmentation of Imagery Using Network Snakes. *Photogrammetrie Fernerkundung Geoinformation* 1/2007, pp. 7-16
- CASELLES, V. AND COLL, B. (1996): Snakes in Movement. *Journal on Numerical Analysis* 33(6), pp. 2445-2456
- CASELLES, V., CATTÉ, F., COLL, T. AND DIBOS, F. (1993): A Geometric Model for Active Contours in Image Processing. *Numerische Mathematik* 66(1), pp. 1-31
- CASELLES, V., KIMMEL, R. AND SAPIRO, G. (1997): Geodesic Active Contours. *International Journal of Computer Vision* 22(1), pp. 61-79
- CHAN, T. F. AND VESE, L. A. (2001): Active Contours Without Edges. *IEEE Transactions on Image Processing* 10(2), pp. 266-277
- CHEN, Y., HUANG, F., TAGARE, H. D. AND RAO, M. (2007): A Coupled Minimization Problem for Medical Image Segmentation with Priors. *International Journal of Computer Vision* 71(3), pp. 259-272
- CHENG, L., YANG, J. AND FAN, X. (2005): A New Region-Based Active Contour for Object Extraction Using Level Set Method. In: J. S. Marques, N. Perez de la Blanca and P. Pina (eds.), *Pattern Recognition and Image Analysis, Lecture Notes in Computer Science* 3522, Springer, pp. 285-291
- CHICUREL, M. (2002): Cell Migration Research is on the Move. *Science* 295(5555), pp. 606-609
- CHOPP, D. L. (1993): Computing Minimal Surfaces via Level Set Curvature Flow. *Journal of Computational Physics* 106(1), pp. 77-91
- COHEN, L. D. AND COHEN, I. (1993): Finite Element Methods for Active Contour Models and Balloons for 2D and 3D Images. *IEEE Transactions on Pattern Analysis and Machine Intelligence* 15(11), pp. 1131-1147
- COHEN, L. D. (1991): On Active Contour Models and Balloons. *CVGIP: Image Understanding* 53(2), pp. 211-218
- CREMERS, D., ROUSSON, M. AND DERICHE, R. (2007): A Review of Statistical Approaches to Level Set Segmentation: Integrating Color, Texture, Motion and Shape. *International Journal of Computer Vision* 72(2), pp. 195-215
- DANIELSSON, P. E. (1980): Euclidean Distance Mapping. *Computer Graphics and Image Processing* 14, pp. 227-248
- DAVATZIKOS, C. A. AND PRINCE, J. L. (1995): An Active Contour Model for Mapping the Cortex. *IEEE Transactions on Medical Imaging* 14(1), pp. 65-80
- DELAGNES, P., BENOIS, J. AND BARBA, D. (1995): Active Contours Approach to Object Tracking in Image sequences with Complex Background. *Pattern Recognition Letters* 16(2), pp. 171-178

- DELINGETTE, H. AND MONTAGNAT, J. (2000): New Algorithms for Controlling Active Contours Shape and Topology. In: D. Vernon (ed.), *Computer Vision - ECCV 2000*, Lecture Notes in Computer Science 1843, Springer, pp. 381-395
- DELINGETTE, H. AND MONTAGNAT, J. (2001): Shape and Topology Constraints on Parametric Active Contours. *Computer Vision and Image Understanding* 83(2), pp. 140-171
- DERVIEUX, A. AND THOMASSET, F. (1979): A Finite Element Method for the Simulation of a Rayleigh-Taylor Instability. In: R. Rautmann (ed.), *Approximation Methods for Navier-Stokes Problems*, Lecture Notes in Mathematics 771, Springer, pp. 145-158
- DERVIEUX, A. AND THOMASSET, F. (1981): Multifluid Incompressible Flows by a Finite Element Method. In: O. Steinmann (ed.), *Perturbation Expansions in Axiomatic Field Theory*, Lecture Notes in Physics 11, Springer, pp. 158-163
- DICKINSON, S. J., JASIOBEDZKI, P., OLOFSSON, G. AND CHRISTENSEN, H. I. (1994): Qualitative Tracking of 3-D Objects Using Active Contour Networks. In: *Proceedings Computer Vision and Pattern Recognition*, pp. 812-817
- DUFOUR, A., SHININ, V., TAJBAKHSH, S., GUILLEN-AGHION, N., OLIVO-MARIN, J. AND ZIMMER, C. (2005): Segmentation and Tracking Fluorescent Cells in Dynamic 3-D Microscopy with Coupled Active Surfaces. *IEEE Transactions on Image Processing* 14(9), pp. 1396-1410
- FISCHLER, M. A. AND ELSCHLAGER, R. (1973): The Representation and Matching of Pictorial Structures. *IEEE Transactions on Computers* 22(1), pp. 67-92
- FORSYTH, D. A. AND PONCE, J. (2002): *Computer Vision: A Modern Approach*. Prentice Hall, 693 p.
- FREEDMAN, D. AND ZHANG, T. (2004): Active Contours for Tracking Distributions. *IEEE Transactions on Image Processing* 13(4), pp. 518-526
- FUA, P., GRÜN, A. AND HAIHONG, L. (1999): Optimization-Based Approaches to Feature Extraction from Aerial Images. In: A. Dermanis, A. Grün and F. Sanso (eds.), *Geomatic Methods for the Analysis of Data in the Earth Sciences*, Lecture Notes in Earth Sciences 95, Springer, pp. 190-228
- FUA, P. (1995): Parametric Models are Versatile: The Case of Model Based Optimization. In: *International Archives of Photogrammetry and Remote Sensing XXX(III/2)*, pp. 828 - 833
- FÖRSTNER, W. AND LÄBE, T. (2003): Learning Optimal Parameters for Self-diagnosis in a System for Automatic Exterior Orientation. In: J. Crowley, J. Piater, M. Vincze and L. Paletta (eds.), *Computer Vision Systems*, Lecture Notes in Computer Science 2626, Springer, pp. 236-246
- GAGE, M. E. (1984): Curve Shortening Makes Convex Curves Circular. *Inventiones Mathematicae* 76(2), pp. 357-364
- GALANDA, M. AND WEIBEL, R. (2003): Using an Energy Minimization Technique for Polygon Generalization. *Cartography and Geographic Information Science* 30(3), pp. 263-279
- GOLDENBERG, R., KIMMEL, R., RIVLIN, E. AND RUDZSKY, M. (2001): Fast Geodesic Active Contours. *IEEE Transactions on Image Processing* 10(10), pp. 1467-1474
- GRAYSON, M. A. (1987): The Heat Equation Shrinks Embedded Plane Curves to Round Points. *Journal of Differential Geometry* 26(2), pp. 285-314
- GRÜN, A. AND LI, H. (1997): Semi-Automatic Linear Feature Extraction by Dynamic Programming and LSB-Snakes. *Photogrammetric Engineering & Remote Sensing* 63(8), pp. 985-995

- GUNN, S. R. AND NIXON, M. S. (1997): A Robust Snake Implementation; A Dual Active Contour. IEEE Transactions on Pattern Analysis and Machine Intelligence 19(1), pp. 63-68
- GURARI, E. M. AND WECHSLER, H. (1982): On the Difficulties in the Segmentation of Pictures. IEEE Transactions on Pattern Analysis and Machine Intelligence 4(3), pp. 304-306
- GÜLCH, E. (1990): Extraction of Contours in Digital Images by Active Contour Models. In: International Archives of Photogrammetry and Remote Sensing 28(3/2), pp. 211-220
- GÜLCH, E. (1995): From Control Points to Control Structures for Absolute Orientation and Aerial Triangulation in Digital Photogrammetry. Zeitschrift für Photogrammetrie und Fernerkundung 3/1995, pp. 130-136
- HAN, X., XU, C. AND PRINCE, J. L. (2003): A Topology Preserving Level Set Method for Geometric Deformable Models. IEEE Transactions on Pattern Analysis and Machine Intelligence 25(6), pp. 755-768
- HARALICK, R. M. AND SHAPIRO, L. G. (1985): Survey: Image Segmentation Techniques. Computer Vision, Graphics, and Image Processing 29(1), pp. 100-132
- HARARY, F. (1994): Graph Theory. Westview Press, 288 p.
- HINZ, S. AND WIEDEMANN, C. (2004): Increasing Efficiency of Road Extraction by Self-diagnosis. Photogrammetric Engineering & Remote Sensing 70(12), pp. 1457-1466
- HOCH, M. AND LITWINOWICZ, P. C. (1996): A Semi-Automatic System for Edge Tracking with Snakes. The Visual Computer 12(2), pp. 75-83
- IVINS, J. AND PORRILL, J. (1995): Active Region Models for Segmenting Textures and Colours. Image and Vision Computing 13(5), pp. 431-438
- JAIN, A. K., ZHONG, Y. AND DUBUISSON-JOLLY, M. (1998): Deformable Template Models: A Review. Signal Processing 71(2), pp. 109-129
- JASIOBEDZKI, P. (1993): Adaptive Adjacency Graphs. In: B. C. Vemuri (ed.), Geometric Methods in Computer Vision II, SPIE 2031, pp. 294-303
- JETZEK, F. AND KAISER, H. (2007): A Geometric Model of Cytoskeletal Tension in Adherent Cells. In: P. Perner (ed.), Machine Learning and Data Mining in Pattern Recognition, IBAI Publishing, pp. 105-119
- Ji, L. AND YAN, H. (2002a): Loop-Free Snakes for Highly Irregular Object Shapes. Pattern Recognition Letters 23(5), pp. 579-591
- Ji, L. AND YAN, H. (2002b): Robust Topology-Adaptive Snakes for Image Segmentation. Image and Vision Computing 20(2), pp. 147-164
- JONES, T. R., CARPENTER, A. AND GOLLAND, P. (2005): Voronoi-Based Segmentation of Cells on Image Manifolds. In: Y. Liu, T. Jiang and C. Zhang (eds.), Computer Vision for Biomedical Image Applications, Lecture Notes in Computer Science 3765, Springer, pp. 535-543
- KANIZSA, G. (1976): Subjective Contours. Scientific American 234(4), pp. 48-52
- KASS, M., WITKIN, A. AND TERZOPOULOS, D. (1987): Snakes: Active Contour Models. In: Proceedings IEEE International Conference on Computer Vision, pp. 259-268
- KASS, M., WITKIN, A. AND TERZOPOULOS, D. (1988): Snakes: Active Contour Models. International Journal of Computer Vision 1(4), pp. 321-331
- KERSCHNER, M. (2003): Snakes für Aufgaben der digitalen Photogrammetrie und Topographie. PhD thesis, Technische Universität Wien, 115 p.

- KICHENASSAMY, S., KUMAR, A., OLVER, P., TANNENBAUM, A. AND YEZZI, A. (1995): Gradient Flows and Geometric Active Contour Models. In: *Proceedings International Conference on Computer Vision*, pp. 810-815
- KICHENASSAMY, S., KUMAR, A., OLVER, P., TANNENBAUM, A. AND YEZZI, A. (1996): Conformal Curvature Flows: From Phase Transitions to Active Vision. *Archive for Rational Mechanics and Analysis* 134(3), pp. 275-301
- KIMIA, B. B., TANNENBAUM, A. AND ZUCKER, S. W. (1990): Toward a Computational Theory of Shape: An Overview. In: O. Faugeras (ed.), *Computer Vision - ECCV 90, Lecture Notes in Computer Science* 427, Springer, pp. 402-407
- KIMIA, B. B., TANNENBAUM, A. R. AND ZUCKER, S. W. (1992): On the Evolution of Curves via a Function of Curvature, I: The Classical Case. *Journal of Mathematical Analysis and Applications* 163(2), pp. 438-458
- KIMMEL, R., AMIR, A. AND BRUCKSTEIN, A. (1995): Finding Shortest Paths on Surfaces Using Level Sets Propagation. *IEEE Transactions on Pattern Analysis and Machine Intelligence* 17(6), pp. 635-640
- KOZERKE, S., BOTNAR, R., OYRE, S., SCHEIDEGGER, M. B., PEDERSEN, E. M. AND BOESIGER, P. (1999): Automatic Vessel Segmentation Using Active Contours in Cine Phase Contrast Flow Measurements. *Journal of Magnetic Resonance Imaging* 10(1), pp. 41-51
- LACHAUD, J. AND MONTANVERT, A. (1999): Deformable Meshes with Automated Topology Changes for Coarse-to-fine Three-Dimensional Surface Extraction. *Medical Image Analysis* 3(2), pp. 187-207
- LAPTEV, I., MAYER, H., LINDBERG, T., STEGER, C. AND BAUMGARTNER, A. (2000): Automatic Extraction of Roads from Aerial Images Based on Scale Space and Snakes. *Machine Vision and Applications* 12(1), pp. 23-31
- LEITNER, F. AND CINQUIN, P. (1992): Complex Topology 3-D Objects Segmentation. In: R. M. Larson and H. N. Nasr (eds.), *Model-Based Vision Development and Tools*, SPIE 1609, pp. 16-26
- LEROY, B., HERLIN, I. L. AND COHEN, L. D. (1996): Multi-Resolution Algorithms for Active Contour Models. In: *Proceedings International Conference on Analysis and Optimization of Systems*, pp. 58-65
- LEVENTON, M. E., GRIMSON, W. E. L. AND FAUGERAS, O. (2000): Statistical Shape Influence in Geodesic Active Contours. In: *Proceedings Conference on Computer Vision and Pattern Recognition*, pp. 316-323
- LEYMARIE, F. AND LEVINE, M. (1993): Tracking Deformable Objects in the Plane Using an Active Contour Model. *IEEE Transactions on Pattern Analysis and Machine Intelligence* 15(6), pp. 617-634
- LI, C., LIU, J. AND FOX, M. D. (2005): Segmentation of External Force Field for Automatic Initialization and Splitting of Snakes. *Pattern Recognition* 38(11), pp. 1947-1960
- LINDBERG, T. (1990): Scale-Space for Discrete Signals. *IEEE Transactions on Pattern Analysis and Machine Intelligence* 12(3), pp. 234-254
- LINDBERG, T. (1994): *Scale-Space Theory in Computer Vision*. Kluwer Academic Publishers, 423 p.
- LÖCHERBACH, T. (1994): Fusion of Multi-Sensor Images and Digital Map Data for the Reconstruction and Interpretation of Agricultural Land-Use Units. In: *International Archives of Photogrammetry and Remote Sensing* XXX(3/2), pp. 505-511
- LÖCHERBACH, T. (1998): *Fusing Raster- and Vector-Data with Applications to Land-Use Mapping*. PhD thesis, Universität Bonn, 107 p.
- MALLADI, R., KIMMEL, R., ADALSTEINSSON, D., SAPIRO, G., CASELLES, V. AND SETHIAN, J. (1996): A Geometric Approach to Segmentation and Analysis of 3D Medical Images. In: *Proceedings Mathematical Methods in Biomedical Image Analysis*, pp. 244-252

- MALLADI, R., SETHIAN, J. A. AND VEMURI, B. C. (1993): A Topology-Independent Shape Modeling Scheme. In: B. C. Vemuri (ed.), *Geometric Methods in Computer Vision II*, SPIE 2031, pp. 246-259
- MALLADI, R., SETHIAN, J. A. AND VEMURI, B. C. (1994): Evolutionary Fronts for Topology-Independent Shape Modeling and Recovery. In: J. Eklundh (ed.), *Computer Vision - ECCV 94*, Lecture Notes in Computer Science 800, Springer, pp. 1-13
- MALLADI, R., SETHIAN, J. A. AND VEMURI, B. C. (1995): Shape Modeling with Front Propagation: A Level Set Approach. *IEEE Transactions on Pattern Analysis and Machine Intelligence* 17(2), pp. 158-175
- MALLADI, R. (2002): *Geometric Methods in Bio-Medical Image Processing*. Springer, 147 p.
- MCINERNEY, T. AND TERZOPOULOS, D. (1995): Topologically Adaptable Snakes. In: *Proceedings International Conference on Computer Vision*, pp. 840-845
- MCINERNEY, T. AND TERZOPOULOS, D. (1996): Deformable Models in Medical Image Analysis: A Survey. *Medical Image Analysis* 1(2), pp. 91-108
- MCINERNEY, T. AND TERZOPOULOS, D. (2000): T-Snakes: Topology Adaptive Snakes. *Medical Image Analysis* 4(2), pp. 73-91
- MENET, S., SAINT-MARC, P. AND MEDIONI, G. (1990a): Active Contour Models: Overview, Implementation and Applications. In: *IEEE Conference on Systems, Man and Cybernetics*, pp. 194-199
- MENET, S., SAINT-MARC, P. AND MEDIONI, G. (1990b): B-Snakes: Implementation and Application to Stereo. In: *Proceedings DARPA Image Understanding Workshop*, pp. 720-726
- MERRIMAN, B., BENCE, J. K. AND OSHER, S. J. (1994): Motion of Multiple Junctions: A Level Set Approach. *Journal of Computational Physics* 112(2), pp. 334-363
- MÜLLER, M., SEGL, K. AND KAUFMAN, H. (2004): Edge- and Region-Based Segmentation Techniques for the Extraction of Large, Man-Made Objects in High-Resolution Satellite Imagery. *Pattern Recognition* 37(8), pp. 1619-1628
- MÜLLER, M. (2001): *Extraktion großflächiger Strukturen in hochauflösenden, panchromatischen Satellitendaten*. PhD thesis, Universität Bielefeld, 158 p.
- NEUENSCHWANDER, W., FUA, P., IVERSON, L., SZEKELY, G. AND KÜBLER, O. (1997): Ziplock Snakes. *International Journal of Computer Vision* 25(3), pp. 191-201
- NEUENSCHWANDER, W., FUA, P., SZEKELY, G. AND KÜBLER, O. (1994a): Making Snakes Converge from Minimal Initialization. In: *Proceedings International Conference on Pattern Recognition*, pp. 613-615
- NEUENSCHWANDER, W., FUA, P., SZEKELY, G. AND KÜBLER, O. (1994b): Initializing Snakes. In: *Proceedings Conference on Computer Vision and Pattern Recognition*, pp. 658-663
- OESTERLE, M. AND WILDMANN, R. (2003): Land Parcel Identification as a Part of the Integrated Administration and Control System (IACS). In: *Proceedings ISPRS Workshop 'Challenges in Geospatial Analysis, Integration and Visualization II'*, pp. 117-123
- ORTIZ DE SOLORZANO, C., MALLADI, R., LELIEVRE, S. A. AND LOCKETT, S. J. (2001): Segmentation of Nuclei and Cells Using Membrane Related Protein Markers. *Journal of Microscopy* 201(3), pp. 404-415
- OSHER, S. AND PARAGIOS, N. (2003): *Geometric Level Set Methods in Imaging, Vision, and Graphics*. Springer, 513 p.
- OSHER, S. AND SETHIAN, J. A. (1988): Fronts Propagating with Curvature Dependent Speed: Algorithms Based on Hamilton-Jacobi Formulations. *Journal of Computational Physics* 79(1), pp. 12-49

- PARAGIOS, N. AND DERICHE, R. (1999): Geodesic Active Contours for Supervised Texture Segmentation. In: Proceedings IEEE Conference on Computer Vision and Pattern Recognition, pp. 422-427
- PARAGIOS, N. AND DERICHE, R. (2000a): Geodesic Active Contours and Level Sets for the Detection and Tracking of Moving Objects. IEEE Transactions on Pattern Analysis and Machine Intelligence 22(3), pp. 266-280
- PARAGIOS, N. AND DERICHE, R. (2000b): Coupled Geodesic Active Regions for Image Segmentation: A Level Set Approach. In: D. Vernon (ed.), Computer Vision - ECCV 2000, Lecture Notes in Computer Science 1843, Springer, pp. 224-240
- PARAGIOS, N. AND DERICHE, R. (2002a): Geodesic Active Regions and Level Set Methods for Supervised Texture Segmentation. International Journal of Computer Vision 46(3), pp. 223-247
- PARAGIOS, N. AND DERICHE, R. (2002b): Geodesic Active Regions: A New Framework to Deal with Frame Partition Problems in Computer Vision. Journal of Visual Communication and Image Representation 13(1), pp. 249-268
- PETERI, R. AND RANCHIN, T. (2003): Multiresolution Snakes for Urban Road Extraction from IKONOS and Quickbird Images. In: EARSeL Symposium 'Remote Sensing in Transition', pp. 141-147
- PETERI, R., CELLE, J. AND RANCHIN, T. (2003): Detection and Extraction of Road Networks from High Resolution Satellite Images. In: Proceedings International Conference on Image Processing, pp. 301-304
- POGGIO, T., TORRE, V. AND KOCH, C. (1985): Computational Vision and Regularization Theory. Nature 317, pp. 314-319
- PUJOL, O. AND RADEVA, P. (2003): Texture Segmentation by Statistical Deformable Models. International Journal of Image and Graphics 4(3), pp. 433-452
- RADEVA, P., SERRAT, J. AND MARTI, E. (1995): A Snake for Model-Based Segmentation. In: Proceedings International Conference on Computer Vision, pp. 816-822
- RAY, N., ACTON, S. T. AND LEY, K. (2002): Tracking Leukocytes In Vivo with Shape and Size Constrained Active Contours. IEEE Transactions on Medical Imaging 21(10), pp. 1222-1235
- RAY, N., ACTON, S. T., ALTES, T., DE LANGE, E. E. AND BROOKEMAN, J. (2003): Merging Parametric Active Contours Within Homogeneous Image Regions for MRI-Based Lung Segmentation. IEEE Transactions on Medical Imaging 22(2), pp. 189-199
- ROCHERY, M., JERMYN, I. H. AND ZERUBIA, J. (2006): Higher Order Active Contours. International Journal of Computer Vision 69(1), pp. 27-42
- RONFARD, R. (1994): Region-Based Strategies for Active Contour Models. International Journal of Computer Vision 13(2), pp. 229-251
- ROSENFELD, A. AND DAVIS, L. S. (1979): Image Segmentation and Image Models. Proceedings of the IEEE 67(5), pp. 764-772
- ROSIN, P. L. (1998): Refining Region Estimates. International Journal of Pattern Recognition and Artificial Intelligence 12(6), pp. 841-866
- ROUSSON, M. AND PARAGIOS, N. (2002): Shape Priors for Level Set Representation. In: A. Heyden, G. Sparr, M. Nielsen and P. Johansen (eds.), Computer Vision - ECCV 2002, Lecture Notes in Computer Science 2351, Springer, pp. 416-418
- SAMADANI, R. (1989): Changes in Connectivity in Active Contour Models. In: Proceedings Workshop on Visual Motion, pp. 337-343

- SAPIRO, G. AND TANNENBAUM, A. (1993): On Invariant Curve Evolution and Image Analysis. *Indiana University Mathematics Journal* 42(3), pp. 985-1009
- SARTI, A., MALLADI, R. AND SETHIAN, J. (2002): Subjective Surfaces: A Geometric Model for Boundary Completion. *International Journal of Computer Vision* 46(3), pp. 201-221
- SEGONNE, F., PONS, J., GRIMSON, E. AND FISCHL, B. (2005): Active Contours Under Topology Control Genus Preserving Level Sets. In: Y. Liu, T. Jiang and C. Zhang (eds.), *Computer Vision for Biomedical Image Applications*, Lecture Notes in Computer Science 3765, Springer, pp. 135-145
- SETHIAN, J. A. (1989): A Review of Recent Numerical Algorithms for Hypersurfaces Moving with Curvature-Dependent Speed. *Journal of Differential Geometry* 31, pp. 131-161
- SETHIAN, J. A. (1996a): *Level Set Methods: Evolving Interfaces in Geometry, Fluid Mechanics, Computer Vision, and Materials Science*. Cambridge University Press, 218 p.
- SETHIAN, J. A. (1996b): A Fast Marching Level Set Method for Monotonically Advancing Fronts. In: *Proceedings of the National Academy of Sciences, USA* 93(4), pp. 1591-1595
- SHAPIRO, L. G. AND STOCKMANN, G. C. (2001): *Computer Vision*. Prentice Hall, 580 p.
- SINGH, A., GOLDBOF, D. B. AND TERZOPOULOS, D. (1998): *Deformable Models in Medical Image Analysis*. IEEE Computer Society Press, 388 p.
- SMITH, K. A., SOLIS, F. J. AND CHOPP, D. L. (2002): A Projection Method for Motion of Triple Junctions by Level Sets. *Interfaces and Free Boundaries* 4(3), pp. 263-276
- SONG, W., HAITHCOAT, T. L. AND KELLER, J. M. (2006): A Snake-Based Approach for TIGER Road Data Conflation. *Cartography and Geographic Information Science* 33(4), pp. 287-298
- SONKA, M. AND FITZPATRICK, J. M. (2000): *Handbook of Medical Imaging II: Medical Image Processing and Analysis*. SPIE Press, 1218 p.
- SRINARK, T. AND KAMBHAMETTU, C. (2001): A Framework for Multiple Snakes. In: *Proceedings Conference on Computer Vision and Pattern Recognition*, pp. 202-210
- SRINARK, T. AND KAMBHAMETTU, C. (2006): A Framework for Multiple Snakes and its Applications. *Pattern Recognition* 39(9), pp. 1555-1565
- STARK, K. AND FUCHS, S. (1996): A Method for Tracking the Pose of Known 3-D Objects Based on an Active Contour Model. In: *Proceedings International Conference on Pattern Recognition*, pp. 905-909
- SURI, J. S., SETAREHDAN, S. K. AND SINGH, S. (2002): *Advanced Algorithmic Approaches to Medical Image Segmentation: State-of-the-Art Applications in Cardiology, Neurology, Mammography and Pathology*. Springer, 668 p.
- TERZOPOULOS, D. AND FLEISCHER, K. (1988): Deformable Models. *The Visual Computer* 4(6), pp. 306-331
- TERZOPOULOS, D., PLATT, J., BARR, A. AND FLEISCHER, K. (1987a): Elastically Deformable Models. *Computer Graphics* 21(4), pp. 205-214
- TERZOPOULOS, D., WITKIN, A. AND KASS, M. (1987b): Symmetry-Seeking Models and 3D Object Reconstruction. *International Journal of Computer Vision* 1(3), pp. 211-221
- TERZOPOULOS, D. (1986): Regularization of Inverse Visual Problems Involving Discontinuities. *IEEE Transactions on Pattern Analysis and Machine Intelligence* 8(4), pp. 413-424

- THIERMANN, A., SBRESNY, J. AND SCHÄFER, W. (2002): GIS in WEELS - Wind Erosion on European Light Soils. *GeoInformatics* 5, pp. 30-33
- TIKHONOV, A. N. (1963): Regularization of Incorrectly Posed Problems. *Soviet Mathematics Doklady* 4, pp. 1624-1627
- TORRE, M. AND RADEVA, P. (2000): Agricultural Field Extraction from Aerial Images Using a Region Competition Algorithm. In: *International Archives of Photogrammetry and Remote Sensing XXXIII(B2)*, pp. 889-896
- TORRE, M. AND RADEVA, P. (2004): Agricultural-Field Extraction on Aerial Images by Region Competition Algorithms. In: *Proceedings International Conference on Pattern Recognition*, pp. 313-316
- TRIAS-SANZ, R., PIERROT-DESEILLIGNY, M., LOUCHET, J. AND STAMON, G. (2007): Methods for Fine Registration of Cadastre Graphs to Images. *IEEE Transactions on Pattern Analysis and Machine Intelligence* 29(11), pp. 1990-2000
- TRIAS-SANZ, R. (2006): Semi-Automatic Rural Land Cover Classification from High-Resolution Remote Sensing Images. PhD thesis, 374 p.
- VESE, L. A. AND CHAN, T. F. (2002): A Multiphase Level Set Framework for Image Segmentation Using the Mumford and Shah Model. *International Journal of Computer Vision* 50(3), pp. 271-293
- WIDROW, B. (1973): The 'Rubber-Mask' Technique. *Pattern Recognition* 5(3), pp. 199-211
- WILLIAMS, D. J. AND SHAH, M. (1992): A Fast Algorithm for Active Contours and Curvature Estimation. *CVGIP: Image Understanding* 55(1), pp. 14-26
- WOLF, B. AND HEIPKE, C. (2007): Automatic Extraction and Delineation of Single Trees from Remote Sensing Data. *Machine Vision and Applications* 18(5), pp. 317-330
- WONG, S. AND WONG, K. K. (2004): Robust Image Segmentation by Texture Sensitive Snake Under Low Contrast Environment. In: *Proceedings International Conference on Informatics in Control, Automation and Robotics*, pp. 430-434
- XU, C. AND PRINCE, J. L. (1997): Gradient Vector Flow: A new External Force for Snakes. In: *Proceedings IEEE Conference on Computer Vision and Pattern Recognition*, pp. 66-71
- XU, C. AND PRINCE, J. L. (1998): Snakes, Shapes, and Gradient Vector Flow. *IEEE Transactions on Image Processing* 7(3), pp. 359-369
- XU, C., PHAM, D. L. AND PRINCE, J. L. (2000): Image Segmentation Using Deformable Models. In: M. Sonka and J. M. Fitzpatrick (eds.), *Handbook of Medical Imaging II*, SPIE Press, pp. 129-174
- YEZZI, A., KICHENASSAMY, S., KUMAR, A., OLVER, P. AND TANNENBAUM, A. (1997): A Geometric Snake Model for Segmentation of Medical Imagery. *IEEE Transactions on Medical Imaging* 16(2), pp. 199-209
- YEZZI, A., TSAI, A. AND WILLSKY, A. (1999): A Statistical Approach to Snakes for Bimodal and Trimodal Imagery. In: *Proceedings International Conference on Computer Vision*, pp. 898-903
- YHANN, S. R. AND YOUNG, T. Y. (1995): Boundary Localization in Texture Segmentation. *IEEE Transactions on Image Processing* 4(6), pp. 849-856
- YOUNG, D., GLASBEY, C. A., GRAY, A. J. AND MARTIN, N. J. (1998): Towards Automatic Cell Identification in DIC Microscopy. *Journal of Microscopy* 192(2), pp. 186-193
- ZAGORCHEV, L., GOSHTASBY, A. AND SATTER, M. (2007): R-Snakes. *Image and Vision Computing* 25(6), pp. 945-959

- ZHANG, B., ZIMMER, C. AND OLIVO-MARIN, J. (2004): Tracking Fluorescent Cells with Coupled Geometric Active Contours. In: Proceedings International Symposium on Biomedical Imaging: Nano to Macro, pp. 476-479
- ZHAO, H., CHAN, T., MERRIMAN, B. AND OSHER, S. (1996): A Variational Level Set Approach to Multiphase Motion. *Journal of Computational Physics* 127(1), pp. 179-195
- ZHU, S. C. AND YUILLE, A. (1996): Region Competition: Unifying Snakes, Region Growing, and Bayes/MDL for Multiband Image Segmentation. *IEEE Transactions on Pattern Analysis and Machine Intelligence* 18(9), pp. 884-900
- ZHU, S. C., LEE, T. S. AND YUILLE, A. L. (1995): Region Competition: Unifying Snakes, Region Growing, and Bayes/MDL for Multiband Image Segmentation. In: Proceedings International Conference on Computer Vision, pp. 416-425
- ZIMMER, C. AND OLIVO-MARIN, J. (2005): Coupled Parametric Active Contours. *IEEE Transactions on Pattern Analysis and Machine Intelligence* 27(11), pp. 1838-1842
- ZIMMER, C., LABRUYERE, E., MEAS-YEDID, V., GUILLEN, N. AND OLVO-MARIN, J. (2002): Segmentation and Tracking of Migrating Cells in Videomicroscopy with Parametric Active Contours: A Tool for Cell-Based Drug Testing. *IEEE Transactions on Medical Imaging* 21(10), pp. 1212-1221
- ZIMMER, C., ZHANG, B., DUFOUR, A., THEBAUD, A., BERLEMONT, S., MEAS-YEDID, V. AND OLIVO-MARIN, J. (2006): On the Digital Trail of Mobile Cells. *IEEE Signal Processing Magazine* 23(3), pp. 54-62

Curriculum Vitae

Personnel Details

Name	Matthias Butenuth
Date of Birth	24.02.1976
Place of Birth	Bielefeld
Citizenship	German
Marital Status	Single

Work Experience

Since 09/2007	Remote Sensing Technology Technische Universität München <i>Research assistant</i>	München
08/2002 – 08/2007	Institute of Photogrammetry and GeoInformation Leibniz Universität Hannover <i>Scientific collaborator</i>	Hannover

Education

09/1996 – 06/2002	Geodesy and Geoinformatics (Dipl.-Ing.) <i>Leibniz Universität Hannover</i>	Hannover
05/1996 – 09/1996	Internship, engineering company <i>Dipl.-Ing. U. Elschen (ÖbVI), Dipl.-Ing. W. Schumann (ÖbVI)</i>	Herford, Löhne
09/1995 – 04/1996	Mathematics and Geography <i>Ruhr-Universität Bochum</i>	Bochum
08/1986 – 06/1995	High-school diploma (Abitur) <i>Weser-Gymnasium Vlotho</i>	Vlotho

Acknowledgements

An dieser Stelle möchte ich den Menschen danken, die auf ganz unterschiedliche Art und Weise zum Gelingen der Arbeit beigetragen haben:

- Bei meinem Doktorvater Prof. Dr.-Ing. Christian Heipke möchte ich mich für die konstruktive Begleitung der Arbeit bedanken. Insbesondere die wissenschaftlich und kritisch ausgerichteten Diskussionen haben zu meiner Motivation und zum Erfolg der Arbeit beigetragen. Darüberhinaus war die Freiheit, die ich bei meinen Forschungen hatte, sehr förderlich für das Entstehen der Arbeit.
- Bei Prof. Dr.-Ing. Wolfgang Förstner und Prof. Dr.-Ing. Monika Sester möchte ich mich für die Übernahme der Korreferate bedanken.
- Bei meinen alten und neuen Kollegen möchte ich mich für die Unterstützung durch viele fachliche und auch nicht fachliche Gespräche während der Entstehung der Arbeit bedanken. Ganz besonders möchte ich Dr.-Ing. „Benz“ Wolf danken, der zu Beginn meiner Forschung und beim Einstieg in die Snakes sehr hilfsbereit war.
- Bei Dr.-Ing. Markus Gerke, Prof. Dr.-Ing. Uwe Sörgel und ganz besonders bei Dr.-Ing. Stefan Hinz möchte ich mich für das Korrekturlesen der Arbeit und die vielen Anregungen bedanken.
- Bei Fritz Jetzek und der Firma Evotec Technologies möchte ich mich für die Bereitstellung der medizinischen Bilddaten bedanken, die IKONOS-Daten entstammen dem EC-MARS Programm – European Space Imaging, EUSI, 2004.
- Bei meiner Mutter und meinen Geschwistern möchte ich mich für das Zuhören und das Verständnis bedanken, das sie während der Entstehung der Arbeit aufgebracht haben. Außerdem möchte ich mich bei Ninas Familie für die Unterstützung bedanken.
- Bei Nina reicht Danke zu sagen sicherlich nicht aus, denn ihr Beitrag während der Entstehung der Arbeit war viel größer – aber dazu fehlen mir die Worte.